The number of neutrino species

D. Denegri

CERN, Geneva, Switzerland and Département de Physique des Particules Élémentaires, Centre d'Études Nucléaires de Saclay, Gif-sur-Yvette, France

B. Sadoulet

Center for Particle Astrophysics, Department of Physics, and Lawrence Berkeley Laboratory, University of California, Berkeley, California 94720

M. Spiro

Département de Physique des Particules Élémentaires, Centre d'Études Nucléaires de Saclay, Gif-sur-Yvette, France

The authors review the methods used before the operation of the high energy Stanford and CERN e^+e^- colliders to determine the number of neutrino species N_ν, or an upper limit on this number, within the framework of the Standard Model of light stable neutrinos interacting according to the SU(2)×U(1) universal couplings. The astrophysical limit based on the neutrino burst from supernova 1987A is discussed first, followed by a discussion of the cosmological constraint based on the observed He/H abundance ratio. Finally, the particle physics methods based on single-photon production in e^+e^- collisions, on the production of monojets in $p\bar{p}$ collisions, and on the determination of N_ν from the ratio of the $W\to l\bar{\nu}$ to $Z^0\to l\bar{l}$ partial cross sections in $p\bar{p}$ collisions are discussed. The various sources of uncertainty and the experimental backgrounds are presented, as well as an idea of what may be expected on this subject in the future. There is a remarkable agreement between the various methods, with central values for N_ν between 2 and 3 and with upper limits $N_\nu<6$. Combining all determinations, the authors obtain a central value $N_\nu=2.1^{+0.6}_{-0.4}$ for $m_{\rm top}=50$ GeV/c^2 and $N_\nu=2.0^{+0.6}_{-0.4}$ if $m_{\rm top}\geq m_W$. The results are perfectly compatible with the *a priori* knowledge that at least three families of neutrinos should exist. The observed consistency between this *a priori* knowledge, the laboratory determinations of N_ν, and determinations from SN 1987A and cosmology represent an astounding success for the Standard Model and for the current descriptions of stellar collapse and the Big-Bang primordial nucleosynthesis. These results, however, severely limit the number of additional families. Although the consistency is significantly worse, four families still provide a reasonable fit. In the framework of the Standard Model, a fifth light neutrino is, however, unlikely. A noted added in proof summarizes the results recently obtained at the Fermilab $\bar{p}p$ and the Stanford and CERN e^+e^- colliders which confirm these conclusions.

CONTENTS

I. INTRODUCTION

With the discovery of the W and Z bosons at the CERN SPS collider (Arnison *et al.*, 1983a, 1983b, 1983c, 1983d; Bagnaia *et al.*, 1983; Banner *et al.*, 1983) and the measurements of their properties, production rates, and decay features, the SU(3)×SU(2)×U(1) Standard Model of electroweak and strong interactions is on a firm footing. The model, however, does not predict the number of fermion generations or their masses.

The quarks and leptons observed so far can be organized into three families (or generations) of weak isodoublets (for left-handed states) as follows:

u	c	t	quark doublets
d	s	b	
ν_e	ν_μ	ν_τ	lepton doublets
e	μ	τ	

Each leptonic doublet contains a distinct type of neutrino, labeled ν_e, ν_μ, ν_τ. One of the basic questions is this: are there more families than the three observed so far? In view of the regularity prevailing in the first three generations, counting the number of neutrino types may also mean counting the number of fundamental fermion generations.

Until now the direct detection of neutrinos has been achieved only for the neutrinos ν_e and ν_μ. The third generation ν_τ has not been detected directly through its characteristic interactions with matter. The evidence for ν_τ as an independent species, with the same (universal) Fermi coupling to its third-generation charged-lepton partner τ, as is the case for the two lighter generations, is indirect. It is obtained either from the τ lifetime (Braunschweig *et al.*, 1988; Hitlin, 1988) or from the tests of e-μ-τ universality based on the W partial production cross-section ratios $\sigma(W\to e\nu)/\sigma(W\to\mu\nu)/\sigma(W\to\tau\nu)$ measured at the SPS collider by the UA1 collaboration (Albajar *et al.*, 1987a). While the τ lifetime tests the hypothesis of the universality of weak charged currents at a low $Q^2\le M_\tau^2$, the collider results test it at $Q^2\approx M_W^2$.

Information on the number of light neutrino species N_ν (or an upper limit on N_ν) can be obtained from various fields: astrophysics, cosmology, and particle physics. It should be noted that limits from particle physics apply to a much wider range of neutrino masses ($M_\nu < M_Z/2$) than the limits from astrophysics and cosmology, which apply to neutrinos lighter than a few MeV. However, we will show that the limits are comparable, demonstrating an astounding consistency in our current understanding of diverse phenomena (for a brief discussion, see Cline *et al.*, 1987).

The astrophysical and cosmological methods rely on the equipartition of energy between the relativistic degrees of freedom at temperatures of a few MeV at stellar-collapse time or primordial nucleosynthesis time, respectively. Thermal equilibrium is established through weak neutral-current interactions of the type $e^+e^-\leftrightarrow Z^0\leftrightarrow\nu_i\bar{\nu}_i$. The astrophysical limit on N_ν is based on the observation of antineutrinos emitted by SN 1987A and is obtained by comparison with the expected neutron-star binding energy (Ellis and Olive, 1987; Krauss, 1987; Schaeffer *et al.*, 1987; Schramm, 1987, 1988). This astrophysical limit is discussed in Sec. II. The cosmological results are based on the comparison of the observed cosmological He/H abundance ratio with Big-Bang-model calculations (see, e.g., the review by Boesgaard and Steigman, 1985). The most recent attempt along those lines have been by Steigman *et al.* (1986) and Ellis *et al.* (1986). The cosmological upper limit on N_ν is discussed in detail in Sec. III. The laboratory particle physics results from e^+e^- and $p\bar{p}$ colliders are based on the fact that, in the Standard Model, all neutrino species ν_i are universally coupled to the Z^0 boson. Each neutrino species contributes to the Z^0 total width $\Gamma_{\rm tot}^Z$ with a partial rate $\delta\Gamma^z=\Gamma_{\nu\nu}^Z$, which is given by

$$\Gamma_{\nu\nu}^Z=\frac{G_F}{12\pi\sqrt{2}}M_Z^3 ,$$

where G_F is the Fermi constant and M_Z is the Z^0 mass. For $M_Z=91.9$ GeV, which is obtained from the Standard Model prediction $M_Z=(38.68\pm0.03\ \text{GeV})/\sin\theta_W\cos\theta_W$ [including electroweak radiative corrections (Marciano, 1987)] and from the latest world average for $\sin^2\theta_W=0.230\pm0.005$ (Amaldi *et al.*, 1986; Costa *et al.*, 1988), this partial width amounts to $\approx$170 MeV. The above equation is valid for neutrino masses $M_\nu \ll M_Z/2$. The various particle physics methods employed to obtain N_ν all amount to either an (indirect) measurement of the Z^0 total width or a measurement of the partial width corresponding to the sum over all neutrino species $\sum\Gamma_{\nu\nu}^Z$. More generally, these results can be interpreted as a limit on the Z^0 partial decay rate into noninteracting particles, as, for example, $Z^0\to\tilde{\nu}\tilde{\nu}$. The most significant accelerator experiment limits or values for N_ν obtained until now are from searches for $e^+e^-\to\gamma+Z^0\to\gamma\nu\bar{\nu}$ (Z^0 off shell) at PEP and PETRA (Ford *et al.*, 1986; Hearty *et al.*, 1987; Behrend *et al.*, 1988), from results on $p\bar{p}\to Z^0(\to\nu_i\bar{\nu})+$jet ($Z^0$ on shell) (Albajar *et al.*,, 1987b), and from the measured ratio of partial W to Z production rates $\sigma(W\to l\nu)/\sigma(Z\to ll)$ from the CERN $p\bar{p}$ collider (Albajar *et al.*, 1987c; Ansari *et al.*, 1987a; Colas *et al.*, 1988). In Secs. IV, V, and VI we discuss each of these results in turn.

In Sec. VII we conclude with an overview of the various results on N_ν. In this review, we have attempted to treat consistently the statistical and systematic errors and have adopted a "classical" point of view of statistics as opposed to a "Bayesian" approach (see, e.g., Eadie *et al.*, 1971). The number of neutrino families is considered as a

parameter to be estimated and not as a random variable on which some *a priori* information exists. Our justification for this approach is mainly that of consistency with the common practice in experimental physics and of objectivity in summarizing the information carried by the measurements we review (cf. Appendix).

II. NUMBER OF NEUTRINO SPECIES FROM SUPERNOVA 1987A

On February 23, 1987, the optical and the neutrino flashes resulting from the ultimate collapse of a star (SN 1987A) were detected by astronomers and elementary-particle physicists. A supernova exploded in the Large Magellanic Cloud (LMC), which is 154 000±10 000 light years away. This is the first supernova ever detected through neutrinos. The most significant numbers of detected neutrino events, almost free of background, appeared in the two large water Čerenkov detectors, one at the Kamioka Mine nucleon decay experiment (Kamiokande) and the other at the Irvine-Michigan-Brookhaven (IMB) experiment, which were initially designed for proton lifetime measurements. A less significant signal has also been detected with scintillator detectors at Baksan and possibly in the Mont Blanc tunnel, although not at the same time in this latter case.

These events, as discussed below, were most likely due to $\bar{\nu}_e$ interactions on protons:

$$\bar{\nu}_e + p \rightarrow n + e^+ .$$

Figure 1 shows the spike (<13 s) of events, which is the time signature of the burst in Kamiokande (Hirata *et al.*, 1987). Tables I(a) and I(b) give the information collected on the 11 events detected by Kamiokande and the eight events detected by the IMB experiment (Bionta *et al.*, 1987). Figures 2(a) and 2(b) show the time sequence and energy spectrum of events. Most of the events are concentrated in the first few seconds. This is precisely what is expected for a stellar collapse. The proximity in time to the visual observation of SN 1987A, the difficulty in finding an alternative interpretation of the short burst of events in the observed low-energy range, and the approximate time coincidence for observations in several detectors, make it most plausible to attribute these events to neutrinos originating in a stellar collapse. In the following we show how the number of species of neutrinos N_ν can be derived from this information. We first briefly discuss the mechanism leading to stellar collapse.

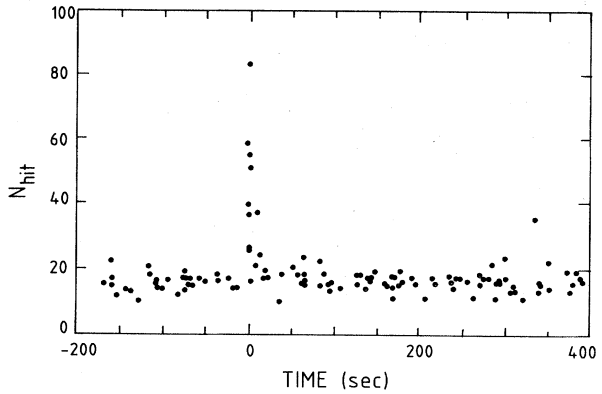

FIG. 1. Neutrino burst from SN 1987A observed in the Kamiokande II detector on February 23. The vertical axis is a measure of recoil electron energy in terms of the number of photomultipliers hit ($E_{el} \sim 10$ MeV corresponds to $N_{hit} \sim 25$), from Hirata *et al.* (1987).

TABLE I. (a) Measured properties of the 12 electron events detected in the neutrino burst, from Hirata *et al.* (1987). The electron angle is relative to the direction of SN 1987A. (b) Characteristics of the contained neutrino events recorded on 23 February 1987 by the IMB collaboration, from Bionta *et al.* (1987).

(a)

Event number	Event time (s)	Number of PMT's (N_{hits})	Electron energy (MeV)	Electron angle (deg)
1	0	58	20.0±2.9	18±18
2	0.107	36	13.5±3.2	15±27
3	0.303	25	7.5±2.0	108±32
4	0.324	26	9.2±2.7	70±30
5	0.507	39	12.8±2.9	135±23
6	0.686	16	6.3±1.7	68±77
7	1.541	83	35.4±8.0	32±16
8	1.728	54	21.0±4.2	30±18
9	1.915	51	19.8±3.2	38±22
10	9.219	21	8.6±2.7	122±30
11	10.433	37	13.0±2.6	49±26
12	12.439	24	8.9±1.9	91±39

(b)

Event number	Time (UT)	No. of PMT's	Energy (MeV)	Electron angle (deg)
33 162	7:35:41.37	47	38	74
33 164	7:35:41.79	61	37	52
33 167	7:35:42.02	49	40	56
33 168	7:35:42.52	60	35	63
33 170	7:35:42.94	52	29	40
33 173	7:35:44.06	61	37	52
33 179	7:35:46.38	44	20	39
33 184	7:35:46.96	45	24	102

A. Star evolution until collapse

A supernova explosion corresponds to the ultimate phase of stellar evolution. A massive star ($>8M_\odot$) evolves with time following the now well-known scenario (see, for instance, Harrison *et al.*, 1965; Clayton, 1968; and Arnett, 1973; for a review article on supernovae, see Trimble, 1982, 1983).

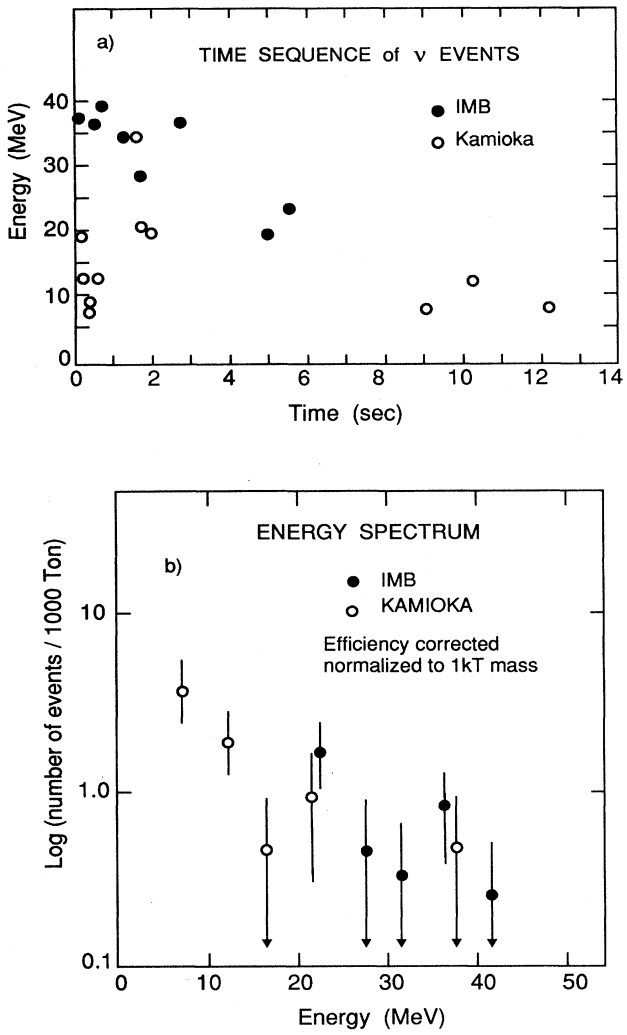

FIG. 2. Comparison of the IBM and Kamiokande neutrino events (Haines, 1987): (a) correlation between the energy and the time of arrival; (b) energy spectrum after efficiency corrections.

(1) At the beginning, a cloud of gas (mostly hydrogen) contracts under gravitation and radiation losses (infrared protostar stage). The central temperature increases until the onset of thermonuclear fusion, where ultimately four hydrogen nuclei fuse into helium:

$$4p+2e^-\rightarrow{}^4\mathrm{He}+2\nu_e \ .$$

(2) The star reaches a steady state (main sequence phase) when the heat produced by the thermonuclear fusion of hydrogen in the center of the start compensates for the radiation losses at the surface. At the center, an ^{4}He core gradually develops. Higher Z elements cannot yet be synthesized, owing to Coulomb barriers which cannot yet be overcome.

(3) The ^{4}He core becomes more massive while the thermonuclear reactions with ^{4}He are not yet effective in the core; at a certain moment, the helium core can no longer sustain the gravitational implosive pressure. This is the first collapse, which takes place less than 10^8 years after the formation of the star, for stars more massive than $8M_\odot$. The temperature of the collapsing He core increases abruptly, allowing the onset of ^{4}He burning into C nuclei.

(4) The He burning lasts for less than 10^6 years. Subsequent collapses will then take place, allowing C, N, O, and ultimately Si burning, giving an onion-shell structure to the star. As Fe is the nucleus with the highest binding energy, this sequence of fusion reactions must end with the development of an iron core at the center of the star. This growing iron core is responsible for the inevitable ultimate collapse of the star. Since all fusion reactions involving iron are endothermic, there are no more thermonuclear reactions that could provide energy to resist the collapse of the iron core. It will then give birth to a new state of matter, either a neutron star or a black hole.

B. Ultimate collapse of the iron core

The iron core collapses when the degenerate electron-gas pressure can no longer sustain the gravitational pressure, that is, when its mass reaches the Chandrasekhar limit (Chandrasekhar, 1957). Let us recall the basic mechanism.

The density of the iron core before collapse is $\rho\approx 4\times 10^9$ g/cm^3, and the radius is $R\approx 500$ km. The gas is an almost relativistic gas of degenerate Fermi-Dirac electrons, and the pressure is dominated by the degeneracy. In this case the pressure p is not temperature dependent and is given as a function of the matter density ρ by

$$p=K\rho^\gamma \ ,$$

with $\gamma=\frac{5}{3}$ for a nonrelativistic, degenerate gas, while $\gamma=\frac{4}{3}$ for a relativistic degenerate one. The proportionality constant K is a function of fundamental constants and is numerically equal to (with p in dyn/cm^2 and ρ in g/cm^3)

$$K=1.0\times 10^{13}/(A/Z)^{5/3}$$

in the nonrelativistic case, while it is

$$K=1.24\times 10^{15}/(A/Z)^{4/3}$$

in the relativistic case. Here $Z/A=e/(n+p)$ is the ratio of number densities for electrons and nucleons in the core. In the stellar core, we then have

$$\gamma=4/3+\varepsilon/3, \quad \text{with } 0<\varepsilon<1 \ .$$

In terms of the mass M and radius R of the core, the restoring forces due to this pressure are then

$$F_p=\frac{dp}{dR}\approx KM^{5/3}/R^6$$

and

$$F_p\approx KM^{4/3}/R^5$$

in the nonrelativistic and relativistic cases, respectively, while the implosive force due to gravity is

$$F_g \approx G_N M^2/R^5$$

($F \approx G_N \rho M/R^2$, with $\rho \approx M/R^3$), where G_N is the gravitational constant. Thus, in the nonrelativistic case, the restoring force due to pressure and the gravitational force have a different power-law variation with radius. The star can therefore adjust its radius to bring the two forces into equilibrium. However, as the mass of the iron core increases, the radius decreases, until the electron Fermi temperature T_F reaches the relativistic regime ($T_F > m_e$). In this case the two forces depend on the same power of the radius, but not on the same power of the mass. For large masses the gravity force F_g exceeds the restoring force F_p from the pressure; the core radius decreases, and eventually the core collapses. The limiting mass is the Chandrasekhar mass $M_{\rm Ch}$, for which the two forces balance. It can be shown that (Chandrasekhar, 1939; Hillebrandt, 1987)

$$M_{\rm Ch} = 5.7(Z/A)^2 M_\odot \sim 1.4 M_\odot \ .$$

For core masses M smaller than $M_{\rm Ch}$, the star expands until the density decreases enough for the outer parts to become nonrelativistic and to reach equilibrium.

As a massive iron core starts to collapse, the density and temperature increase and very soon a new phenomenon takes place—electron capture by nuclei:

$$\mathrm{Fe} + e^- \rightarrow \mathrm{Co} + \nu_e \ ;$$

more generally,

$$p + e^- \rightarrow n + \nu_e \ .$$

This leads to a sharp drop in the electron pressure, and the star collapses in almost free fall until the core reaches a new state of matter. This is associated with the type-II supernova explosion, with a shock wave and neutrino emission (see, for instance, Arnett, 1973; Baym and Pethick, 1975; Irvine, 1978; Weaver and Woosley, 1980; Trimble, 1982, 1983; Bethe and Browne, 1985; and Burrows, 1987a, 1987b).

C. Energy released by the ultimate collapse of a star

1. Neutron-star final state

For stars with a mass below $8M_\odot$, the above mechanism does out occur because the star never develops a massive enough iron core. For stars with a mass between $8M_\odot$ and $50M_\odot$, the predictions are that about $1.4M_\odot$ of iron collapses to form a neutron star (all electrons and protons have combined to give neutrons and escaping neutrinos) of roughly the same mass. However, due to possible rotation, convection, or accretion, the predictions of the mass ranges involved extend from $1.2M_\odot$ and $1.8M_\odot$.

The density, temperature, and radius of neutron stars can be predicted from the equation of state of nuclear matter. Various computations have been made (Pandharipande, 1971; Malone *et al.*, 1975). They all converge towards nearly the same values: $\rho \approx 3\times10^{14}$ g/cm^3, $T \approx 10$ MeV, and $R \approx 10$ km. The energy that is expected to be released in the collapse is related directly to the difference of gravitational binding energies between the initial and final states:

$$\Delta E \approx G_N M^2 (1/R_{\text{neutron star}} - 1/R_{\text{iron core}})$$
$$\approx G_N M^2/R_{\text{neutron star}} \ .$$

The predicted values for the daughter neutron-star binding energies extend from 1.5×10^{53} to 4×10^{53} ergs for masses varying from $1.2M_\odot$ to $1.8M_\odot$ and the acceptable equations of state.

The masses of a few neutron stars—members of binary systems—have been measured experimentally. The results are shown in Fig. 3 (Trimble, 1987). The range of observed masses is indeed in agreement with these theoretical expectations. Supporting evidence for this picture is also provided by the gravitational redshift. The surface gravitational redshift is proportional to $\Delta\lambda/\lambda \sim G_N M/R$ and is predicted to be 0.25 ± 0.1, which is in good agreement with available experimental measurements (Fujimoto and Taam, 1986; Schaeffer *et al.*, 1987). Furthermore, by measuring the rate at which the rotation of a neutron star slows down, and by taking into account the total radiated energy, it is also possible to derive the moment of inertia of such an object. This has been done for the remnant neutron star of the Crab nebula; again, the result agrees fairly well with expectations (Schaeffer, 1984). Thus all experimental data now available agree with the expectations from this neutron-star-formation scenario.

2. Black-hole formation

For very massive stars ($> 50M_\odot$), one expects the collapse to end with the formation of a black hole (Woosley

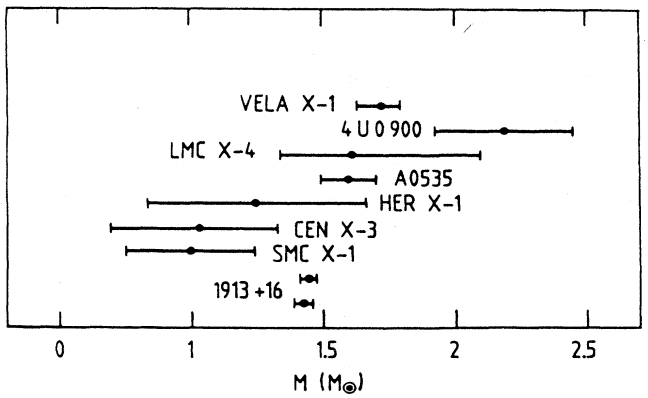

FIG. 3. Masses for the few neutron stars that have been measured (Trimble, 1987).

et al., 1986, and references therein). Would this mean an energy release much superior to the one resulting from neutron-star formation? Computations given in Woosley *et al.* (1986) indicate that this is not the case, unless we are dealing with ultramassive stars ($>150M_\odot$). In the $50M_\odot$ to $150M_\odot$ range, however, the energy released is expected to be in the range 3×10^{53} to 4×10^{53} ergs. Above $150M_\odot$, there is a dramatic increase. But the possibility of a $150M_\odot$ progenitor—which from general arguments is unlikely—has been excluded for SN 1987A, from the type of progenitor, from the analysis of the light curve, and from the neutrino pulse duration (Burrows, 1987a, 1987b; Mayle and Wilson, 1987; Woosley, 1987).

In conclusion, the total energy release in the ultimate collapse of the core of a star of $8M_\odot$ to $150M_\odot$ (!) ranges from 1.5×10^{53} to 4×10^{53} ergs.

D. Neutrino emission

The gravitational binding energy that is released in the collapse of the stellar core is considerably larger than the (more easily measured) energy that is released in the form of electromagnetic radiation and as kinetic energy of the expelled layers of matter (10^{50} to 10^{51} ergs), and larger than the energy carried away by neutrinos during the initial neutronization phase $p+e^-\rightarrow n+\nu_e$. For a $1.5M_\odot$ neutron star, for example, neutronization is expected to take place within the first 100 ms of the collapse and to release $\approx10^{52}$ ergs in the form of ν_e's of ~8 MeV average energy (Burrows, 1987a, 1987b). This is still an order of magnitude smaller than the neutron-star binding energy ΔE.

According to conventional neutron-star-formation theory, most of this energy is expected to be evacuated in a few seconds (80% in the first 10 s, according to Burrows, 1984) in the form of neutrinos and antineutrinos of all species, maintained in thermal equilibrium (equipartition of energy) through neutral-current interactions $e^+e^-\leftrightarrow\nu_i\bar{\nu}_i$ at temperatures ~3 to 6 MeV (the average energy of neutrinos is ≈3.15 times the temperature for a Fermi-Dirac gas and is thus in the 10 to 15 MeV range). These are the surface temperatures for neutrinos escaping from the neutrinosphere, and they are expected to be smaller than the 20–70 MeV central temperature. The temperatures of ν_μ and ν_τ are expected to be slightly larger than those of $\bar{\nu}_e$ and ν_e, as the latter ones can interact through charged currents, in addition to neutral currents, and are thus more efficiently cooled down by outer core layers. However, the energy fluxes, which depend on both the temperatures and the radii of the neutrinospheres, are the same for all neutrinos, owing to the equipartition principle. All species of neutrinos means here species for which the mass is much smaller than the temperature, i.e., less than, or of the order of, 1 MeV.

E. Energy release in the case of supernova 1987A

The progenitor, which has been identified finally as Sanduleak-69202 (after some hesitation), was a blue star.

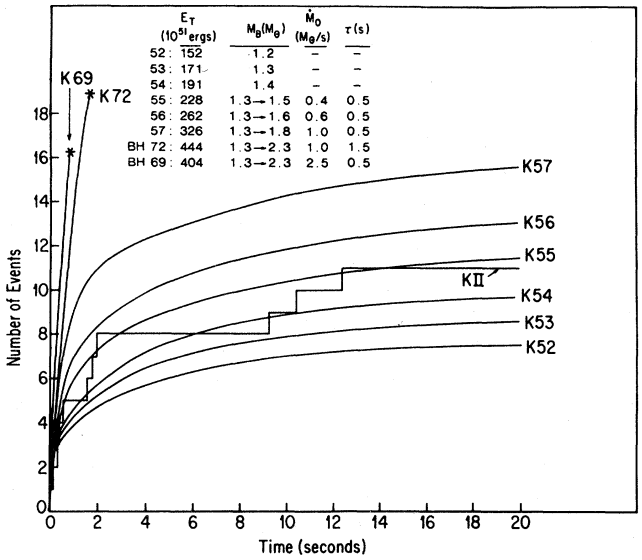

FIG. 4. Integrated distribution of the detected neutrino events of Kamiokande. The various curves correspond to the models computed by Burrows (1988) and described in the inset. In particular, K54 refers to a model with no accretion and $1.4M_\odot$. K55 involves accretion bringing the mass of the core from $1.3M_\odot$ initially to $1.5M_\odot$. Note that the black-hole models (K69, K72) are in clear contradiction with the data.

The analysis of the light curves (Woosley, 1987) is consistent with the explosion of a star that on the main sequence, had a mass of $(19\pm3)M_\odot$ and that, according to Burrows (1987a, 1987b) and Mayle and Wilson (1987), would give birth to a $(1.45\pm0.1M_\odot$ neutron star. Furthermore, the integrated time distribution of the detected neutrino events shown in Fig. 4 is in excellent agreement with the predictions (Burrows, 1984, 1987a, 1987b) for a $1.4M_\odot$ neutron star formation and is in disagreement with black-hole formation ($>1.8M_\odot$). The total length of the pulse is ~13 s. Black-hole formation would lead to much shorter pulses (<2 s) in Fig. 4, since only the prompt neutrino signal would be seen.

In conclusion, the range for the total gravitational energy release ΔE, consistent with all observations until now, is $\Delta E=(1.5-3.5)\times10^{53}$ ergs. This range does not cover all possible published values, but there seems to be a consensus among nuclear astrophysicists that it indeed covers all "reasonable models" without exotic equations of state (Schaeffer *et al.*, 1987). As explained in the Appendix, we shall assume that this range represents a $\pm2\sigma$ interval, and in the subsequent fit we shall take $\Delta E=(2.5\pm0.5)\times10^{53}$ ergs.

F. Energy carried by $\bar{\nu}_e$'s and the number of neutrino families

1. Neutrino detection

The Kamiokande and IMB detectors are sensitive to electrons and positrons through Čerenkov light emission.

The $e^{\pm}$ detection threshold is, however, lower for the Kamiokande experiment ($\sim$7.5 MeV) than for the IMB experiment ($\sim$18 MeV).

As already stated, the initial neutronization ν_e's are expected to give a negligible contribution to the detected signal. For the main (thermalization) neutrino pulse, the dominant contribution to the signal in these detectors should come from the inelastic reaction $\bar{\nu}_e p \rightarrow n e^+$, whose rate is expected to be at least an order of magnitude larger than the rate of elastic scattering of ν_e ($\bar{\nu}_e$) on electrons. This can be seen from Fig. 5, which shows the cross sections as a function of the neutrino energy for various reactions to which the detectors are sensitive, together with the expected flux of neutrinos and antineutrinos. The temperatures of ν_μ and ν_τ are expected to be somewhat larger than those of $\bar{\nu}_e$ and ν_e, as explained above, but their energy fluxes are the same owing to the equipartition principle. From Fig. 5 then, for the neutrinos emitted at the thermalization stage, the total elastic-scattering rate on electrons for all species of neutrinos amounts to $\sim$10% of the total interaction rate. However, this elastic-scattering contribution should represent a smaller-yet fraction of the detected events, since in the elastic scattering the recoil electron has an approximately flat energy distribution (from zero to the incident neutrino energy), and has thus a much reduced triggering probability, while in the inelastic scattering of $\bar{\nu}_e$ on protons, $\bar{\nu}_e p \rightarrow n e^+$, the positron carries the entire energy of the incident antineutrino, diminished by the reaction threshold (1.3 MeV). Thus in a first approximation the contribution from the elastic scattering of neutrinos on electrons can also be ignored in the detected signal. Background events (radioactivity, noise, etc.) in the first 13 seconds amount to 0.2 events in Kamiokande and 0.8 events in IMB (Bionta *et al.*, 1987; Hirata *et al.*, 1987) and can also be neglected.

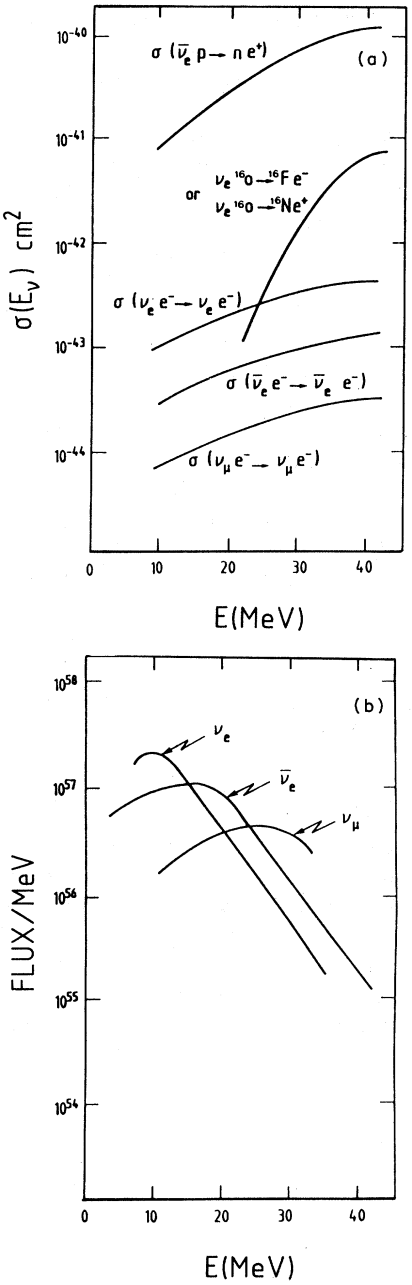

FIG. 5. Energy dependence of (a) cross sections for ν ($\bar{\nu}$) induced reactions; (b) expected ν ($\bar{\nu}$) fluxes.

Additional information could, in principle, be gained from the angular distribution of the events. In the elastic scattering of neutrinos on electrons, the recoil electron is strongly correlated with the incident neutrino direction ($\cos\theta > 0.85$), thus giving an indication of the direction of the source. For antineutrino absorption on protons, on the other hand, the positrons are almost isotropically distributed. The data, shown in Fig. 6, exhibit an excess of events in the forward direction, which is at the limit of statistics ($\sim$5% confidence level) and is mainly present in the IMB data. Two authors (van der Velde, 1988; LoSecco, 1989) have recently suggested that the effect is real and have attributed it to the combined effect of elastic scattering of all neutrino species on electrons and to some exotic new particles. Their proposals, however, are not very convincing.

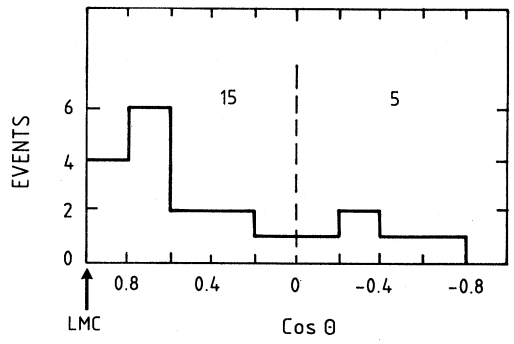

FIG. 6. Angular distribution of observed neutrino events as measured by the electron angle, the forward direction being away from the LMC.

2. $\bar{\nu}_e$ luminosity of supernova 1987A

Assuming, therefore, that the detected events are due to $\bar{\nu}_e$ interactions ($\bar{\nu}_e p \rightarrow n e^+$), the luminosity in $\bar{\nu}_e$ of SN 1987A can then be derived from a maximum-likelihood adjustment of a few parameters on the collected data.

(1) The number density of $\bar{\nu}_e$ is assumed to have a Fermi-Dirac thermal spectrum

$$n(E)dE = NE^2 dE/[\exp(E/kT)+1] ,$$

where E is the neutrino energy, k is the Boltzmann constant, and T is the emission temperature and is here a free parameter. The relation between the average energy and temperature in a Fermi-Dirac gas is given by

$$\langle E \rangle = 3.15kT \quad (kT \text{ in MeV}) .$$

(2) The temperature T might decrease as a function of time during neutrino emission:

$$T = T_0 \exp(-t/\tau) ,$$

where τ is a characteristic neutrinosphere cooling time and a second free parameter.

(3) Finally, the overall normalization N, related to the total number of events, can be adjusted and translated into a third parameter, the most relevant one for this study, i.e., the total $\bar{\nu}_e$ luminosity $L(\bar{\nu}_e)$.

Many such computations have been performed by various authors (Burrows, 1987a, 1987b; Ellis and Olive, 1987; Krauss, 1987; Lamb *et al.*, 1987; Schaeffer *et al.*, 1987; Schramm, 1987; Spergel *et al.*, 1987; Piran and Spergel, 1988). The results are shown in Table II. They cluster around $L(\bar{\nu}_e) \approx 6.0 \times 10^{52}$ ergs for a source distant 49 ± 5 kpc. This number has to be (1) increased by $\approx 10\%$ for the energy dissipated after the first 13 s and the energy that is lost below the threshold of the detectors, (2) decreased by about 5% for possible background events in the data, and (3) decreased by a further 5% for the elastic-scattering contribution. This leads to

$$L(\bar{\nu}_e) = (6.0 \pm 1.8) \times 10^{52} (D/49 \text{ kpc})^2 \text{ ergs} ,$$

where D is the distance from SN 1987A in the LMC to Earth.

One should note that the fit is applied to the high-energy tail of the neutrino energy spectrum (which might not be monothermal; Schramm, 1987), especially for the IMB experiment, so that the energy might be underestimated. In that sense, the Kamiokande data are more reliable, as they have a lower electron energy detection threshold (with the above assumptions $E_\nu = E_e + 1.3$ MeV), and these data favor somewhat lower neutrino temperatures and higher luminosities (Schramm, 1987). It is worth mentioning that in all these calculations the $e^\pm$ triggering efficiency, the detection threshold effects, the electron energy reconstruction, and the energy resolution of detectors are taken into account by simple analytical formulas. It would certainly be worthwhile to include in the maximum likelihood a full Monte Carlo simulation of the experiments (apparatus response near detection threshold) in order to deal with these instrumental effects properly and to get the final numerical answer.

It should be said that similar calculations have also been performed for the five events detected by the Baksan scintillator detector (Pomanski, 1987). They lead to an even higher luminosity: $L(\bar{\nu}_e) = (17 \pm 8) \times 10^{52}$ ergs (Alexeyev *et al.*, 1988). The Mont Blanc signal (Aglietta *et al.*, 1987) cannot be included in this analysis, since it occurred about 4.7 hours earlier than the other detected signals and, if real, would thus correspond to a different physics content (De Rújula, 1987). Furthermore, it would probably cast doubt upon the overall understanding of the mechanism of supernova explosions, and our analysis then would not be justified. It is nonetheless true that the Kamiokande and IMB bursts agree very well with the standard scenario of stellar collapse adopted by us in this analysis. A discussion of the mutual compatibility of the various observations is given by Schramm (1988).

TABLE II. Compilation of neutrino luminosities $L(\bar{\nu}_e)$ for SN 1987A obtained by various authors, in units of 10^{52} ergs.

Krauss (1987)	5 within a factor 2
Schaeffer *et al.* (1987)	8±2.5
Ellis and Olive (1987)	6.6 within a factor 2
Schramm (1987, 1988)	4.5±1.5
Lamb *et al.* (1987)	6.6 within a factor 3
Burrows (1987a, 1987b)	4 within a factor 1.3
Piran and Spergel (1988)	5.9±1.8
Spergel *et al.* (1987)	6.1±1.8

G. Conclusions on the number of neutrino species from supernova 1987A

There is a good general agreement between theoretical expectations and observations regarding the neutrino physics of SN 1987A. The energy spectrum and the time distribution of events are in excellent agreement with expectations. We can thus rely on the theory to predict the total number of species of light neutrinos ($M_\nu \lesssim 1$ MeV). The prediction is that the total gravitational energy release is shared equally by all neutrino species. The number of families is then derived directly from the ratio of the total expected luminosity ΔE to the one observed in $\bar{\nu}_e$:

$$\Delta E \approx 2 N_\nu L(\bar{\nu}_e) .$$

The factor 2 takes into account the presence of particles and antiparticles.

Starting from

$$\Delta E = (2.5 \pm 0.5) \times 10^{53} \text{ ergs} ,$$

$$D = 49 \pm 5 \text{ pc} ,$$

and

$$L(\bar{\nu}_e)=(6\pm1.8)\times10^{52}\left[\frac{D}{49\text{ kpc}}\right]^2,$$

we obtain

$$N_\nu=2^{+1.1\,+1}_{-0.4\,-0.8},$$

where the second errors correspond to the systematic uncertainty on the total luminosity ($1.5\times10^{53}<\Delta E<3.5\times10^{53}$ ergs). If we consider this error as Gaussian with a rms of 0.5×10^{53} ergs (so that the above interval corresponds to $\pm2\sigma$), then using the χ^2 minimization described in the Appendix, the combined fit leads to

$$N_\nu=2^{+1.4}_{-0.7},$$

with $N_\nu<3.9$ (4.8) at the 90% (95%) confidence level. These central values and limits on N_ν apply only to neutrinos with masses much less than ~1 MeV.

H. Future prospects for supernova detection

It is worth mentioning again that SN 1987A in the LMC occurred at a distance of ~49 kpc and resulted in the observation of ~20 events worldwide. A stellar collapse occurring within our galaxy (thus at <10 kpc) would produce $\gtrsim25$ times as many events in detectors of the same sensitivity. With samples of ~500 events, the elastic neutrino interactions on electrons should be observable (at the few % level), with their characteristic directionality. We note also that $\sim50\%$ of these directional (elastic) events should be due to ν_μ ($\bar{\nu}_\mu$), ν_τ ($\bar{\nu}_\tau$), and therefore have a higher average energy (Fig. 5).

Larger and more sensitive volume detectors are now being considered. The Super-Kamiokande project, for example, with ~32 ktons of water in the active part of the detector (as compared to ~2.1 ktons in the present one), is expected to yield ~4000 detectable neutrino events for a supernova explosion in the region of the galactic center. Clearly, once the high statistics from the SLC and LEP experiments definitively determine the number of neutrino species, such observations would powerfully constrain the models of stellar collapse.

III. NUMBER OF NEUTRINO SPECIES FROM THE PRIMORDIAL NUCLEOSYNTHESIS

A. Principle of the method

There is now a wide consensus that our universe originated in a Big Bang. The three major facts behind that belief are the following (see, for example, Weinberg, 1972).

(1) The observed galaxy recession indicates that the universe is not static (which agrees with general relativity) and that it is expanding. This implies that at earlier times it had a higher temperature.

(2) This means that, at earlier times, fusion reactions could have occurred (Gamow, 1946, 1948) and formed ^{4}He, ^{3}He, D, and ^{7}Li. This is usually referred to as the primordial nucleosynthesis. The primordial abundances deduced from present observations are, at least to the first order, in agreement with this model, and, in particular, it is unlikely that the amount of ^{4}He that is observed could have been made in stars.

(3) The blackbody radiation from this hot epoch is expected to have survived until today (Gamow, 1946, 1948) and is indeed observed as a universal microwave background of temperature 2.7 K (Penzias and Wilson, 1965). For a recent review see, for instance, Wilkinson (1987).

The constraints provided by cosmology on the number of light neutrino families are based on the primordial nucleosynthesis in the early universe. The greater the number of relativistic degrees of freedom at the times of decoupling of proton and neutron weak interactions (at a temperature of about 0.75 MeV), the faster the universe's expansion, the higher the decoupling temperature, the higher the number of neutrons (that are less depressed by the Boltzmann factor), and thus the larger the primordial abundance of helium. The exact amount depends on the ratio η of the number of nucleons to the number of photons in the universe, which in turn can be determined by the observed amount of D, ^{3}He, and ^{7}Li. This method has been discussed extensively by many authors (Olive, Schramm, *et al.*, 1981; Olive, Schramm, and Steigman, 1981; Yang *et al.*, 1984; Boesgaard and Steigman, 1985; Ellis *et al.*, 1986; Steigman, 1987), and our task will be mainly to summarize the observations and update the estimate of the number of neutrino species.

B. Summary of the standard cosmology model

Before we go into the detailed predictions, let us summarize the classical results of cosmology (see, for instance, Weinberg, 1972).

1. Expansion of the universe

If the universe is homogeneous and isotropic on a scale large enough—as it appears to be—it can be characterized simply by a scale parameter $a(t)$ [often also written as $R(t)$; this notation has the drawback of leading to the wrong interpretation of $R(t)$ as a "radius" of the universe]. The physical coordinate x of a galaxy at rest with respect to the expansion is given at time t by

$$x=a(t)r,$$

where r is the fixed comoving coordinate. The rate of expansion is given by the Hubble "constant"

$$H=\frac{1}{a}\frac{da}{dt}.$$

Experimentally, we find that the universe is expanding and that light from distant galaxies is redshifted. If we define the redshift as

$$z=\frac{\Delta\lambda}{\lambda} ,$$

it can easily be shown to be given, for an object at rest with respect to the Hubble flow, by the ratio of the scale parameter at the present time ($t=t_0$) to the value at the time of emission ($t=t_1$)

$$1+z=\frac{a(t_0)}{a(t_1)} .$$

At a very large scale, our universe can be considered as a spatially homogeneous and isotropic space; its metric is the Robertson-Walker metric:

$$ds^2=dt^2-a^2(t)\left[\frac{dr^2}{1-kr^2}+r^2d\theta^2+r^2\sin^2\theta\, d\varphi^2\right] ,$$

where k is a constant that can be set to 0 or ±1 by proper choice of the units and is related to the space curvature.

The theory of general relativity then allows us to relate the Hubble constant to the average energy density ρ of the universe by the so-called Friedman equation:

$$H^2=\frac{8\pi G_N}{3}\rho-\frac{k}{a^2}+\frac{\Lambda}{3} .$$

This equation, which can also be derived (except for the cosmological constant Λ) in Newtonian mechanics, expresses the balance of the kinetic energy given by H^2 and the potential energy (proportional to ρ). The constant k arises then as an integration constant.

Let us discuss first the case in which Λ is zero. It is obvious that if $k=0$ the density is

$$\rho_c=\frac{3H^2}{8\pi G_N} ,$$

the so-called critical density. Since ρ_c is positive, the expansion rate cannot go through zero and the universe is always expanding. If we define

$$\Omega=\frac{\rho}{\rho_c} ,$$

then $\Omega=1$, and the universe is spatially flat (but curved in space-time). On the other hand, if $k>0$, that is, if $\Omega>1$, then the expansion rate can go through zero and the universe will recollapse. This corresponds to a closed universe, which is spatially isometric to a 3-sphere. If $k<0$, which corresponds to $\Omega<1$, then the universe is open and will expand forever.

The additional term Λ is called the cosmological constant. It arises naturally in many particle-physics models (but with rather larger values) and, when it is positive, can be interpreted as the energy density of vacuum (but with negative pressure). The present value of Ω can be determined by weighing galaxies, by measuring their peculiar velocities, or by attempting to measure the spatial curvature directly. The current consensus is that the value of Ω today is $0.1\le\Omega_0\le2$. (For references and a recent summary for particle physicists, see Sadoulet, 1988.)

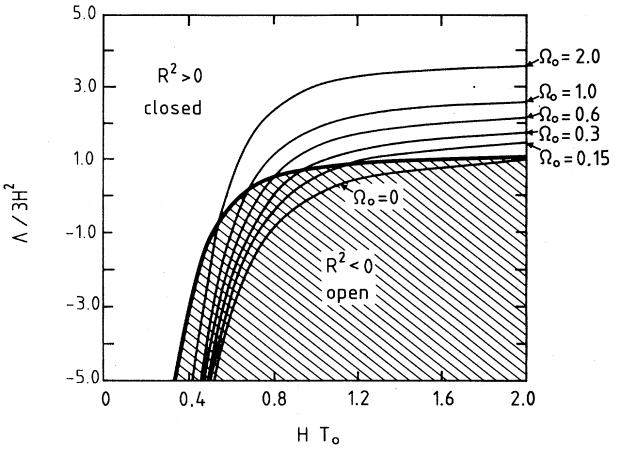

FIG. 7. Relation between the cosmological constant Λ, the Hubble constant H, and the age of the universe T_0, for various values of the average density Ω_0. The regions of positive and negative curvatures are indicated.

The cosmological constant is obtained by measuring simultaneously the Hubble constant, the age of the universe, and Ω, which are related as shown in Fig. 7. Currently, the data constrain Λ to the interval

$$-1<\frac{\Lambda}{3H_0^2}<3 ,$$

where H_0 is the present value of the Hubble "constant."

The Friedman equation has to be complemented by two equations expressing the relation between the pressure and the density (equation of state) and the conservation of energy. Let us examine the evolution of the basic parameters for the case of zero cosmological constant.

In the present matter-dominated universe, the pressure is negligible ($p=0$). The conservation of energy states then that

$$\frac{d}{dt}[\rho a^3(t)]=0 .$$

The Friedman equation can then be solved. For instance, in the absence of a cosmological constant and if $k=0$,

$$a(t)\propto t^{2/3} .$$

For $t\to0$, there is an initial singularity. The Friedman equation shows that the universe cannot be static and that there has been a Big Bang. The present age T_0 of the universe is of the order of

$$T_0\approx\frac{1}{H_0}\quad(\text{e.g., } T_0=2/3H_0 \text{ for } \Lambda=0 \text{ and } k=0) .$$

Unless Ω is equal to 1, it evolves very rapidly. For $\Lambda=0$, it can be shown that during this matter-dominated period

$$1-\Omega(z)^{-1}=\frac{1-\Omega_0^{-1}}{1+z} , \tag{3.1}$$

where $\Omega(z)$ is the value of Ω at redshift z, and Ω_0 is the

value of Ω today.

During the matter-dominated epoch, the background photon (and neutrino) energies and temperatures evolve as $1/a(t)$ and their energy densities as $a(t)^{-4}$. Therefore at sufficiently early times ($z \gtrsim 3\times 10^4$), the energy density of the universe becomes radiation dominated. It is easy to show that given the above-quoted experimental range for Ω_0 and Λ, the spatial curvature term and the cosmological term are negligible in the radiation-dominated period. For instance, in the case of null cosmological constant, Eq. (3.1) shows that even at the end of the radiation-dominated era, Ω is equal to 1 within 3×10^{-4}. For a relativistic fluid

$$p=\frac{\rho}{3} ,$$

the conservation of energy leads to

$$\rho \propto a(t)^{-4} ,$$

and the combination of the Friedman equation and thermal equilibrium gives a temperature

$$T^{-1} \propto a(t) \propto (\mathrm{NDF})^{1/4} t^{1/2} ,$$

where NDF is the effective number of relativistic degrees of freedom, i.e., the sum of the number of boson states and of $\frac{7}{8}$ of the number of fermion states (see, for instance, Weinberg, 1972). The time is related to the temperature by

$$t \sim 2.4(\mathrm{NDF})^{-1/2} \left[\frac{1\ \mathrm{MeV}}{kT}\right]^2 \mathrm{s} .$$

The important point of the equation above is that the evolution speed depends on the number of degrees of freedom: the larger it is, the faster $a(t)$ grows. This is the basis for the constraints on the number of neutrino species provided by primordial nucleosynthesis.

2. Thermal equilibrium and decoupling

During early times, all interacting species i, j, l, and m are in thermodynamic equilibrium through reactions of the type

$$ij \leftrightarrow lm ;$$

this goes on as long as the mean collision time is much less than the expansion time $1/H$. When the collision time becomes too large, the species involved decouple and their abundance is frozen out. Quantitatively (see, e.g., Barrow, 1983), if n_i is the density of particles of a given species i, the evolution of this species is given by

$$\frac{dn_i}{dt} = -3n_i \frac{da/dt}{a(t)} - \langle \sigma_{ij\to lm} v \rangle n_i n_j + \langle \sigma_{lm\to ij} v \rangle n_l n_m , \quad (3.2)$$

where the σv terms are the thermally averaged reaction rates in both directions. The first term on the right-hand side accounts for the dilution due to the expansion. The second term accounts for the disappearance of the species i, and the third term for its production. Detailed balance relates the two reactions rates at temperature T:

$$\frac{\langle \sigma_{ij\to lm} v \rangle}{\langle \sigma_{lm\to ij} v \rangle} = \frac{n_i^* n_j^*}{n_l^* n_m^*} ,$$

where the n^*'s are the *thermodynamical equilibrium* densities at the temperature (given by the Fermi-Dirac or Bose-Einstein distributions)

$$n_i^* = g_i \int \frac{4\pi q^2 dq}{h^3} \left[\exp\left[\frac{E-\mu_i}{kT}\right] \pm 1\right]^{-1} ;$$

μ_i is the chemical potential, E is the energy, g_i the number of spin states, and the integral is evaluated over the momenta q. The integral indeed gives the density because of the presence of the chemical potential μ_i, which acts as a normalization constant. The μ_i can be determined through the relation

$$\mu_i + \mu_j = \mu_l + \mu_m ,$$

which guarantees the equilibrium between the number of particles in the reaction being considered. In particular, if j is the antiparticle $\bar{i}$ of i, we have

$$\mu_i = -\mu_{\bar{i}} ,$$

since they are in equilibrium with photons (which have $\mu=0$). If there is no asymmetry between the number of particles and antiparticles,

$$\mu_i = \mu_{\bar{i}} = 0 .$$

For the more realistic case in which the difference between the number of particles and antiparticles is small compared to the number of photons ($\propto T^3$),

$$\left|\frac{\mu_i}{kT}\right| = \left|\frac{\mu_{\bar{i}}}{kT}\right| \ll 1$$

and the chemical potential can also be neglected. This is often referred to as the nondegeneracy of particle i (cf. Weinberg, 1972, p. 542).

At temperatures and densities high enough for the reaction rates to be much larger than the expansion rate, the last two terms in Eq. (3.2) are essentially equal, and the relative densities of particles are the thermodynamical equilibrium values. At the other extreme, when the last two terms are individually negligible, the particle species i is decoupled from the rest of the system and is just diluted by the expansion $n_i \propto a^{-3}$. Its density per comoving volume is frozen out. We can approximate the smooth transition between these two regimes by a sharp transition between thermodynamical equilibrium and free evolution at the "freeze-out temperature" T_f. Two cases can be singled out.

(1) If the freeze-out occurs when the particle i is still relativistic, then its subsequent abundance is proportional to the cube of the decoupling temperature:

$$n_i \propto \left[\frac{a_f}{a}\right]^3 T_f^3 .$$

(2) If the freeze-out occurs when the particle i is nonrelativistic, and if it is nondegenerate, then its subsequent abundance is determined by the Boltzmann factor at freeze-out:

$$n_i \propto \left[\frac{a_f}{a}\right]^3 \exp\left[-\frac{m_i c^2-\mu_i}{kT_f}\right]\left[\frac{m_i c^2 kT_f}{2h^2\pi}\right]^{3/2} g_i \tag{3.3}$$

(e.g., Weinberg, 1972). Such a case occurs when the cross sections are large enough for the equilibrium to be maintained until T_f is much smaller than the mass m_i. In particular, if j is the antiparticle of i, and if there is no initial asymmetry ($\mu_i=-\mu_{\bar{i}}=0$), then most of the $i\,\bar{i}$ pairs will disappear before freeze-out.

C. Primordial nucleosynthesis

After the initial suggestion of Gamow, these calculations were originally performed by Alpher and coworkers (Alpher and Herman, 1950; Alpher *et al.*, 1953) and by Wagoner (1973). Recent reviews include Boesgaard and Steigman (1984) and Matzner (1986). Let us now apply the results just discussed to the period of nucleosynthesis. At about a temperature of 10 MeV, the universe is made up of protons, neutrons, ν's, $\bar{\nu}$'s, $e^{\pm}$'s, and γ's in thermodynamic equilibrium. At about 2 MeV, light neutrinos decouple because the rate of the weak-interaction reactions,

$$\nu e \rightarrow \nu e, \quad e^+e^- \rightarrow \nu\bar{\nu} ,$$

becomes too small. But they are relativistic at that time, and their energy density continues to evolve as a^{-4} and to be important in determining the expansion rate.

At $T_f \approx 0.75$ MeV ($t\sim 1$ s), the protons and neutrons fall out of equilibrium, since the reaction rates

$$n+\nu \leftrightarrow p+e, \quad n+e^+ \leftrightarrow p+\bar{\nu}, \quad n \leftrightarrow p+e+\nu ,$$

become too small. The relative abundance is frozen out at a value that can be computed with the techniques outlined above. While in equilibrium, we have

$$\mu_n+\mu_\nu=\mu_p+\mu_{e^-} ,$$

$$\mu_\nu=-\mu_{\bar{\nu}}, \quad \mu_{e^+}=-\mu_{e^-} .$$

If, as is usually assumed, there is no strong initial asymmetry between e^+ and e^- and between ν and $\bar{\nu}$, we have

$$\mu_\nu \approx \mu_{e^-} \approx 0$$

and

$$\mu_p \approx \mu_n .$$

Then, since $m_p \approx m_n$, we have, according to Eq. (3.3),

$$\frac{n}{p}=\exp\left[-\frac{\Delta m c^2}{kT_f}\right] , \tag{3.4}$$

where $\Delta m = m_n - m_p$.

The freeze-out temperature is related to the number of relativistic species

$$\mathrm{NDF}=g_\gamma+\tfrac{7}{8}(g_e+N_\nu g_\nu)=\tfrac{43}{4} \quad \text{for } N_\nu=3 ,$$

since there are two states for the photon ($g_\gamma=2$), two spin states for e^+ and e^- ($g_e=4$), and one spin state for each ν and $\bar{\nu}$ ($g_\nu=2$).

The larger the number of species is, the faster is the expansion, the earlier is the weak-interaction freeze-out, and the higher is the decoupling temperature. It can be shown (e.g., Weinberg, 1972, Eqs. 15.7.17, 15.7.18) that

$$T_f \sim (\mathrm{NDF})^{+1/6} .$$

Finally, according to Eq. (3.4), the higher the decoupling temperature, the higher the n/p ratio.

After this episode, the n/p ratio evolves slowly through the decay of the neutron:

$$n \rightarrow p+e+\bar{\nu} .$$

At $T\sim 150$ keV, the electron-positron pairs annihilate, reheating the photon bath, but not the already decoupled neutrinos.

In spite of the fact that the binding energy of nuclei such as helium is much greater than this temperature, nuclei cannot yet be formed in significant quantities. At the present density, the reactions can only occur through two-body processes;

$$p+n \rightarrow \mathrm{D}+\gamma, \quad \mathrm{D}+\mathrm{D} \rightarrow {}^3\mathrm{He}+n, \quad {}^3\mathrm{He}+\mathrm{D} \rightarrow {}^4\mathrm{He}+n ;$$

however, deuterium is too fragile and is continuously destroyed by the ambient photon flux. This mechanism is described in the same formalism as above, with the deuterium-to-nucleon ratio behaving as (cf. Weinberg, 1972, Eq. 15.7.28)

$$\frac{\mathrm{D}}{N} \sim \exp\left[-\frac{Q}{kT}\right] ,$$

where Q is the deuterium binding energy. Between 0.5 and 0.1 MeV, the D concentration, and therefore the reaction rates, are too low for higher elements to reach their thermodynamic equilibrium, too. We have to wait until the temperature falls below 100 keV (that is ~ 2 minutes after the Big Bang) for the deuterium "bottleneck" to disappear and higher Z elements to be formed. Rapidly, the elements below ^{7}Be are formed (Fig. 8). Higher Z elements are not produced in significant numbers because of the Coulomb barriers and the absence of a suitable, stable intermediate state; these elements will have to wait for fusion in stars to occur in order to be produced.

All cross sections are reasonably well known (except for some of the ^{7}Li reactions) in this energy region. Detailed calculations can be performed (Fig. 9), giving the

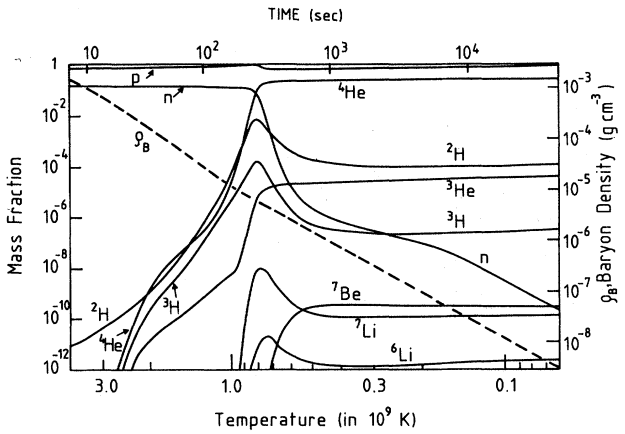

FIG. 8. Evolution with time and temperature of the primordial abundances and the baryon density ρ_B, as calculated by Wagoner (1973).

primordial abundances as a function of the ratio η of the number of protons to the number of photons (which determines the exact temperature at which deuterium begins to be formed), and giving the number of species that are relativistic at 0.75 MeV, which, as we have seen, determines the neutron-to-proton ratio at freeze-out. The higher this number is, the higher will be the amount of ^{4}He. The minimum expected in the ^{7}Li fraction as a function of η is due to the fact that a low baryon density, the interplay between the two reactions

$$^4\text{He}+^3\text{H}\rightarrow^7\text{Li}, \quad ^7\text{Li}+p\rightarrow^4\text{He}+^4\text{He},$$

leads to a decrease of ^{7}Li with increasing proton concentration, while at higher densities

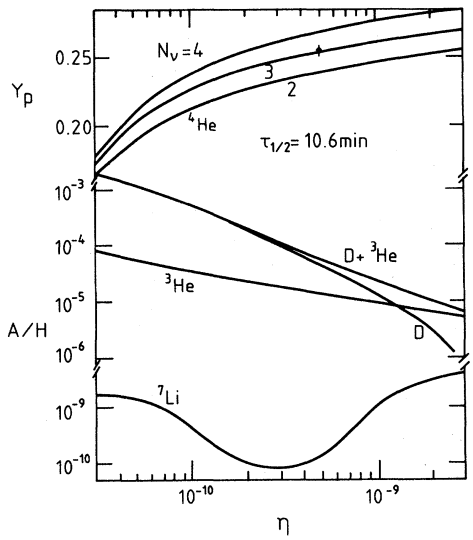

FIG. 9. Predicted abundances relative to H of ^{4}He (by mass), D, ^{3}He, and ^{7}Li (by number) as a function of η for $\tau_{1/2}=10.6$ min, as calculated by Yang *et al.* (1984). For ^{4}He, the predictions for $N_\nu=2,3,4$ are shown; the size of the error bar shows the range of Y_p that corresponds to $10.4<\tau_{1/2}<10.8$.

$$^4\text{He}+^3\text{He}\rightarrow^7\text{Be}\rightarrow^7\text{Li}$$

becomes appreciable and rises with proton concentration.

Our task then is to determine η from the measured primordial abundances of D, ^{3}He, and ^{7}Li, which are rapidly varying functions of η but which are not sensitive [at the present level of measurement accuracy (see, e.g., Matzner, 1986)] to the number of neutrinos, and to compare the predicted amount of ^{4}He for various numbers of neutrinos with the observed value.

D. Observed primordial abundances

1. Experimental difficulties

Unfortunately the measurements of primordial abundances via optical spectra are difficult because, apart from ^{4}He, the abundances are small and the signal is extremely weak, especially in absorption. It is often somewhat easier to observe the signal in emission through, for instance, recombination in ionized regions (H II regions), but the excitation mechanisms have to be estimated carefully.

Even more fundamental is the fact that it is quite difficult to ensure that it is indeed the primordial abundance that is being measured. The best candidate would be the intergalactic medium, but it is too tenuous to allow any measurement. The best approximation would be the metal-poor gas clouds, which are observed in absorption against quasars and which may not have evolved to galaxies. However, these Lyman α "forests" of absorption lines are very difficult to disentangle. Most determinations rely on the interstellar medium, which gives more intense signals, but then they have to be corrected for the chemical evolution due to processing by earlier generations of stars. This is usually done by extrapolating to zero metallicity, as "metals" (everything heavier than He) are produced mainly in stars. For rarer elements, such as ^{7}Li, only the stellar atmospheres allow positive observations; as discussed below, the question of whether it is really the primordial abundance that is being observed is even more crucial. Finally, the determinations of the solar system, from the composition of the solar wind and the spectra of planetary atmospheres or from the analysis of meteorites, are even more uncertain because of the large corrections for astration and fractionation. Table III gives a summary of the present determinations.

2. Deuterium

Deuterium is extremely fragile and is transformed into ^{3}He in stars as soon as the temperature is greater than 6×10^5 K through the reaction $p+\text{D}\rightarrow^3\text{He}+\gamma$. The more certain determinations of its abundance are those based on intergalactic and interstellar gases.

Recently, Carswell *et al.* (1986) may have observed

TABLE III. Primordial abundances.

Elements	"Intergalactic"	Interstellar optical	Interstellar radio	Stellar Atmosphere	Solar system	Results by number
D	Low metallicity Lyman-α forest but not first generation of HST	COPERNICUS H II region UV Lyman $\Delta\lambda/\lambda \cong 80$ km/s *Difficulties*: High-velocity clouds, reprocessing correction	D I line (91.6 cm) in the direction of the galactic anticenter *Difficulties*: Long excitation temperature	Unreliable	Meteorites, Solar wind, spectrum of planets *Difficulties*: Evolution, fractionation	$D/H = 10^{-5}$–(2×10^{-4})
^{3}He		*Future*: FUSE—Blue wing of ^{4}He Lyman (60 nm) $\Delta\lambda/\lambda \cong 17$ km/s	H II regions $^3He^+$ 3.46 cm	Unreliable	Solar wind, meteorites	$^3He/H = (0.5\times10^{-5})$–$10^{-4}$
^{3}He+D					Meteorites	$(^3He+D)/H = (2.5\times10^{-5})$–$10^{-4}$
^{4}He	Low metallicity Lyman α forest but not first generation of HST	H II regions in compact blue galactic (Young/low metallicity) *Difficulties*: Ionization correction factor, correction for evolution		Fit to HR plot in population-II stars, *B* stars		By mass: $Y_p = 0.235\pm0.010$ By number: $^4He/H = 0.077\pm0.003$
^{7}Li				Population-II stars $\lambda = 671$ nm *Difficulties*: Convection, population-I stars?	Solar wind, meteorites (not primordial)	$^7Li/H = (1.4\pm0.2)\times10^{-10}$ [population I $= (1.6\pm0.3)\times10^{-9}$]

deuterium in absorption against the quasar 90420-288 at the level of $(D/H)\sim 4\times 10^{-5}$. The high redshift ($z_{abs}\sim 3.08571$) and the low metallic ($\sim\frac{1}{5}$ solar) of the intervening gas suggest that this value may be close to the primordial value. We may thus infer that

$$4\times 10^{-5}\leq \left.\frac{D}{H}\right|_p \leq 10^{-4}\ .$$

Absorption lines generated by intervening gas clouds were observed in the emission spectrum of stars (Laurent *et al.*, 1979; Ferlet *et al.*, 1980; Vidal-Madjar *et al.*, 1983; York, 1983), which may be attributed to deuterium. However, the isotopic shift $\Delta\lambda/\lambda$ from the main hydrogen line is only 80 km/s and could be simulated by velocities in the observed clouds (see, e.g., Gry *et al.*, 1983). This may explain why the observed values vary widely from 5×10^{-6} to 10^{-4}. Figure 10 [from Boesgaard and Steigman (1985)] summarizes the results for the cleaner lines of sight, suggesting that the interstellar D abundance is 0.8×10^{-5}–2×10^{-5}. These numbers have to be corrected for astration, which may have depleted the amount of deuterium by a factor of 2 to 10 (Audouze and Tinsley, 1976; Clayton, 1985; Delbourgo-Salvador *et al.*, 1985). We are led to believe that

$$10^{-5}\leq \left.\frac{D}{H}\right|_p \leq 2.10^{-4}\ .$$

Blitz and Heiles (1987) have recently searched for radio emission of D at 91.6 cm in the direction of the galactic anticenter. Unfortunately, this determination is difficult to make because of both the weakness of the signal compared with terrestrial interferences and the uncertainties in the excitation mechanism. They may have detected a signal at the level of 5×10^{-5} (compatible with the above estimates). However, this signal is only marginally larger than the noise fluctuations in adjacent channels and therefore needs to be confirmed.

3. ^{3}He

Stars can either produce ^{3}He through the *pp* cycle and the destruction of D or convert it into ^{4}He (Dearborn, *et al.*, 1986). Low-mass stars are net producers, while high-mass ones destroy ^{3}He. Rood and co-workers (Rood *et al.*, 1984; Bania *et al.*, 1987) have been measuring the radio-emission line of $^3He^+$ (3.46 cm) in various H II regions. Figure 11 summarizes their result as a function of the distance to the galactic center. They observe a very large variation, from upper limits at 10^{-5} level to 1.5×10^{-4}. Even though, on the average (over the mass distribution of stars), ^{3}He is produced, the largest H II regions that they use for their observation may contain gas that has recently been reprocessed through massive stars and may thus have been depleted in ^{3}He. The allowed range is therefore quoted as

$$0.5\times 10^{-5}\leq \left.\frac{^3He}{H}\right|_p \leq 10^{-4}\ .$$

4. D+^{3}He

In order to circumvent the difficulty of the destruction of D in stars, Yang *et al.* (1984) have proposed to study the sum D+^{3}He. The observed ratio D/H represents only a fraction f of the primordial ratio

$$\frac{D}{H}=f\left.\frac{D}{H}\right|_p\ ,$$

but the destroyed D has gone into the making of ^{3}He. So the observed ratio ^{3}He is

$$\frac{^3He}{H}=(1-f)g\left.\frac{D}{H}\right|_p+g\left.\frac{^3He}{H}\right|_p+\frac{^3He_{prod}}{H}\ ,$$

where g is the fraction of ^{3}He destroyed and $^3He_{prod}$ is the produced ^{3}He. The second equation gives

$$g^{-1}\frac{^3He}{H}>(1-f)\left.\frac{D}{H}\right|_p+\left.\frac{^3He}{H}\right|_p\ .$$

Then, adding the first equation,

$$\left.\frac{D+^3He}{H}\right|_p<\left.\frac{D}{H}\right|_p+g^{-1}\frac{^3He}{H}$$

or

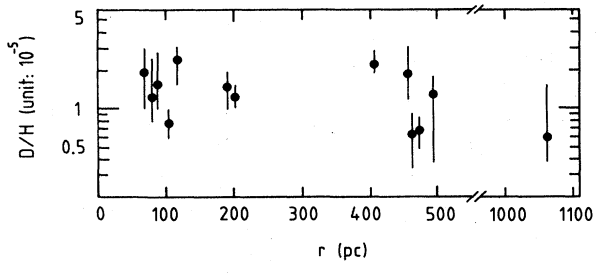

FIG. 10. Observed D/H ratios inferred for the interstellar medium toward hot stars. The distances on the x axis are uncertain, but they serve to spread out the data points (Boesgaard and Steigman, 1985).

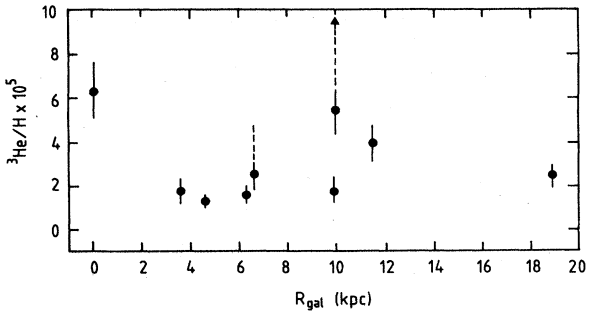

FIG. 11. Observed ^{3}He/H abundance (by number), in units of 10^{-5}, as a function of the galactic radius for each detected H II region.

$$\left.\frac{D+{}^3He}{H}\right|_p < \frac{D+{}^3He}{H} + (g^{-1}-1){}^3He/H \ .$$

It may then be safe to use the presolar observations made with meteorites (carbonaceous chondrites):

$$\left.\frac{D+{}^3He}{H}\right|_p < [4.3+1.9(g^{-1}-1)]\times 10^{-5} \ .$$

Taking $g > \frac{1}{4}$, which is usually considered to be a reasonable estimate (Dearborn *et al.*, 1986), we obtain

$$\left.\frac{D+{}^3He}{H}\right|_p \leq 10^{-4} \ .$$

5. ^{7}Li

The proportion of primordial ^{7}Li is so small that there is generally no possibility of measuring it in the intergalactic or interstellar medium. Stellar atmospheres have to be used, with all the above-mentioned dangers of destruction or production. It is, however, the use of this method that has recently led to the most striking advances being made in the field of primordial nucleosynthesis. Spite and Spite (1982) were able to measure ^{7}Li in halo dwarfs, which are very old stars of very low metallicity (i.e., population II). Their results have been confirmed and refined in the last few years by two other groups (Hobbs and Duncan, 1987; Rebolo, Molaro, and Beckman, 1988). Figure 12 summarizes the results.

(1) When plotted against the effective temperature ($T_{\rm eff} \propto$ mass) of the star [Fig. 12(a)], the ^{7}Li abundance appears to be more or less constant for temperatures above 5500 K. Below this temperature, it decreases; this effect is at least qualitatively understood (D'Antona and Mazzitelli, 1984; Brown and Schramm, 1988) as being due to the increase at low temperature of the convective layer, which drags ^{7}Li to hotter regions of the stars, where it is destroyed.

(2) For stars above 5500 K, the ^{7}Li abundance is independent of metallicity at low metallicity [Fig. 12(b)].

(3) An upper limit on ^{9}Be/H of 2.5×10^{-12} for three low-metallicity stars has been obtained by Rebolo, Molaro, Abia, and Beckman, 1988. This means that the ^{7}Li observed in these stars has not been produced by cosmic rays.

These experimental facts suggest that we do observe the primordial abundance at the level

$$\left.\frac{{}^7Li}{H}\right|_p = (1.4\pm 0.2)\times 10^{-10}$$

(combining the Rebolo *et al.*, and Hobbs and Duncan results at high $T_{\rm eff}$ and low metallicity).

However, some younger stars (population-I stars such as the Hyades) have a higher ^{7}Li concentration [Fig. 12(c); Hobbs and Pilachowski, 1986, 1988]: ^{7}Li/H $\sim(1.6\pm 0.3)\times 10^{-9}$. The ^{7}Li can indeed be formed in a red giant and in novae (Audouze *et al.*, 1983) and supernovae (Dearborn *et al.*, 1989), or it can be produced as a spallation product of cosmic-ray interactions. So, having a higher abundance is not disturbing in itself. But this fact raises the obvious question: which of the two concentrations is the primordial one? Is it not possible to imagine that population-II stars, which are 10 times older than the Hyades, have depleted an initial ^{7}Li abundance of 10^{-9} down to 10^{-10}? Several plausibility arguments favor the hypothesis that the population-II value is primordial.

(1) As emphasized, the simple behavior observed for population-II stars as a function of metallicity and temperature is at least qualitatively understood (Kawano *et al.*, 1988) and is suggestive that this is indeed the primary abundance. However, Vauclair (1988a, 1988b) has recently suggested that a mixing mechanism proposed by Zahn (1987) for rotating stars could give a depletion rate independent of the effective temperature, therefore generating a plateau such as the one observed in Fig. 12(a). The weakness of this argument is that, for this mechanism to work, all stars must have the same rotation velocities, and no good mechanism has yet been proposed for such a constancy for population-II stars.

(2) Two groups, Baade and Magain (1988) and Sahu *et al.* (1988), recently set an upper limit on the ^{7}Li abundance in the (low-metallicity) interstellar gas in the Large Magellanic Cloud using SN 1987A as a light source. Their result is compatible with the 1.4×10^{-10} determination from population-II stars and incompatible with the higher estimates. The argument would obviously be stronger if there had been a positive observation.

(3) Rebolo, Molaro, and Beckman (1988) argue that it is difficult to understand why the depletion in population-II stars at low temperature should be slower than that for the Hyades and much faster at temperatures of 6000–6300 K. However, this may be in agreement with the qualitative behavior expected with metallicity. Lower metallicity naturally leads to a shallower convection zone at a given temperature and therefore, for a given depletion, lower $T_{\rm eff}$ are necessary for population-II stars than for population-I stars. It remains to be seen if this mechanism works quantitatively.

Therefore, although arguments of simplicity favor the population-II abundance value, there is still a theoretical possibility that the population-I value is the primordial one. Answering this question unambiguously would require an understanding of the complex behavior observed in population-I stars as a function of their age and their temperature [Fig. 12(c)], including the dip at 6600 K for which several mechanisms have been proposed (Michaud *et al.*, 1984; Vauclair, 1988a, 1988b). It should also be noted that the interpretation of the population-II abundances as primordial requires that ^{7}Li be produced very rapidly at early galactic times, in order to explain a high ^{7}Li value for population-I stars of a wide range of ages. This may be compatible with a supernova origin of ^{7}Li (Dearborn *et al.*, 1989).

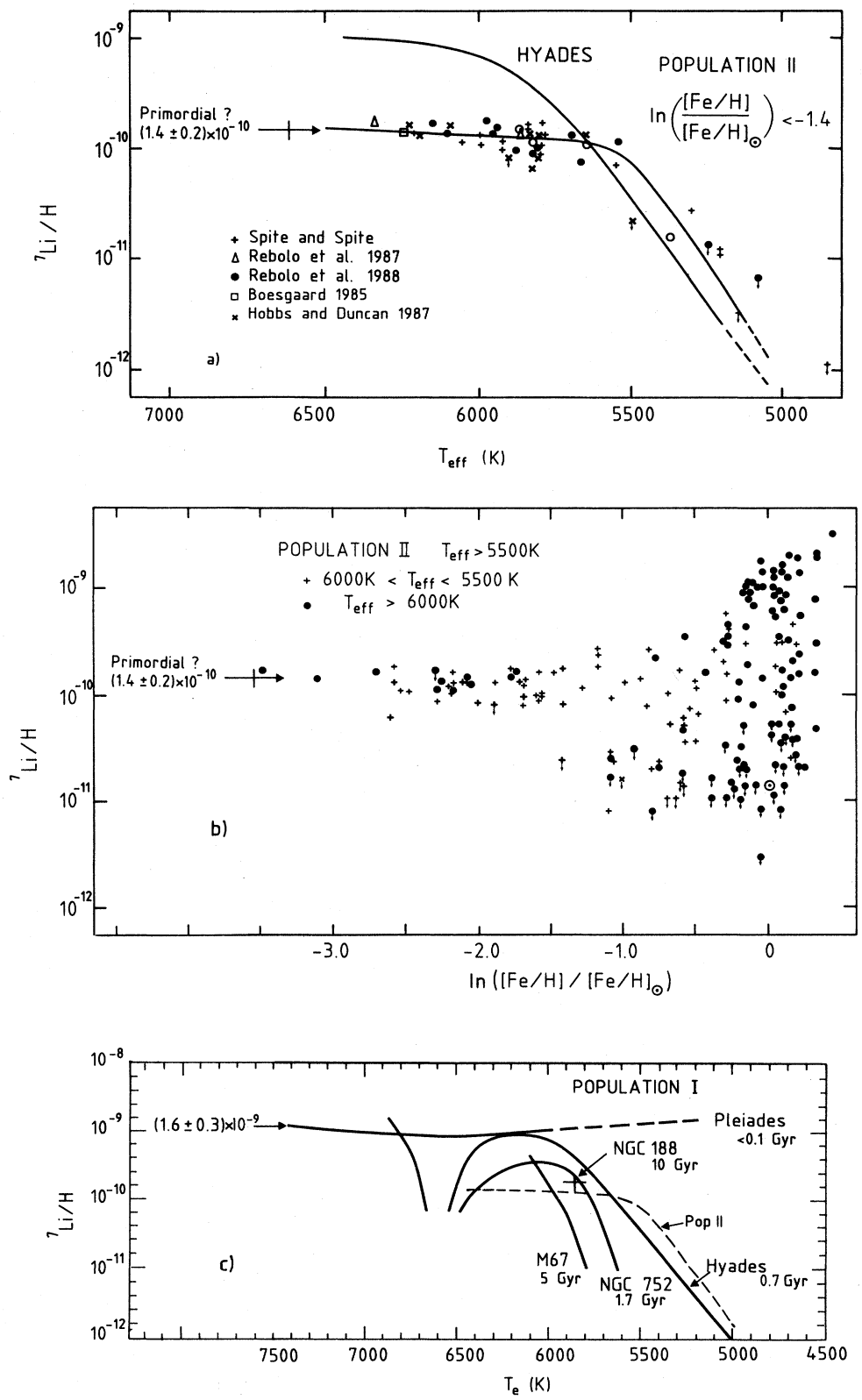

FIG. 12. Observed ^{7}Li abundances for population II, as a function of effective temperature (a) and metallicity (b) (Rebolo, Molaro, and Beckman, 1988; Rebolo, Molaro *et al.*, 1988; Hobbs and Duncan, 1987) and for population I (c) (Hobbs and Pilachowski, 1988).

Given the above doubts, for our purpose, we would then have to use the two values of ^{7}Li, corresponding to the population II and population I stars, respectively.

6. ^{4}He

Let us finally turn to the determination of the abundance of ^{4}He. It relies on the emission lines of He^+ produced by recombination in blue compact galaxies. Shields (1987) has recently reviewed the experimental difficulties and uncertainties in correcting for neutral helium, He^{++}, and collisional excitation. It is important to realize, in particular, that the H II regions used are not resolved and contain many stars. The assumption of a common temperature is a gross oversimplification. In order to correct for chemical evolution due to stellar nucleosynthesis, the abundance by mass,

$$Y=\frac{3.97N_{\rm He}}{N_{\rm H}+3.97N_{\rm He}} ,$$

is plotted against the abundance of some higher A element, which would be synthesized by stars [oxygen (Kunth and Sargent, 1983; Kunth, 1986; Peimbert, 1986), nitrogen (Pagel *et al.*, 1986), and carbon (Steigman *et al.*, 1986)], and extrapolated to zero (Fig. 13).

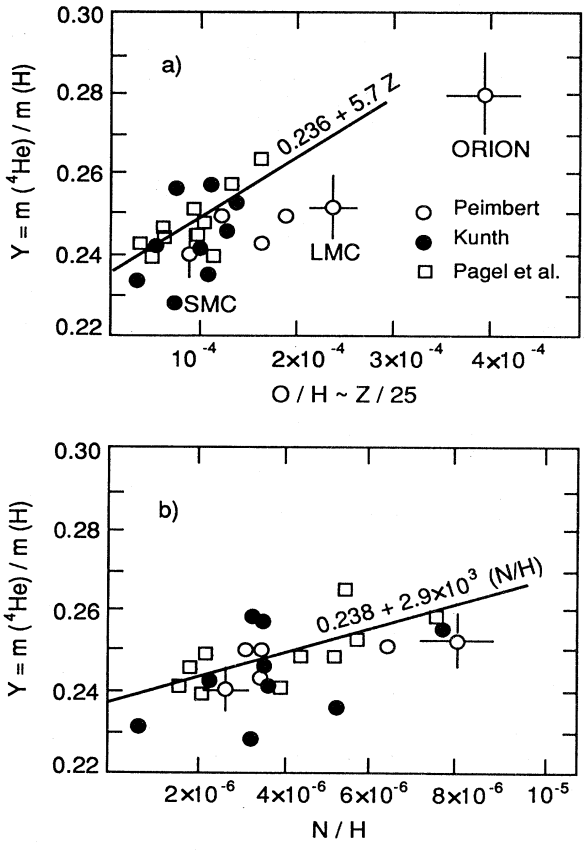

FIG. 13. Observed ^{4}He abundances in metal-poor dwarf galaxies and other objects as a function of O/H (a) and N/H (b). After Pagel *et al.* (1986).

These authors obtain for the mass fraction

0.243±0.0003 (Kunth),

0.232±0.0013 (Peimbert),

0.236±0.0005 (Pagel O/H),

0.238±0.0005 (Pagel N/H),

0.235±0.0004 (Steigman *et al.*).

These results, which use partially overlapping data, are compatible, yielding a weighted average of

$$Y_p=0.236\pm0.003 ,$$

which may have to be decreased somewhat to take into account the collisional excitation. We propose to take

$$Y_p=0.235\pm0.003(\text{statistical})\pm0.010(\text{systematic}) ,$$

where we have followed Shields's estimate of the systematic error.

E. Number of neutrinos

In order to treat statistically the observations summarized above, we chose the following central values and errors:

$$\ln\frac{\rm D}{\rm H}\bigg|_p=\ln(4.5\times10^{-5})\pm0.75 ,$$

$$\ln\frac{^3{\rm He}}{\rm H}\bigg|_p=\ln(2.25\times10^{-5})\pm0.75 ;$$

for the solar system determination,

$$\ln\frac{\rm D+^3He}{\rm H}\bigg|_p=\ln(5\times10^{-5})\pm0.35 ,$$

spanning the ranges 10^{-5} to 2×10^{-4}, 0.5×10^{-5} to 10^{-4}, and 2.5×10^{-5} to 10^{-4}, respectively, at the 2σ level. We take for the lithium

$$\ln\left[\frac{^7{\rm Li}}{\rm H}\bigg|_p\right]=\ln(1.4\times10^{-10})\pm16\% \quad \text{(population II)}$$

or

$$=\ln(1.6\times10^{-9})\pm30\% \quad \text{(population I)} .$$

Because of the uncertainty in the ^{7}Li cross sections mentioned above, we have added a theoretical uncertainty of 30% (rms on the logarithm). For ^{4}He we take

$$Y_p=0.235\pm0.010 .$$

The neutron lifetime is taken from the latest issue of the *Tables of Particles Properties* (1988) as

$$\tau_{1/e}=896\pm10 \text{ s} ,$$

leading to

$$\tau_{1/2}=10.35\pm0.12 \text{ min} ,$$

a value definitely smaller than the one chosen by Yang *et al.* We can then construct as explained in the Appendix a χ^2 with the theoretical predictions for abundances as a function of η from Yang *et al.* (1984) (except for the ^{7}Li value, which is from Kawano *et al.*, 1988). Minimizing this χ^2 yields the following estimates.

(1) For population-II ^{7}Li abundance, we get

$$N_\nu = 2.2 \pm 0.7 \pm 0.2 \quad \text{(solution I)} ,$$

where the second error arises from the theoretical uncertainty on ^{7}Li cross sections. If the theoretical uncertainty is treated as being random, we obtain

$$N_\nu = 2.3 \pm 0.8$$

and

$$N_\nu < 3.3 \ (3.6) \text{ at the } 90\% \ (95\%) \text{ C.L.}$$

The goodness of fit is 93%, indicating an excellent consistency between the data and the model. We have also

$$\eta = (4.35^{+0.4}_{-0.6}) \times 10^{-10} .$$

Note that η is related to a ratio Ω_b of the baryon density to the critical density:

$$\Omega_b = 0.37 \frac{a}{k} m_p \left[\frac{8\pi G_n}{3H^2} \right] T^3 \eta ,$$

where a and k are the blackbody and the Boltzmann constants, m_p the mass of the proton, and T the present temperature of the microwave background. If h is the Hubble constant measured in units of 100 km/s Mpc, then

$$\Omega_b h^2 = 3.7 \times 10^7 \eta \quad \text{for } T = 2.74 \text{ K}$$
$$= (1.61^{+0.16}_{-0.22}) \times 10^{-2} ,$$

and

$$\Omega_b h^2 < 1.85 \times 10^{-2} \quad (90\% \text{ C.L.})$$
$$< 1.92 \times 10^{-2} \quad (95\% \text{ C.L.}) .$$

(2) If, on the other hand, we take the population-I ^{7}Li abundance, we obtain two solutions.

(a) Solution II:

$$N_\nu = 1.8 \pm 0.75$$

and

$$N_\nu < 2.6 \quad (90\% \text{ C.L.})$$
$$< 3.1 \quad (95\% \text{ C.L.}) ,$$

corresponding to $\eta = (8.6 \pm 0.6) \times 10^{-10}$ with a goodness of fit to 1.9%. This solution is a poor fit and presumably should be rejected as incompatible with the Standard Model, unless our errors are grossly underestimated.

(b) Solution III:

$$N_\nu = 3.4 \pm 0.8$$

and

$$N_\nu < 4.4 \quad (90\% \text{ C.L.})$$
$$< 4.7 \quad (95\% \text{ C.L.}) .$$

corresponding to $\eta = (1.6 \pm 0.6) \times 10^{-10}$, but with a very poor goodness of fit of less than 10^{-6} because of the incompatibility with D and D+^{3}He abundances. This fit is so poor that this solution cannot be retained.

F. Discussion

The excellent agreement of the Standard Model with the ^{7}Li abundance of population-II stars is another indication that favors this value as the primordial one. However, it should be noted that the only solution with population-I ^{7}Li abundance that could be considered (solution II) leads to *more restrictive* bounds on the number of neutrinos.

For the population-II solution, it should be noted that our limit

$$N_\nu < 3.6 \quad (95\% \text{ C.L.})$$

is strongly dependent on the systematic error we have chosen to place on the amount of ^{4}He. Had we chosen 0.05 by arguing that it is more representative of the dispersion by the three determinations above, and that the systematic errors that worry Shields would average out the objects and methods, we would have obtained

$$N_\nu \leq 3.1 \quad (95\% \text{ C.L.})$$

a value that we do not, however, recommend because of the possible systematic effect of commonly used assumptions and because of the potential bias in the community in favor of the Standard Model, which may cluster the observations more than is warranted.

Let us remind the reader that our limit is a limit on the number of relativistic degrees of freedom at 0.75 MeV, and that, if we exclude three neutrino families, the electron, and the photon, the number of additional degrees of freedom, NDF, is bounded by

$$\text{NDF} < 1.2 \quad (95\% \text{ C.L.}) ,$$

where the fermions are computed for $\frac{7}{8}$ times their number of spin states. This assumes that the temperature of these particles is the same as that of the neutrinos. However, this will not be the case if they have decoupled much earlier. This would be the case, for instance, for right-handed neutrinos (Olive, Schramm, *et al.*, 1981; Ellis *et al.*, 1986). The compatibility of our result with the presence of three light, right-handed neutrinos would require a decoupling before the quark-hadron transition (Olive, Schramm, *et al.*, 1981), which can easily be arranged with sufficiently massive additional vector bosons.

Finally, it should be kept in mind that the Standard Model could be wrong. Two unconventional mechanisms are at the moment close to reproducing the primordial abundance data. The quark-hadron transition could lead to a spatial segregation between the neutrinos

and protons (Alcock *et al.*, 1987; Applegate *et al.*, 1987; Fuller *et al.*, 1988), But the model with $\Omega_b = 1$ has considerable difficulty reproducing in detail the amount of ^{4}He and ^{7}Li (even if the population-I value is chosen; Alcock *et al.*, 1988). A late release of energy due, for instance, to the decay of a supersymmetric particle (Dimopoulos *et al.*, 1988a, 1988b, 1989) could also change the standard picture and allow $\Omega_b = 1$. However, much ^{6}Li is also produced, and this may be close to being ruled out (Brown and Schramm, 1988; Schramm, 1989). Unconventional models with $\Omega_b < 1$ are probably viable and will weaken the limit of the number of neutrino families. The motivation to add the additional parameters they will need becomes, however, unclear.

Other exotic scenarios have been reviewed recently by Matzner (1986). Most increase the abundance of ^{4}He, thus making the limit on the number of neutrinos more strict. However, an electron-neutrino degeneracy that would accelerate neutron decay in the early universe, or a variable gravitational constant, could increase the limit. But here, again, there is no justification for the required additional parameters.

G. Outlook

Presumably the most important improvement to be made in the next decade on nucleosynthesis would be a reliable measurement of deuterium in the intergalactic medium through the detailed study of the Lyman α systems in the absorption spectra of quasars. Unfortunately, the first generation of spectrometers aboard the Hubble Space Telescope (HST, to be launched in 1990) may have insufficient resolution to unravel their complexity. Radio determination in emission and absorption in the interstellar medium may also be interesting.

More detailed studies of H II regions in young galaxies, made with better angular resolution, will help in refining ionization models and in determining ^{4}He. The Far UV Satellite Explorer (FUSE), at present in its final stages of study, would help in determining both the ^{3}He and the deuterium abundance in the same objects, and in checking for an anticorrelation between ^{3}He and D.

Refinement of stellar models and more data should allow us to improve our understanding of convection and diffusion and to clarify the ^{7}Li question. A better knowledge of the nuclear cross sections for the ^{7}Li abundance calculation is also important.

IV. NEUTRINO COUNTING FROM SINGLE-PHOTON PRODUCTION IN e^+e^- ANNIHILATION

A. The method

Single-photon production in e^+e^- annihilation as a means of determining the number of neutrino species was first suggested by Dolgov *et al.* (1972) and by Ma and Okada (1978). The method is based on the radiative correction diagram to Z^0 production, shown in Fig. 14(a). Depending on the center-of-mass energy, the Z^0 can be on-shell or off-shell. The final state is characterized by the production of a single isolated photon, recoiling against a noninteracting system. Within the Standard Model there is, however, another source of single-photon events leading to noninteracting final-state particles, which is due to the diagram shown in Fig. 14(b). All neutrino species are produced through the Z^0 diagram (a), while the charged-current diagram (b) gives rise only to $\nu_e\bar{\nu}_e$ pairs. Clearly, this direct counting method can measure, or put a limit on, the sum $\sum\Gamma(Z\to\nu_i\bar{\nu}_i)$, or more generally on the partial width for all Z^0 decay modes into noninteracting particles (ν, $\tilde{\nu}$, $\tilde{\gamma}$, etc.).

If we assume that the only relevant extensions of the Standard Model are additional neutrino families, for N_ν species of (light) neutrinos, the lowest-order cross section for $e^+e^-\to\gamma\nu_i\bar{\nu}_i$ is given by (Gaemers *et al.*, 1979)

$$\frac{d^2\sigma}{dE_t^\gamma d\cos\theta_\gamma}=\frac{G_F^2\alpha}{6\pi^2}\frac{s(1-x_\gamma)}{E_t^\gamma\sin^2\theta_\gamma}[(1-\tfrac{1}{2}x_\gamma)^2+\tfrac{1}{4}x_\gamma^2\cos^2\theta_\gamma]\left[\frac{M_Z^4\{N_\nu(g_V^2+g_A^2)+2(g_V+g_A)[1-s(1-x_\gamma)/M_Z^2]\}}{[s(1-x_\gamma)-M_Z^2]^2+M_Z^2\Gamma_Z^2}+2\right],$$

where E_t^γ is the photon momentum transverse to the beam, and θ_γ is the polar angle of emission, $x_\gamma=2E_\gamma/\sqrt{s}$. The term in the curly bracket proportional to N_ν is due to the s-channel Z^0 propagator, and the last term is due to the production of electron-neutrinos by W exchange. The second term is the interaction between W and Z exchange for electron-neutrinos. M_Z and Γ_Z are the Z^0 mass and total width, and g_V, g_A are the vector and axial-vector $Z^0\to e^+e^-$ couplings: $g_V=-\frac{1}{2}+2\sin^2\theta_W$ and $g_A=-\frac{1}{2}$.

This is a bremsstrahlung process, and the photon distribution is proportional to $(1/E_\gamma)(1/\sin^2\theta_\gamma)$. It is peaked at low energy E_γ and at polar angles θ_γ close to the beam. Because of this, the cross sections observable

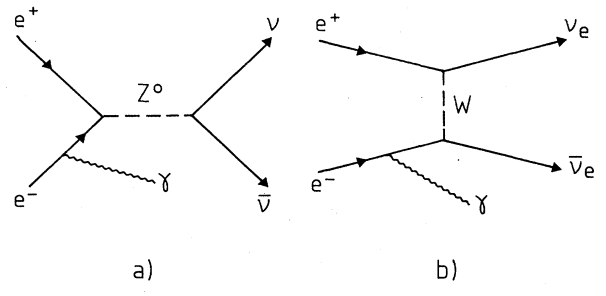

FIG. 14. Single-photon production accompanied by neutrinos in e^+e^- annihilation, in (a) through a Z^0 exchange and in (b) through a W exchange.

in practice are rather small at present (PEP, PETRA) c.m. energies $\sqrt{s}$, which are much smaller than M_{Z^0}. An experiment designed to study this process thus would need good photon detection at low E_γ and low θ_γ; at the same time, the veto capability of the detector would have to extend over as large a solid angle as possible. For example, at $\sqrt{s}=29$ GeV (PEP) the detectable cross section for $E_\gamma > 1$ GeV, $\theta_\gamma > 20°$, and $N_\nu = 3$ is 0.04 pb (Hearty *et al.*, 1987). In typical PEP or PETRA experiments with a sensitivity of ~ 100 events per picobarn, this leads us to expect only a few events. At present, therefore, this method is barely able to determine N_ν, but rather places an upper limit on N_ν. A substantial improvement over the present situation is already expected at TRISTAN energies, where the rate for $\gamma\nu\bar{\nu}$ at $\sqrt{s}=68$ GeV should be larger by a factor ≈ 6 for comparable cuts. The situation will drastically change with the Z^0 factories SLC and LEP, where the cross section is enhanced by a factor $\sim 10^3$. At these machines, N_ν can be determined in several ways: from a direct measurement of the Z^0 total width with a beam scan across the peak (Altarelli *et al.*, 1986); by operating at the Z^0 peak (Feldman, 1986); and by operating at a c.m. energy $\sqrt{s}$ slightly above M_Z, if this $\gamma\nu\bar{\nu}$ method is employed (Barbiellini *et al.*, 1981; Simopoulou, 1986).

In the single-photon final state, the photon is the main experimental signature. One must, however, be sure that it is produced in association with no other interacting particles; i.e., it is necessary to be able to detect any other particle that might be produced, down to the smallest possible angle to the beams.

As this is a direct counting experiment, good control is needed over physical and instrumental backgrounds of the same topology. Momentum balance in the transverse plane is the essential background rejection criterion. The main physical background is due to $e^+e^- \to \gamma e^+e^-$, with the final-state e^+e^- escaping detection, mostly through the beam pipe. This background can be reduced, at the expense of rate, by raising the γ transverse energy threshold E_t^γ, as either the e^+ or the e^- must emerge at a laboratory angle

$$\theta_{\rm lab} < E_t^\gamma/\sqrt{s} = E_t^\gamma/(2E_{\rm beam}) .$$

Hermetic calorimetry and particle detection down to low angles to the beams is therefore essential in this search, in order to avoid physical backgrounds from $ee \to \gamma ee, \gamma\gamma, \gamma\gamma\gamma$ (Hearty *et al.*, 1987; Behrend *et al.*, 1988). Instrumental backgrounds arise from cosmics and beam-gas interactions producing π^0's along the beam lines.

B. Results from PEP and PETRA

We discuss in more detail the search performed in the ASP detector at PEP at $\sqrt{s}=29$ GeV (Bartha *et al.*, 1986; Hearty *et al.*, 1987). This experiment has the largest sensitivity of all e^+e^- experiments until now (115 events/pb) and is best suited for this search. The ASP detector is shown in Fig. 15. It has charged-particle detection and electromagnetic calorimetry over the full solid angle down to 21 mrad from the beam lines. Only radiative Bhabha events $e^+e^- \to e^+e^-\gamma$, with $E_t^\gamma < 0.6$ GeV, could possibly be mistaken for $e^+e^- \to \gamma\nu\bar{\nu}$. Photon recognition is achieved in the angular range $20° < \theta_\gamma < 160°$ with lead glass counters, and single-photon candidates are required to satisfy $E_t^\gamma > 0.8$ GeV and $E_\gamma < 10$ GeV. The requirement $E_\gamma < 10$ GeV is introduced to eliminate background due to $e^+e^- > \gamma\gamma$ and $\gamma\gamma\gamma$, with a photon escaping detection in the calorimeter or the beam tube. The ASP collaboration expected three such events and found four.

For rejection of cosmic-ray interactions, it is required to have an electromagnetic shower shape with a vertex matching for the extrapolated electromagnetic shower direction (expressed in terms of the distance of closest approach to the interaction point). Timing between the calorimeter signal and the beam crossing has to be con-

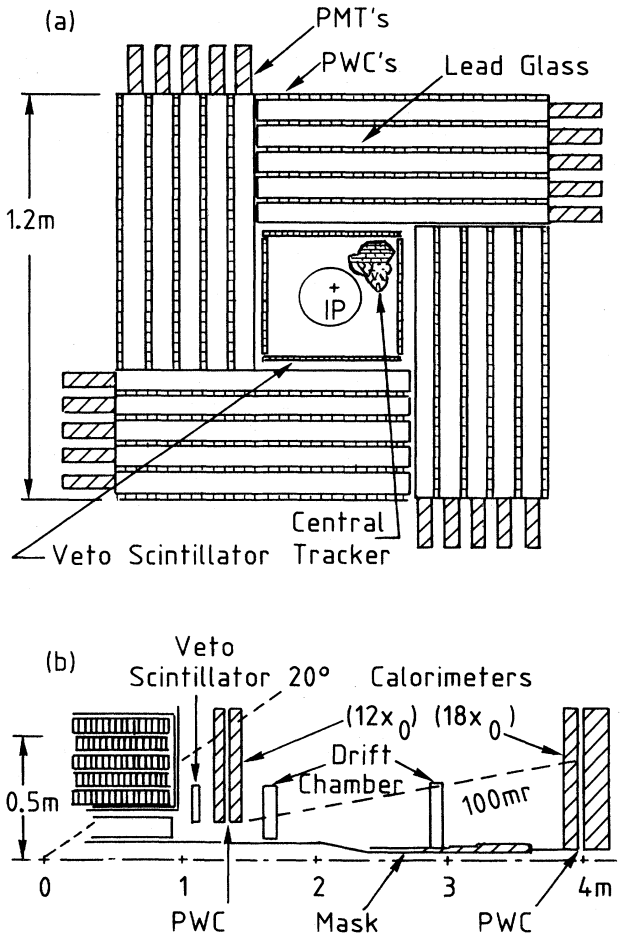

FIG. 15. Transverse (a) and longitudinal (b) views of the ASP detector at PEP. For a detailed description of the apparatus, see Bartha *et al.* (1986) and Hearty *et al.* (1987).

sistent with a shower developing outwards from the interaction region.

The efficiency with which photons pass the various selection criteria is determined, as a function of E_t^γ and θ_γ, from the sample at radiative $e^+e^-\gamma$ final states (40 000 kinematically fitted events). A display of an $e^+e^-\gamma$ event in the ASP detector is shown in Fig. 16(a). The overall efficiency for single photons accompanying $\nu\bar{\nu}$ production is 75% in the ASP fiducial region $20° < \theta_\gamma < 160°$. The requirement that there be no evidence of another particle produced in the event is a crucial one. No significant signal is allowed in any part of the detector, other than for the γ candidate. The efficiency of this veto is found to be 89%. There are additional signal losses of 6.8%, due to backscattering from the γ shower, to γ conversions in the beam pipe and tracking chamber, to late γ conversions, and to triggering efficiency. The overall efficiency for detecting single-photon annihilation processes in the signal region of ASP is 61% (Hearty *et al.*, 1987).

The most probable signal and background contributions from the 24 candidate single-photon events with $E_t^\gamma > 0.8$ GeV, Fig. 17, are estimated by a maximum-likelihood method. The expected signal and background probability distributions in the distance of closest approach of the shower to the interaction point (R in Fig. 17) and in E_t^γ are used in the analysis. This procedure yields a signal of 1.6 events for $E_t^\gamma > 0.8$ GeV, $E_\gamma < 10$ GeV, and $20° < \theta_\gamma < 160°$, while 2.7 $\gamma\nu\bar{\nu}$ events are expected for $N_\nu = 3$. A schematic display of the clear single-photon event of Fig. 17 with $E_t^\gamma = 3.4$ GeV is shown in Fig. 16(b). The probability of observing ≤ 1.6 events is shown in Fig. 18 as a function of the $e^+e^- \to \gamma\nu\bar{\nu}$ cross section. From this figure we see that $\sigma(ee \to \gamma\nu\bar{\nu}) < 0.069$ pb at 90% C.L.; this is equivalent to $N_\nu < 7.5$ (90% C.L.) and $N_\nu < 9.7$ (95% C.L.). This limit is valid for neutrinos light compared to $\sqrt{s}/2$, i.e., for M_ν less than a few GeV.

A similar search has been conducted with the MAC detector at PEP, with 1 event observed for 1.1 events expected, yielding $N_\nu < 15.5$ (90% C.L.; see Fernandez *et al.*, 1985 and Ford *et al.*, 1986), and with the CELLO detector at PETRA, yielding $N_\nu < 15$ (90% C.L.; see Behrend *et al.*, 1986).

More recently, the CELLO collaboration has analyzed

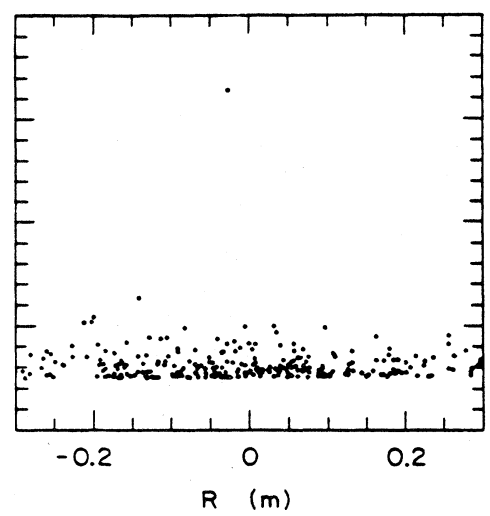

FIG. 17. Scatter plot of the distance of closest approach to the interaction point R vs the photon transverse momentum p_t^γ for the single-photon candidates of the APS collaboration (Hearty *et al.*, 1987).

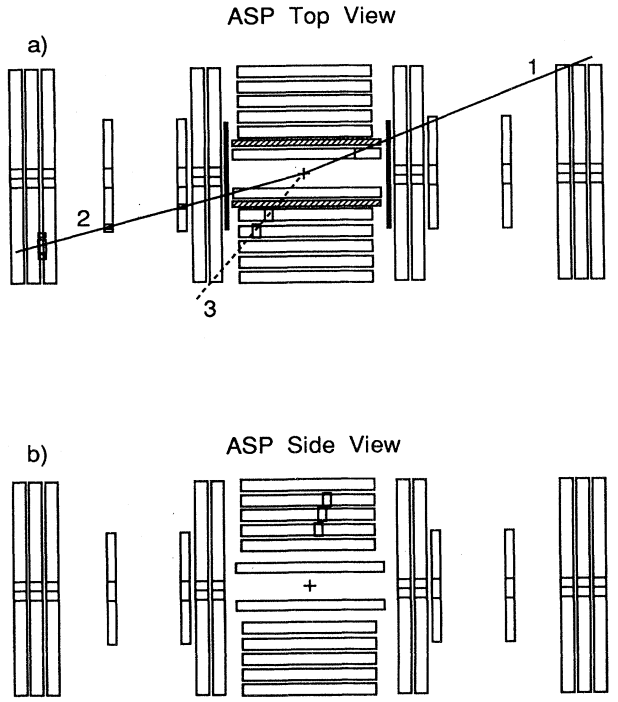

FIG. 16. Events in the ASP detector: (a) Typical radiative $e^+e^- \to \gamma e^+e^-$ Bhabha event (Burke, 1987); (b) single-photon event with $E_t^\gamma = 3.4$ GeV (Burke, 1987).

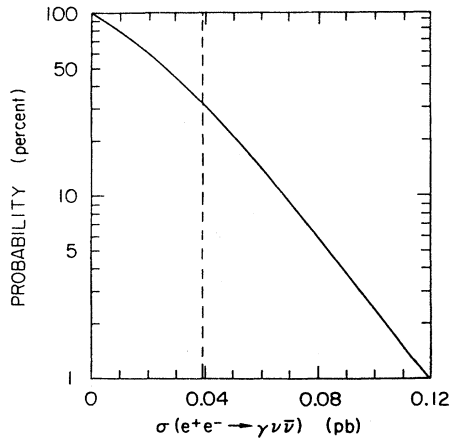

FIG. 18. Probability of observing ≤ 1.6 $\gamma\nu\bar{\nu}$ events as a function of the $e^+e^- \to \gamma\nu\bar{\nu}$ cross section (Hearty *et al.*, 1987).

data at c.m. energies of 35 and ~43 GeV, with experimental sensitivities of 85 and 38 events per picobarn, respectively (Behrend *et al.*, 1988). Within the acceptance of the CELLO detector, ten single-photon candidates are observed in the final selection. This event sample contains one clear-cut example of a single-photon event of $E_t^\gamma = 3.6$ GeV, separated out by a requirement of tight pointing to the interaction point. Using again the distance of closest approach to the interaction point for the single-photon candidates, a maximum-likelihood method gives 1.3-observed $\gamma\nu\bar{\nu}$ events, while 1.9 are expected. The remaining events are cosmic-ray background due to the inefficiency of muon chambers. With the 1.3 observed $\gamma\nu\bar{\nu}$ events, the CELLO collaboration gets a central value $N_\nu = 1.3^{+6.7}_{-1.2}$ and a new limit $N_\nu < 8.7$ at 90% C.L.

The results for N_ν from these three $e^+e^- \to \gamma\nu\bar{\nu}$ searches have been combined in Behrend *et al.* (1988) and Johnson (1987). In all experiments combined, the total number of observed $\gamma\nu\bar{\nu}$ events is estimated to be $N_{\rm est} = 3.9$, while the total expected number of events is

$$N_{\rm exp} = 2.8 + 1.1 N_\nu \ .$$

To arrive at a first approximation, $N_{\rm est}$ can be assumed to be Poisson distributed around $N_{\rm exp}$. It can be checked explicitly that for the CELLO and ASP experiments, which dominate the statistical accuracy, this assumption yields confidence limits very close to those obtained more rigorously by Monte Carlo simulations, taking into account fluctuations of the background. Behrend *et al.* then obtain the central value

$$N_\nu = 1.0^{+2.9}_{-1.0} \quad \text{(all } e^+e^- \text{ experiments combined)}$$

and upper limit $N_\nu \leq 4.6$ (90% C.L.) and $N_\nu \leq 5.8$ (95% C.L.).

These single-photon e^+e^- annihilation searches have also been used to put upper limits on noninteracting supersymmetric-particle final-state production rates, and thus lower limits on $\tilde{\gamma}$, $\tilde{\nu}$ masses (Hearty *et al.*, 1987; Behrend *et al.*, 1988).

C. Prospects for TRISTAN, SLC, and LEP

At LEP it is expected that the Z^0 total width $\Gamma^Z_{\rm tot}$ will be measured with an uncertainty of $\delta\Gamma_{\rm tot} \leq \pm 50$ MeV (Altarelli *et al.*, 1986). This is adequate for neutrino counting, as each neutrino species (with $M_\nu \sim 0$) contributes $\delta\Gamma^Z_{\rm tot} \approx 170$ MeV; thus the uncertainty should be $\delta N_\nu \approx \pm 0.4$. This precision would then allow us to investigate $Z^0 \to \nu_i\bar{\nu}_i$ decays into possibly massive $\geq$ fourth-generation neutrinos with masses up to $M_\nu \sim 30$ GeV.

It is important to reduce the uncertainty $\delta\Gamma_{\rm tot}$ or δN_ν as far as possible, for at the level of $\delta N_\nu < 1.0$ neutrino units, the neutrino-counting methods become sensitive, for instance, to $Z^0 \to \tilde{\nu}\tilde{\nu}$ decays. For a massless scalar neutrino, the partial rate $\delta\Gamma_Z(Z \to \tilde{\nu}\tilde{\nu}) = \frac{1}{2}\delta\Gamma_Z(Z \to \nu\bar{\nu}) \approx 85$ MeV; for increasing $M_{\tilde{\nu}}$, it is suppressed by a kinematics factor $(1-4M^2_{\tilde{\nu}}/M^2_Z)^{3/2}$. A precision of $\delta N_\nu \approx \pm 0.4$ should make the SLC or LEP sensitive to $M_{\tilde{\nu}} \leq 20$ GeV, provided the three sneutrinos are mass degenerate and there are only three massless neutrinos. Otherwise, there could be a trade-off between a possible $\geq$ fourth-generation massive neutrino and scalar neutrinos.

The direct counting method, i.e., measuring the cross section of $e^+e^- \to \gamma\nu\bar{\nu}$, is probably more adequate if a

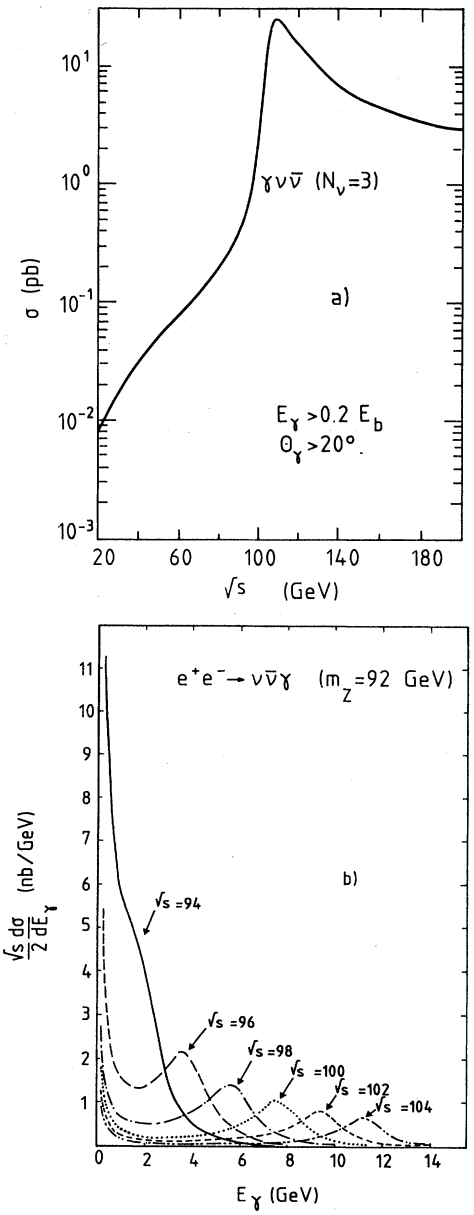

FIG. 19. Using radiative events to count neutrinos: (a) Energy dependence of the cross section for $e^+e^- \to \gamma\nu\bar{\nu}$ (for $N_\nu = 3$), for photons at polar angles $> 20°$ from the beams and with $E_\gamma > 0.2E_{\rm beam}$ (Burke, 1987); (b) photon energy spectra from $e^+e^- \to \gamma\nu\bar{\nu}$ at c.m. energies $\sqrt{s}$ a few GeV above the Z^0 peak ($M_Z = 92$ GeV is assumed); the photon cross section is integrated over the angular range $20° < \theta_\gamma < 160°$ (Simopoulou, 1986).

precise $\delta\Gamma^Z_{\rm tot}$ cannot be directly achieved, as may be the case with the SLC. The rate of $\gamma\nu\bar{\nu}$ events should be measured a few GeV above the Z^0 peak. Figure 19(a) shows the expected cross section for $e^+e^-\to\gamma\nu\bar{\nu}$ versus $\sqrt{s}$, for single photons in the 20°–160° polar-angle range, with $E_\gamma \geq 0.20\, E_{\rm beam}$ (Burke, 1987). Figure 19(b) shows the photon energy spectra is 2 GeV steps from $\sqrt{s}=94$ to 104 GeV ($M_Z=92$ GeV is assumed; see Simopoulou, 1986). As shown in Fig. 19(a), the cross sections at the SLC and LEP will be $\sim 10^3$ times larger than at present PEP and PETRA energies, yielding $\sim 10^3$ single-photon events for similar acceptances and for a sensitivity of 100 pb^{-1}. The gain over the present situation is already substantial at TRISTAN, up to a factor of ~ 6 for $\sqrt{s}=68$ GeV. In the $\sqrt{s}=100$-GeV region, the interesting photon energy range is ~ 2 to ~ 14 GeV [Fig. 19(b)]. The bremsstrahlung spectrum does not fall off as sharply as it does below the Z^0 peak; in fact, it has a bump due to the recoil on-shell Z^0. This makes the counting rate rather insensitive to the threshold cut and to the absolute energy-scale uncertainties. However, for this method to work, as already discussed, a hermetic detector is needed to guarantee the production of a single photon accompanied only by noninteracting particles ($\nu\bar{\nu}$, $\tilde{\nu}\bar{\tilde{\nu}}$, $\tilde{\gamma}\tilde{\gamma}$, etc.). This is not needed for N_ν determination from $\Gamma^Z_{\rm tot}$ obtained by an event-rate measurement in an energy scan across the Z^0 peak.

V. LIMIT ON THE NUMBER OF NEUTRINO TYPES FROM $\bar{p}p\to Z^0(\to\nu_i\bar{\nu}_i)+$JET

A. The method

This method, first suggested by Denegri (1984) and by Chaichian and Hayashi (1984), is based on $p\bar{p}\to Z^0+$jet production followed by $Z^0\to\nu\bar{\nu}$, which is the QCD analog of the QED process $e^+e^-\to Z^0+\gamma$. The simplest Z^0+jet QCD gluon-bremsstrahlung production mechanism is represented in Fig. 20(a). A high-transverse-momentum Z^0 is produced recoiling against a (gluon) jet, with the Z^0 decaying (invisibly) into neutrino pairs. To-

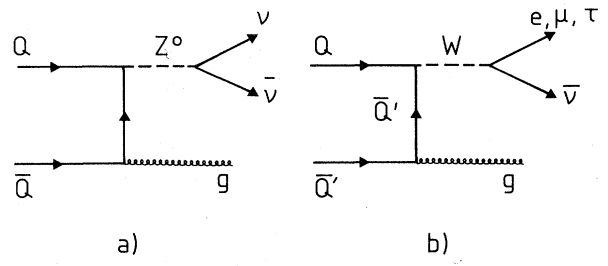

FIG. 20. Gluon-bremsstrahlung diagrams leading to large p_t production of a Z^0 in (a) and a W in (b).

pologically this is a large missing-transverse-energy ($E_t^{\rm miss}$) monojet event. The analogous $W+$jet production mechanism is represented in Fig. 20(b).

The average Z^0 transverse momentum $p_t^Z \approx E_t^{\rm jet}$, balancing the recoil jet transverse energy generated by QCD radiative effects, is ≈ 8.5 GeV/c at $\sqrt{s}=630$ GeV (Ansari *et al.*, 1987b; Stubenrauch, 1987; Albajar *et al.*, 1988a). High-p_t Z^0 production is needed in this method in order to have an adequate experimental signature and a good background rejection. A $Z^0\to\nu\bar{\nu}$ decay with a low p_t^Z cannot be detected in a $p\bar{p}$ collision, since a longitudinal missing energy cannot be measured in hadron colliders where numerous beam fragments always escape detection in the beam pipes. Missing transverse energy, however, can, be detected. It shows up as an energy/momentum imbalance in the transverse plane. Significant missing transverse energy though, requires a cut, which depends on the specific apparatus features. For example, $E_t^{\rm miss}>15$ GeV in the UA1 experiment, and >25 GeV in experiments UA2 (before upgrading) and CDF (Fermilab). The large-E-recoil jet thus provides a selective hardware trigger—which is essential in view of the large $p\bar{p}$ event rates—and a topological event signature.

The neutrino-counting Z^0 mode in Fig. 20(a) is directly connected to the observable $Z^0\to e^+e^-$ decay mode as follows:

$$\frac{d\sigma}{dE_t^{\rm jet}}\left[p\bar{p}\to Z\left[\to\sum_l^{N_\nu}\nu\bar{\nu}\right]+\text{jet}+X\right]=\frac{N_\nu\Gamma(Z\to\nu\bar{\nu})}{\Gamma(Z\to e^+e^-)}\frac{d\sigma}{dE_t^{\rm jet}}[p\bar{p}\to Z(\to e^+e^-)+\text{jet}+X]$$
$$=N_\nu\frac{1}{1-4\sin^2\theta_W+8\sin^4\theta_W}\frac{d\sigma}{dE_t^{\rm jet}}\,.$$

The ratio of $Z^0\to\nu\bar{\nu}$ (for one neutrino flavor) to $Z^0\to e^+e^-$ partial rates is very close to 2; for $\sin^2\theta_W=0.230$, it is equal to 1.99.

The above relation shows explicitly the dependence on N_ν and allows us, in principle, to normalize the expected monojet signal to observed $Z^0\to e^+e^-$ decays. In practice, however, as the cross section for $Z^0\to e^+e^-$ is smaller by a factor of ~ 6 than the neutrino signal [BR($Z^0\to e^+e^-$)$\approx 3\%$, while BR($Z^0\to\sum\nu\bar{\nu}$)$\sim 18\%$ for $N_\nu=3$], the expected signal is estimated using the observed $W(\to e\nu)+$jet [Fig. 20(b)] differential cross-section shape $(1/\sigma_W)(d\sigma_W/dp_t^W)$ shown in Fig. 21 (Arnison *et al.*, 1986; Ansari *et al.*, 1987b; Di Lella, 1987; Stubenrauch, 1987; Albajar *et al.*, 1988a). The rate of $W(\to e\nu)+$jet is comparable to the expected neutrino signal, as the W and Z total production cross sections are

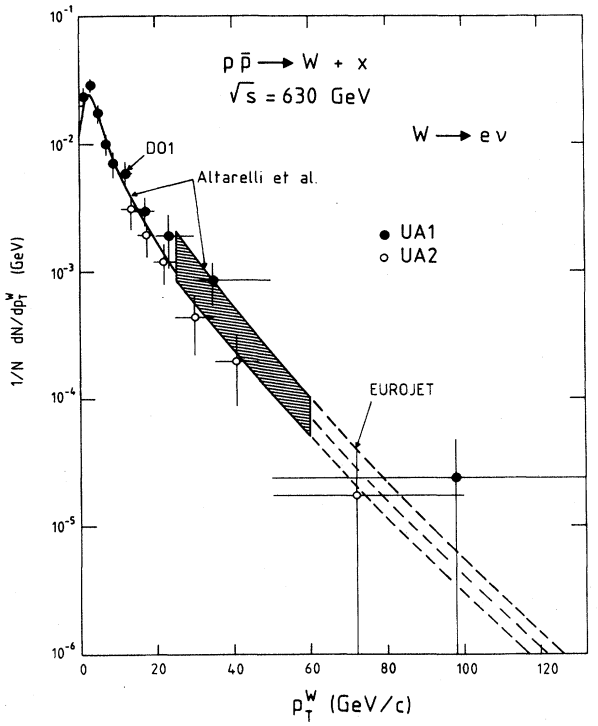

FIG. 21. Shape of the W transverse momentum distribution observed by the UA1 and UA2 collaborations at $\sqrt{s}=630$ GeV [Stubenrauch (1987) for UA1 and Di Lella (1987) for UA2]. The solid line is the QCD calculation of Altarelli *et al.* (1984) for DO1. The shaded area is the perturbative QCD calculation with its theoretical uncertainty, in the range of interest for the neutrino-counting monojet search; this calculation has been extended to higher p_t^W values, as indicated (dashed lines), with the EUROJET Monte Carlo program.

in the ratio $\sigma_W/\sigma_Z \sim 3.5$ (Altarelli *et al.*, 1984), which is partially compensated by the branching ratios $\mathrm{BR}(W\to e\nu)\sim 10\%$ and $\mathrm{BR}(Z\to\sum\nu\bar{\nu})\sim 18\%$ for $N_\nu=3$. The predicted $E_t^{\mathrm{jet}}\approx p_t^{W,Z}$ shapes are very similar, with $\langle p_t^Z\rangle$ being about 15% larger than $\langle p_t^W\rangle$ (Altarelli *et al.*, 1984).

In order to be applicable, this method requires hermetic calorimetry extending to small angles to the beam, and muon detection and momentum measurement to reject $W\to\mu\nu$+jet events [Fig. 20(b)]. Moreover, genuine backgrounds exist: fluctuation of two-jet events, which can be removed by a high-transverse-energy threshold; $W\to\tau\nu$ decays, which can usually be recognized; and semileptonic decays of a W overlapping with accompanying jets.

B. Results of UA1

Monojet events with a significant missing transverse energy E_t^{miss} have been detected and analyzed along these lines by the UA1 experiment at the CERN $p\bar{p}$ collider (Albajar *et al.*, 1987b). A typical monojet event is shown in Fig. 22. The jet, with a large transverse energy, $E_t\approx 43$ GeV, is clearly visible in both the central tracking detector and in the calorimeters. All soft-particle tracks or calorimetric cells with p_t or $E_t\le 1$ GeV produced with the hard collision are suppressed in this display in order to exhibit the monojet topology of the event more clearly.

In UA1 the main instrumental backgrounds are cosmics, beam-halo interactions, and fluctuations in calorimeter response to large-E_t dijet events. Dijet fluctuations are estimated from detailed Monte Carlo studies of the apparatus and of the experimental E_t^{miss} distribution. As in UA1 the calorimetric coverage extends down to 0.2° from the beam lines; the E_t cutoff is in the $E_t^{\mathrm{jet}}\approx E_t^{\mathrm{miss}}$ 10–15-GeV range. Cosmics and halo events are rejected through appropriate technical cuts and scanning of the events on interactive graphics displays. The various physics backgrounds previously mentioned have been Monte Carlo generated, and the UA1 apparatus response has been fully simulated.

UA1 observes a total of 56 events containing one (or more) high-E_t jets ($E_t>12$ GeV), with an (isolated) E_t^{miss} measured at a $\ge 4\sigma$ significance level (Albajar *et al.*, 1987a, 1987b). Most of these events are monojets (53 out of 56 events). A τ likelihood (L_τ) is assigned to each event on the basis of jet collimation and jet charged-particle multiplicity (Albajar *et al.*, 1987a). The scatter plot of L_τ versus the jet E_t is shown in Fig. 23. Most of the τ decays are removed by a $L_\tau<0$ cut, which leaves a sample of 22 relatively broad monojets and two dijet events. These events are then interpreted in terms of residual $W\to\tau\nu$ decays, fluctuations of detector response to dijet production, possible heavy flavor ($c\bar{c}$, $b\bar{b}$) contributions, and high-p_t W and Z^0 production, the last being the signal sought.

Including the effect of the $\ge 4\sigma$ significant selection cut on E_t^{miss}, the net acceptance of UA1 to detect a E_t^{miss} event from $Z^0\to\nu\bar{\nu}$ is 1.8%. This gives approximately 2.0 expected events from $Z^0\to\nu\bar{\nu}$ for each neutrino species. Apart from the $W\to\tau\nu$ events, this is the largest source of high-E_t monojets in the UA1 signal region. All the known Standard Model sources, including $Z^0\to\nu\bar{\nu}$ with $N_\nu=3$, account for 21 ± 5 events, to be compared with the 24 events observed. The error on the expected number of events includes the absolute normalization and Monte Carlo simulation uncertainties. The E_t^{jet} and E_t^{miss} distributions for this sample are shown in Fig. 24. The solid curve is the sum of the expected contributions. The agreement between data and Monte Carlo expectations is satisfactory.

Because of limited statistics, UA1 does not yet determine N_ν by this method, but rather gives an upper limit. From the number of events observed at $E_t^{\mathrm{jet}}<40$ GeV compared with the predicted one, the limit on the number of neutrino species is (Albajar *et al.*, 1987b)

$$N_\nu<10 \text{ at a } 90\% \text{ C.L.}$$

In Fig. 25 the expected contribution for seven extra neu-

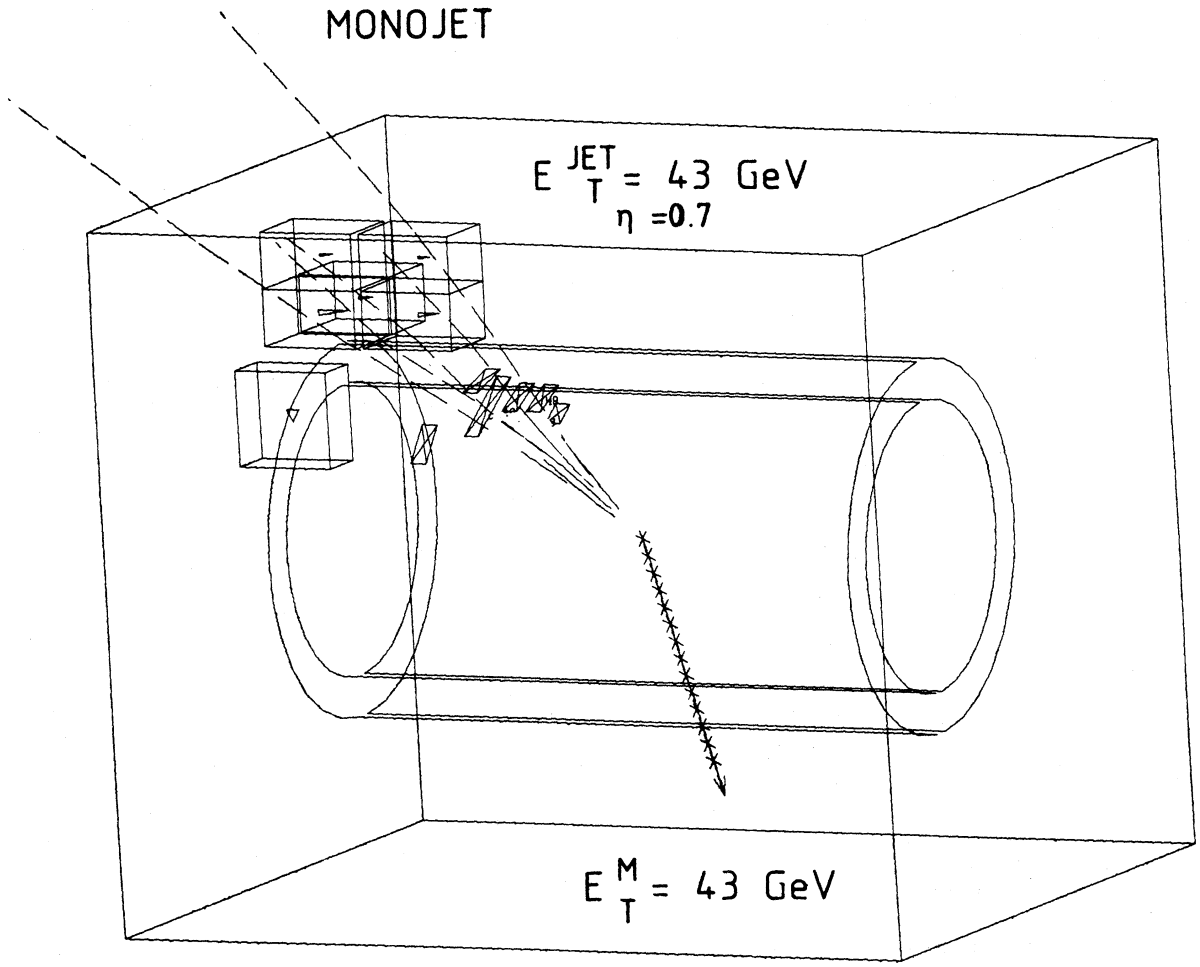

FIG. 22. Typical monojet event seen in the UA1 detector. Only tracks with $p_t > 1$ GeV/c and calorimeter cells with $E_t > 1$ GeV are shown (Albajar *et al.*, 1987b).

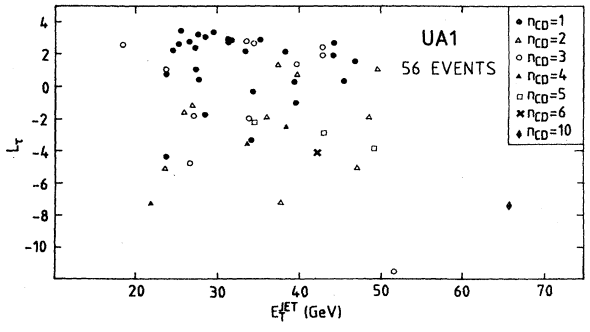

FIG. 23. Scatter plot of the τ likelihood L_τ vs the transverse energy of the highest E_t jet in the sample of 56 large and isolated missing E_t events of UA1. The different symbols indicate the charged multiplicity of the jet (Albajar *et al.*, 1987b).

trino species is compared with the data. The upper limit on N_ν determined by this method is comparable to the one from individual e^+e^- experiments.

The absence of excess E_t^{miss} events has also been used by UA1 to put lower bounds on the masses of the heavy lepton, the squark, and the gluino (Albajar *et al.*, 1987b, 1987c).

C. Discussion and future prospects

The main limitations of this method are the following.

The production of a high-p_t Z^0 represents only a small fraction of the total Z^0 production cross section; the QCD calculations by Altarelli *et al.* (1984) predicts $(4\pm1.5)\%$ of Z^0's produced with $p_t^Z > 30$ GeV/c at $\sqrt{s} = 630$ GeV. The observed W transverse momentum distribution, shown in Fig. 21, confirms the validity of

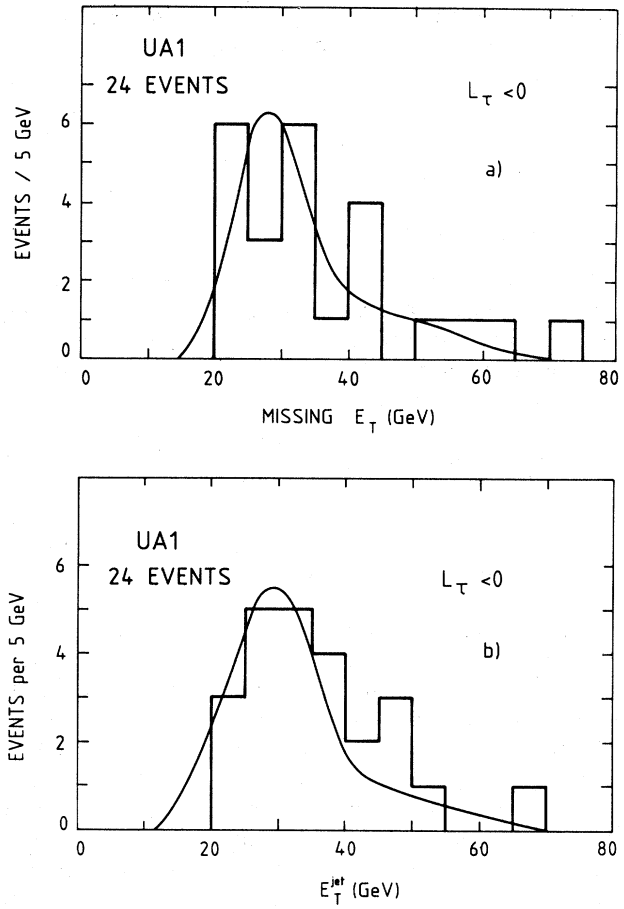

FIG. 24. Missing transverse energy (a) and jet transverse energy (b) for UA1 events passing the cut $L_\tau < 0$ (24 events), compared with the sum of all expected contributions, assuming $N_\nu = 3$ (Albajar *et al.*, 1987b).

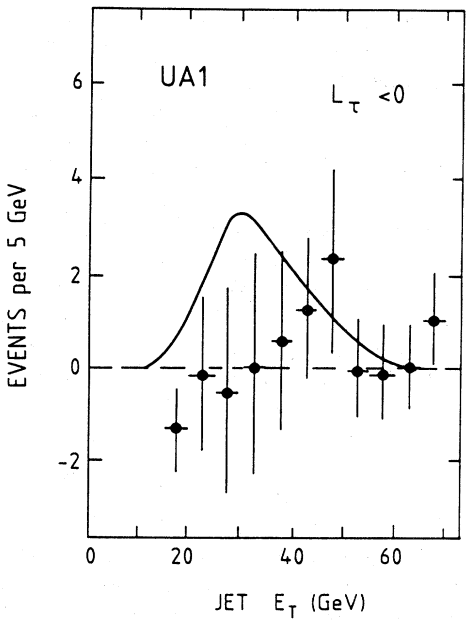

FIG. 25. Jet transverse energy distribution for background-subtracted data (including the contribution for $N_\nu = 3$) passing the cut $L_\tau < 0$ (points with error bars), compared with the expected contribution for seven extra massless neutrino species (solid line) (Albajar *et al.*, 1987b).

this QCD expectation. With present experimental sensitivities of $\lesssim 1$ event/pb, only a few events are thus expected, and the main limitation is statistical. This situation should, however, improve with the future collider runs, particularly at Fermilab collider energies where the Z^0 production rate is larger by a factor of ~ 4 than at the CERN collider and at the same time the p_t^Z spectrum is harder.

Another limitation is the uncertainty in the expected number of known physics background events. The production of a $W \to \tau\nu$ followed by $\tau \to \nu_\tau +$hadrons can be normalized to the observed $W \to e\nu$ cross section. A more difficult background is the high-p_t W production, where the W-decay products e, μ, or τ overlap the recoil jet. The amount of overlap depends on apparatus granularity and the muon recognition capability. In the signal region of UA1, for example, this type of background is estimated at approximately 2.0 events, which is comparable to the contribution of one neutrino species (Albajar *et al.*, 1987b).

This is, moreover, a direct counting method, and a significant part of the error is due to the uncertainty in the expected signal, i.e., in the absolute production rate of high-p_t Z^0's (see Fig. 21). The theoretical uncertainty in the Z^0 production cross section is approximately 30%. This is due to the various possible choices of structure functions, of the value of α_S (or $\Lambda_{\rm QCD}$), and of the Q^2 scale appropriate to high-p_t W and Z production (Altarelli *et al.*, 1984, 1985). Normalizing the expected theoretical p_t^Z distribution to the observed rates of $Z^0 \to e^+e^-$, $\mu^+\mu^-$+jet events, or of $W \to e\nu, \mu\nu, \tau\nu$+jet events, certainly helps. None of these cross sections is, however, larger than the $Z^0(\to \nu\bar{\nu})$+jet signal, as already mentioned. Ultimately, it is the systematics on this absolute normalization that limits the accuracy on N_ν in this method.

Once the high statistics of the SLC and LEP experiments definitely settle the question of the number of light neutrino families, we can use this method to investigate further the possible heavy lepton ($W \to L\nu$) and supersymmetric particle production.

VI. LIMITS ON THE NUMBER OF LIGHT NEUTRINOS FROM THE MEASUREMENT OF $R = \sigma(W \to l\bar{\nu})/\sigma(Z \to l\bar{l})$

A. The method

The number of $W \to l\bar{\nu}$ and $Z^0 \to l\bar{l}$ events observed in experiments UA1, UA2, or CDF is sensitive, through the

W and Z leptonic branching ratios, to additional open channels such as $W\to t\bar{b}$ and $Z^0\to\nu_i\bar{\nu}_i$. The absolute production rates themselves, $\sigma(W\to l\bar{\nu})$ and $\sigma(Z\to l\bar{l})$, are, however, not suitable for deducing N_ν directly, as the uncertainties are too large. This is due, on the one hand, to the $\sim 30\%$ spread in the theoretical predictions on W, Z production rates (Altarelli *et al.*, 1984, 1985) and, on the other hand, to the systematic uncertainty in the experimental luminosity, which is, for example, $\approx 8\%$ for UA2 and $\approx 10\%$ for UA1 (Ansari *et al.*, 1987a; Albajar *et al.*, 1988a). What is considered instead—as initially suggested by Cabibbo (1983; see also Cline and Rolf, 1983; Halzen and Marsula, 1983; Deshpande *et al.*, 1985; Barger *et al.*, 1987; Colas *et al.*, 1988, and references therein)—is the ratio

$$R=\frac{\sigma(W\to l\bar{\nu})}{\sigma(\to l\bar{l})}=\sigma_W/\sigma_Z\frac{\mathrm{BR}(W\to l\bar{\nu})}{\mathrm{BR}(Z\to l\bar{l})}\ ,$$

where BR is the branching ratio of the decay channel since in this ratio most of the experimental and theoretical uncertainties cancel. The number N_ν of neutrino species clearly affects the $Z^0\to l\bar{l}$ branching ratio directly. The ratio R, however, also depends significantly on the top-quark mass if $45<m_{\mathrm{top}}<75$ GeV, because for $m_{\mathrm{top}}<45$ GeV both the $Z\to t\bar{t}$ and $W\to t\bar{b}$ channels are open, while for $45<m_{\mathrm{top}}<75$ GeV, only $W\to t\bar{b}$ remains (Denegri, 1986; Halzen, 1986).

The (top-quark, mass-dependent) central value and upper limit on N_ν is obtained from the comparison of the directly measured value of R with its theoretical expectation at the corresponding center-of-mass energy. The latter can be expressed in terms of the total and partial widths of the W and Z^0 as follows:

$$R_{\mathrm{th}}=\frac{\sigma_W}{\sigma_Z}\frac{\Gamma^W_{e\nu}\Gamma^Z_{\mathrm{tot}}}{\Gamma^Z_{ee}\Gamma^W_{\mathrm{tot}}}=R_\sigma R_\Gamma(m_{\mathrm{top}},\Delta N_\nu)\ . \tag{6.1}$$

The ratio of total production cross sections R_σ can be calculated reliably in QCD and is a slowly varying function of $\sqrt{s}$, while the second term R_Γ, which is predicted by the electroweak Standard Model, contains all the dependence on the number of neutrino families and on the top-quark mass through the ratio $\Gamma^Z_{\mathrm{tot}}/\Gamma^W_{\mathrm{tot}}$.

In conclusion, this method consists in measuring R, assuming all terms on the right-hand side of Eq. (6.1) are known (in particular, Γ^W_{tot}), except for Γ^Z_{tot}. This then allows us to determine Γ^Z_{tot} indirectly, and therefore N_ν. In the following, we briefly discuss each of these points.

B. Experimental measurements of R

The collider experiments UA1 and UA2 have measured the ratio R at $\sqrt{s}=630$ GeV (Albajar *et al.*, 1987d; Ansari *et al.*, 1987a) and have evaluated the uncertainties originating from the relative W and Z^0 selection and detection efficiencies, from the background subtraction, and from the statistical error in the numbers of observed events. The results of the two experiments have been combined (Albajar *et al.*, 1987d) using a maximum-likelihood method, leading to

$$R=8.4^{+1.2}_{-0.9}$$

and

$$R<10.1\ (90\%\ \mathrm{C.L.})\ ,$$

$$R<10.5\ (95\%\ \mathrm{C.L.})\ .$$

The uncertainties in these measurements are predominantly of statistical origin, owing to the limited number of Z^0 events. As discussed in the following, it is this experimental error $\delta R/R\sim 14\%$ that is at present the main limitation in determining N_ν.

C. Standard Model predictions for R

1. Determination of $R_\Gamma=\Gamma^W_{e\nu}\Gamma^Z_{\mathrm{tot}}/\Gamma^Z_{ee}\Gamma^W_{\mathrm{tot}}$

The possible additional neutrinos are assumed to be light with respect to the Z^0, which is here produced on-shell. This allows us to neglect any phase-space suppression in $Z^0\to\nu_i\bar{\nu}_i$ (for $m_\nu<10$ GeV, the suppression does not exceed 4%). It is also assumed that the charged-lepton partners (L_i) of these additional neutrinos, and the quarks of the same generations (Q_i), are heavy enough for their contribution to the W and Z^0 total widths to be neglected; i.e., $W\to L_i\bar{\nu}_i$ or $Z^0\to Q_i\bar{Q}_i$ decays are kinematically forbidden. In Sec. IV.E we will discuss what happens if this requirement is relaxed. The ratio R_Γ depends on the various partial decay widths of the W and Z^0. These can all be expressed in terms of the two partial widths:

$$\Gamma^W_{e\nu}=\frac{G_F}{6\pi\sqrt{2}}M^3_W,\quad \Gamma^Z_{\nu\nu}=\frac{G_F}{12\pi\sqrt{2}}M^3_Z\ . \tag{6.2}$$

More specifically, if we neglect the masses of all fermions except the top quark, the various partial rates are

$$\Gamma^W_{\mu\nu}=\Gamma^W_{\tau\nu}=\Gamma^W_{e\nu}\ ,$$

$$\Gamma^Z_{ee}=\Gamma^Z_{\mu\mu}=\Gamma^Z_{\tau\tau}=C_l\Gamma^Z_{\nu\nu}\ ,$$

$$\Gamma^W_{ud}=\Gamma^W_{cs}=3\cos^2\theta_C K\Gamma^W_{e\nu}\ ,$$

$$\Gamma^Z_{dd}=\Gamma^Z_{ss}=\Gamma^Z_{bb}=3C_d K\Gamma^Z_{\nu\nu}\ ,$$

$$\Gamma^W_{us}=\Gamma^W_{cd}=3\sin^2\theta_C K\Gamma^W_{e\nu}\ ,$$

$$\Gamma^Z_{uu}=\Gamma^Z_{cc}=3C_u K\Gamma^Z_{\nu\nu}\ ,$$

$$\Gamma^W_{tb}=3PS_W(m_{\mathrm{top}})K_W(m_{\mathrm{top}})\Gamma^W_{e\nu}\ ,$$

$$\Gamma^Z_{tt}=3C_u PS_Z(m_{\mathrm{top}})K_Z(m_{\mathrm{top}})\Gamma^Z_{\nu\nu}\ .$$

Here θ_C is the Cabibbo angle; C_l, C_u, and C_d are twice the axial and vector $(c_A^2+c_V^2)$ $Z^0\to f\bar{f}$ couplings for charged leptons and for u-type and d-type quarks, respectively. They are given in Table IV (Albert *et al.*, 1980).

TABLE IV. Values of the lepton, uplike quark, and downlike quark neutral-current coupling strengths, for three values of $\sin^2\theta_W$: the present world average and $\pm 2\sigma$.

$x=\sin^2\theta_W$	0.220	0.230	0.240
$C_l=1-4x+8x^2$	0.5050	0.5032	0.5018
$C_u=1-\frac{8}{3}x+\frac{32}{9}x^2$	0.5800	0.5748	0.5697
$C_d=1-\frac{4}{3}x+\frac{8}{9}x^2$	0.7450	0.7404	0.7358

K is the final-state QCD radiative correction factor $(1+\alpha_s/\pi)$; $K_W(m_{\rm top})$ and $K_Z(m_{\rm top})$ are the top-quark mass-dependent QCD radiative corrections to the processes $W\to t\bar{b}$ and $Z\to t\bar{t}$, respectively (Kühn *et al.*, 1986; Alvarez *et al.*, 1987). The phase-space factors PS_W and PS_Z include a V-A contribution (Albert *et al.*, 1980).

To evaluate the widths, the Standard Model prediction of the W, Z masses (Marciano, 1987) is needed:

$$M_W=38.68\pm0.03\ \text{GeV}/\sin\theta_W,\quad M_Z=M_W/\cos\theta_W\ .$$

With $\sin^2\theta_W=0.230\pm0.005$, which is the present world average (Amaldi *et al.*, 1987; Costa *et al.*, 1988), these relations give

$$M_W=80.7\ \text{GeV},\quad M_Z=91.9\ \text{GeV}\ ,$$

which is in excellent agreement with values measured in UA1 and UA2 (Arnison *et al.*, 1986; Ansari *et al.*, 1987a; Locci, 1987; Albajar *et al.*, 1989).

Figure 26(a) shows the total widths $\Gamma^W_{\rm tot}$ and $\Gamma^Z_{\rm tot}$ as a function of $m_{\rm top}$, for three neutrino flavors. Each additional massless neutrino adds ≈ 170 MeV to $\Gamma^Z_{\rm tot}$. The total variation of $\Gamma^W_{\rm tot}$ as a function of $m_{\rm top}$ is almost 700 MeV. From relation (6.2), a variation of M_W and M_Z by $\pm 1\%$ implies a $\pm 3\%$ variation of partial and total widths. However, R_Γ is independent of the mass scale, if expressed in terms of $m_{\rm top}/M_W$, and depends very slightly on $\sin^2\theta_W$, varying by $<0.5\%$ over the allowed range of $\sin^2\theta_W$. The variation of R_Γ with $m_{\rm top}$ is shown in Fig. 26(b) for $N_\nu=3$, 4, and 5; the steplike behavior is due to the ratio of the total widths shown in Fig. 26(a). For top-quark masses of 50 and 100 GeV, the values of R_Γ (for $N_\nu=3$) are 2.74 and 3.23, respectively.

2. Evaluation of R_σ

The second theoretical input in this method is the ratio R_σ of the total cross sections, which can be quite reliably calculated in QCD. Nonetheless, R_σ is not known with a precision comparable to that of R_Γ. It suffers from uncertainties in $\sin^2\theta_W$ and, more importantly, in the structure functions relating the partonic and hadronic cross sections (Altarelli *et al.*, 1984, 1985; Colas *et al.*, 1988; Diemoz *et al.*, 1988). Simplifying, R_σ can be written as

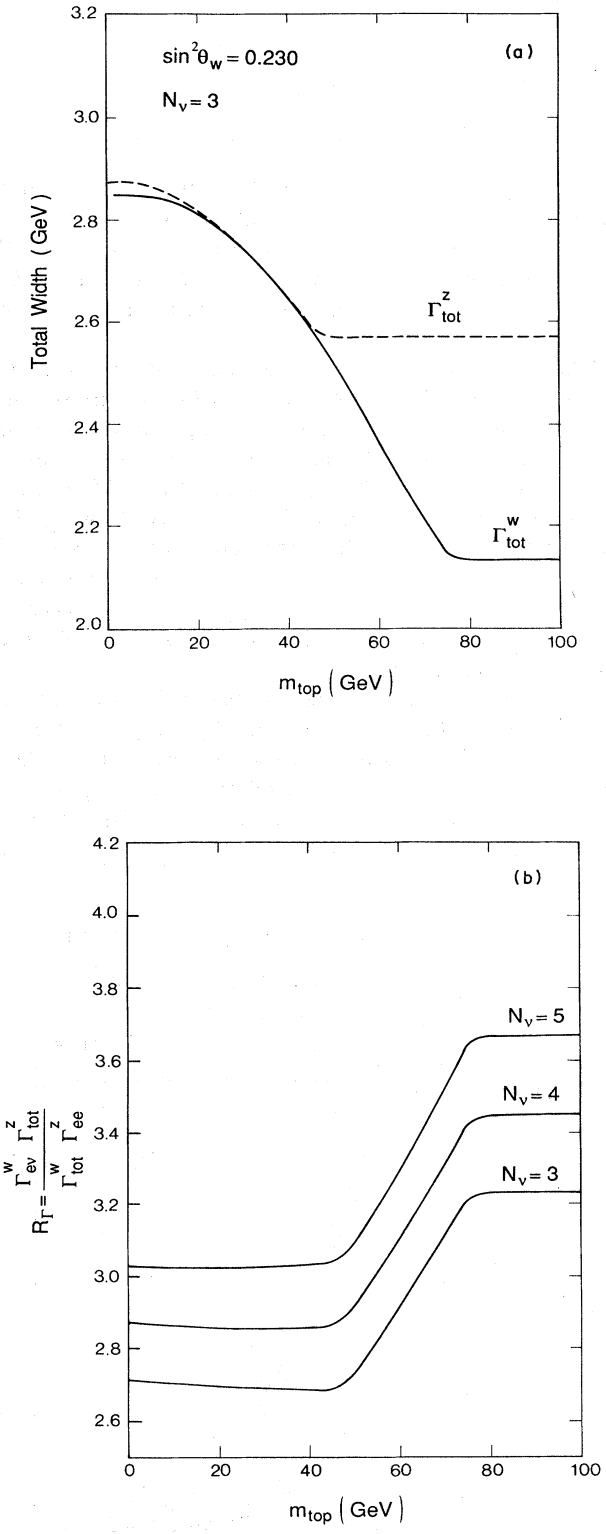

FIG. 26. Dependence on the top-quark mass: (a) Total widths of the W and Z^0 as functions of top-quark mass, assuming three generations, for $\sin^2\theta_W=0.230$, $M_W=80.7$ GeV, and $M_Z=91.9$ GeV; (b) ratio R_Γ of $W\to l\nu$ to $Z\to ll$ branching ratios as a function of $m_{\rm top}$, for $N_\nu=3$, 4, and 5.

$$R_\sigma=\frac{\sigma_W}{\sigma_Z}\approx\frac{2f_{u\bar{d}}\left[\frac{M_W^2}{s}\right]|V_{ud}|^2}{C_u f_{u\bar{u}}\left[\frac{M_Z^2}{s}\right]+C_d f_{d\bar{d}}\left[\frac{M_Z^2}{s}\right]}\,, \tag{6.3}$$

where $f_{qq'}(\tau)=\tau(dL_{qq'}/d\tau)$ are the appropriate partonic luminosities, i.e., constrained products of quark densities. This expression shows explicitly the dependence of R_σ on the structure functions in $\tau(dL_{qq'}/d\tau)$ and on $\sin^2\theta_W$, through M_Z-M_W and the coefficients C_u and C_d (Table IV).

The quark densities, for valence and sea u and d quarks, evaluated at $Q^2=M_W^2$ according to the parametrization of GHR (Glück, Hoffmann, and Reya, 1982), DO (Dukes and Owens, 1984), EHLQ (Eichten, Hinchliffe, Lane, and Quigg, 1984), and DFLM (Diemoz, Ferroni, Longo, and Martinelli, 1988) are shown in Fig. 27. Figure 28 shows the variation of R_σ at $\sqrt{s}=630$ GeV as a function of $\sin^2\theta_W$ for these different sets of structure functions evaluated at $Q^2=M_{W,Z}^2$ (Colas *et al.*, 1988). Theoretical expectations for R_σ at $\sqrt{s}=630$ GeV vary from about 2.95 to 3.5.

As first suggested by Halzen (1986), it is, however, possible to reduce the uncertainty in R_σ using available experimental data on deep-inelastic μ-N scattering at large Q^2. As can be seen from the relation (6.3), R_σ is essentially determined by the ratio $d(x)/u(x)$ of quark densities in the region around $x_W\approx M_W/\sqrt{s}=0.13$ and

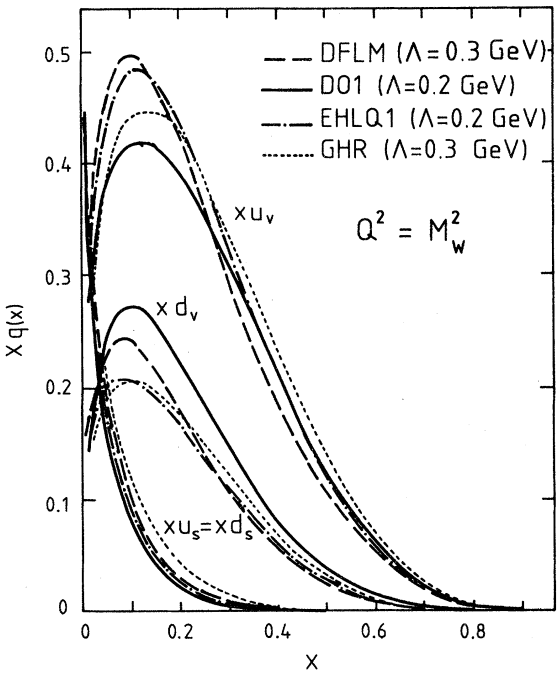

FIG. 27. Valence and sea u- and d-quark momentum distributions for various sets of structure-function parametrizations, evaluated at $Q^2=M_W^2$.

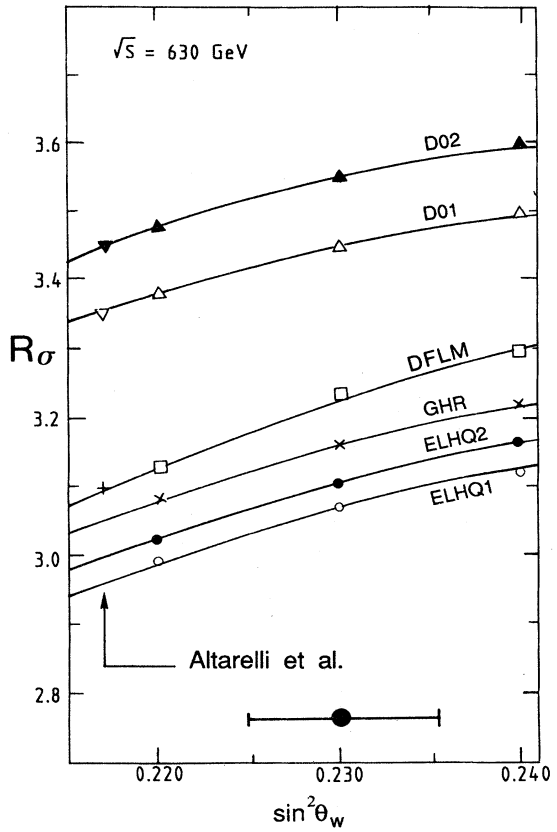

FIG. 28. Dependence of $R_\sigma=\sigma_W/\sigma_Z$, the ratio of W to Z total production cross sections, on $\sin^2\theta_W$ for various choices of structure functions: Duke and Owens sets 1 and 2; Glück, Hoffmann, and Reya; Eichten, Hinchliffe, Lane, and Quigg sets 1 and 2; Diemoz, Ferroni, Longo, and Martinelli, calculated with EUROJET at $\sqrt{s}=630$ GeV. For comparison, the values from Altarelli *et al.* (1984) at $\sin^2\theta_W=0.217$ are also shown.

$x_Z\approx M_Z/\sqrt{s}=0.15$ at $\sqrt{s}=630$ GeV (and at $x\approx 0.05$ for $\sqrt{s}=1.8$ TeV). This ratio $d(x)/u(x)$ in turn is given by the measured ratio of the F_2 deep-inelastic structure functions $F_2^n(x)/F_2^p(x)$.

The data on F_2^n/F_2^p of the two most recent μ-deuterium and μ-hydrogen deep-inelastic experiments, the European Muon Collaboration (EMC, Aubert *et al.*, 1987) and BCDMS (Voss, 1988; Benvenuti *et al.*, 1989; Milsztajn, 1989), are shown in Fig. 29 (Stubenrauch, 1987; Colas *et al.*, 1988). They are compared to theoretical expectations for various sets of structure functions. In the region of interest ($0.05\lesssim x\lesssim 0.4$ for UA1/2), both sets of data are between the EHLQ1 and DO1 curves and close to the GHR or DFLM expectations. According to Fig. 28, this means a value of R_σ between 3.1 and 3.4. The analysis of Colas *et al.* (1988) yields for R_σ

$$R_\sigma(\text{muon data})=3.25\pm 0.10\,,$$

while a comprehensive analysis of neutrino deep-inelastic-scattering data, from which the new set of struc-

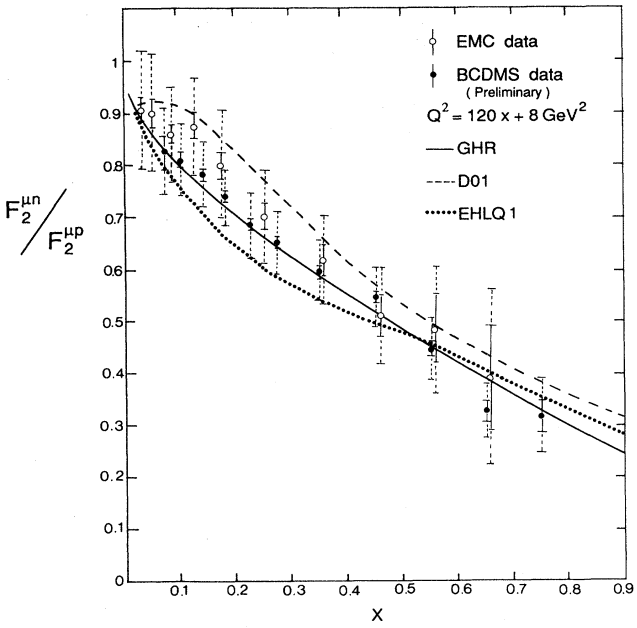

FIG. 29. Comparison of the EMC and BCDMS deep-inelastic muon-scattering data on the ratio of structure functions F_2^n/F_2^p with predictions from various sets of structure functions calculated at the appropriate Q^2, from Stubenrauch (1987) and Colas *et al.* (1988).

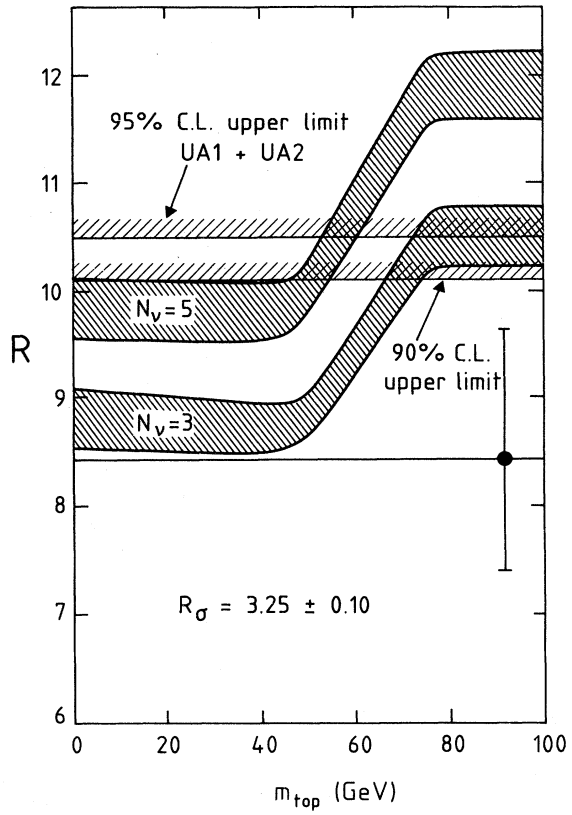

FIG. 30. Comparison of the theoretical predictions for the ratio R as a function of $m_{\rm top}$, with the theoretical input $R_\sigma = 3.25 \pm 0.1$, and the experimental results of UA1/2. The horizontal continuous line represents the UA1 and UA2 combined measurement of R, and the hatched lines are the 90% and 95% C.L. upper limits implied by this measurement (Albajar *et al.*, 1987d). The theoretical expectations are shown for three and five massless neutrinos. The shaded band corresponds to the theoretical uncertainty $\delta R_\sigma = \pm 0.1$.

ture functions (DFLM) is extracted (Diemoz *et al.*, 1988), give similarly

$$R_\sigma(\text{neutrino data}) = 3.28 \pm 0.15 \ .$$

As a central value appropriate for W and Z data at $\sqrt{s} = 630$ GeV, we take $R_\sigma = 3.25$, and as a reasonable lower limit $R_\sigma = 3.15$. At this stage, we will treat the theoretical uncertainty in R_σ as a possible systematic shift. All the ingredients needed to obtain N_ν are now at hand.

D. Limit on N_ν as a function of $m_{\rm top}$

The expected variation of $R = R_\sigma R_\Gamma$ as a function of $m_{\rm top}$ for $N_\nu = 3$ and 5 is shown in Fig. 30 for the central value $R_\sigma = 3.25$, with the hatched band showing the effect of the theoretical uncertainty $\delta R_\sigma = \pm 0.1$. A lower value of R_σ is clearly less constraining for N_ν. These theoretical predictions are compared to the combined UA1 and UA2 experimental central value and upper limits (90% and 95% C.L.) of R in the same figures. Figure 30 shows clearly that N_ν is limited to < 6, and for large top-quark masses the constraint is even stronger.

From the relation (6.1), the (indirect) upper limit on the Z total width is given by

$$\Gamma^Z_{\rm tot} < \Gamma^Z_{\rm tot,\ up}(m_{\rm top}) = \frac{R_{\rm up}}{R_\sigma} \frac{\Gamma^Z_{ee}}{\Gamma^W_{e\nu}} \Gamma^W_{\rm tot}(m_{\rm top}) \ ,$$

where $R_{\rm up}$ is the experimental upper limit on R. If the measured central value R is used instead in this equation, it yields an indirect measure of $\Gamma^Z_{\rm tot}$ itself. The dependence of $\Gamma^W_{\rm tot}$ on $m_{\rm top}$ for three fermion generations is given in Fig. 26(a). With this upper limit on the Z^0 width, and if we assume that the excess over what is expected for three generations [$\Gamma^Z_{\rm tot,\ 3G}$, Fig. 26(a)] can only be due to new neutrino flavors, the upper limit on $\Delta N_\nu = N_\nu - 3$ as a function of $m_{\rm top}$ is given by

$$\Delta N_\nu < [\Gamma^Z_{\rm tot,\ up}(m_{\rm top}) - \Gamma^Z_{\rm tot,\ 3G}(m_{\rm top})]/\Gamma^Z_{\nu\nu} \ .$$

This limit is independent of the precise value of the Z^0 mass.

Figure 31 shows the central value and the upper limit on N_ν as a function of $m_{\rm top}$. The central value of N_ν is obtained from the measured central value of R and from the use of the theoretical central value $R_\sigma = 3.25$. The upper limit on N_ν is obtained by taking the lower value $R_\sigma = 3.15$ from the possible systematic uncertainty range on R_σ and combining it with the experimental 90% C.L. upper limit on R.

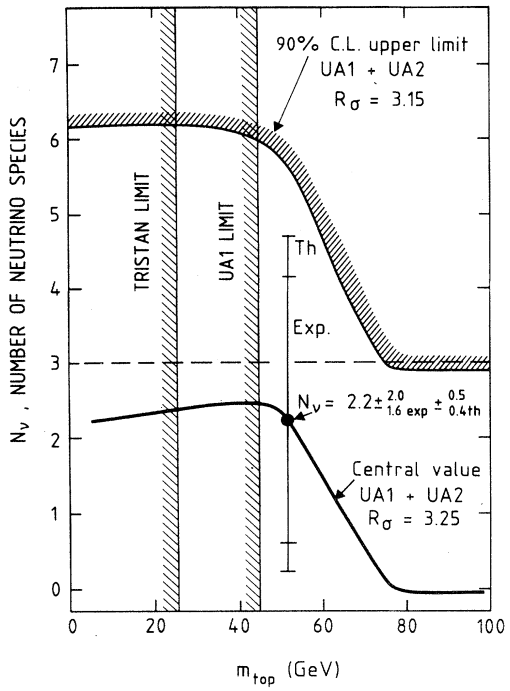

FIG. 31. Total number of light neutrino species N_ν (solid line), as extracted from the combined UA1 and UA2 measurement of R, and the 90% C.L. upper limit on this number, as a function of $m_{\rm top}$. The theoretical input for the central value N_ν is $R_\sigma=3.25$; for the upper limit on N_ν, the value $R_\sigma=3.15$ is used (see text for details). The lower limit of 3 is indicated by the dashed line. The present TRISTAN and UA1 lower limits on $m_{\rm top}$ are shown.

The conclusions are the following. Independent of the top-quark mass, the limits on the number of neutrinos are $N_\nu<5.5\pm0.5$ (90% C.L.) and $N_\nu<6.3\pm0.5$ (95% C.L.; see Albajar *et al.*, 1987d; Ansari *et al.*, 1987a; Colas *et al.*, 1988). The uncertainty in the upper limit reflects the theoretical uncertainty in R_σ, which is treated here as a systematic error. If the top-quark mass is higher than about 75 GeV, then, according to this method, a fourth-generation light neutrino is rather unlikely, as is shown in Figs. 30 and 31. We shall come back to this point in Sec. VII, when combining all results, and discuss it quantitatively in the Appendix. It is also clear from Figs. 30 and 31 that, according to this method, a more accurate knowledge of the ratio R might provide a useful upper limit on the top-quark mass (Halzen, 1986; Albajar *et al.*, 1987d; Barger *et al.*, 1987; Colas *et al.*, 1988; Diemoz *et al.*, 1988).

The central value N_ν itself is given by the central theoretical expectation $R_\sigma=3.25$. As present UA1 results imply that $m_{\rm top}>45$ GeV (Albajar *et al.*, 1988b), Fig. 31 then gives

$$N_\nu=2.2^{+2.0}_{-1.4}{}^{+0.5}_{-0.4} \quad \text{for } m_{\rm top}=50 \text{ GeV},$$

$$N_\nu=0.0^{+1.7}_{-1.3}{}^{+0.4}_{-0.3} \quad \text{for } m_{\rm top}=100 \text{ GeV},$$

where the first error comes from the experimental measurement of R and the second from the theoretical uncertainty on R_σ.

Combining the two errors (as explained in the Appendix), we get for $m_{\rm top}=50$ GeV/c^2

$$N_\nu=2.2^{+2.2}_{-1.5}$$

and

$$N_\nu<5.1 \text{ at 90\% C.L.},$$
$$<5.8 \text{ at 95\% C.L.};$$

for $m_{\rm top}=100$ GeV/c^2 (more generally, for $m_{\rm top}\geq M_W$),

$$N_\nu=0^{+2.0}_{-1.3}$$

and

$$N_\nu<2.5 \text{ at 90\% C.L.}$$
$$<3.1 \text{ at 95\% C.L.}$$

Incidentally, it may be worth noting here that, according to Fig. 30, if $m_{\rm top}>75$ GeV, the observed residual excess of $\Delta N_\nu<0.4$ (at 95% C.L.) would exclude sneutrinos of mass $M_{\tilde\nu}<20$ GeV, provided there are only three neutrino flavors and that the three sneutrinos are mass degenerate.

E. Effects of a possible fourth-generation charged lepton or quark

How would the presence of fourth-generation fermions, a heavy lepton L, or a b' quark, modify these conclusions?

For a heavy lepton with the minimal mass $m_L=41$ GeV allowed by UA1 (Albajar *et al.*, 1987b; Mohammadi, 1987), the total width $\Gamma^W_{\rm tot}$ in the denominator of Eq. (6.1) gets an additional contribution, $\delta\Gamma^W_{\rm tot}=\Gamma(W\to L\nu_4)\approx139$ MeV, while $\Gamma^Z_{\rm tot}$ in the numerator gets, in addition, $\delta\Gamma^Z_{\rm tot}=\Gamma(Z\to\nu_4\nu_4)\approx170$ MeV, as in this case $N_\nu\geq4$ necessarily (we assume that $m_{\nu4}\sim0$). If there is no other fermion lighter than the W, the new upper limit on N_ν is given by the dashed curve in Fig. 32. One more neutrino flavor is allowed for any top-quark mass; i.e., the upper limit in Fig. 31 (shown as a shaded band in Fig. 32) moves up by about one neutrino unit. As m_L tends to M_W, however, this limit on N_ν gradually falls back onto the one shown in Fig. 31.

The presence of a fourth-generation b' quark, on the other hand, with a mass $m_{b'}<M_Z/2$, contributes to $\Gamma^Z_{\rm tot}$ with a $Z^0\to b'\bar b'$ decay mode. This reinforces the limit on N_ν, as, within the measured excess $\Gamma^Z_{\rm tot}$ width, allowance must now be made for $Z^0\to b'\bar b'$. For $m_{b'}=32$ GeV, the minimal mass allowed by UA1 (Albajar *et al.*, 1988b), $\Gamma^Z_{\rm tot}$ gets $\delta\Gamma^Z_{\rm tot}=\Gamma(Z\to b'\bar b')\approx196$ MeV in addition to the ≈170 MeV from the $Z\to\nu_4\nu_4$ mode. If also $m_L>M_W$, the new limit is given by the dotted curve in Fig. 32. It drops by about 1.1 neutrino units for all $m_{\rm top}$,

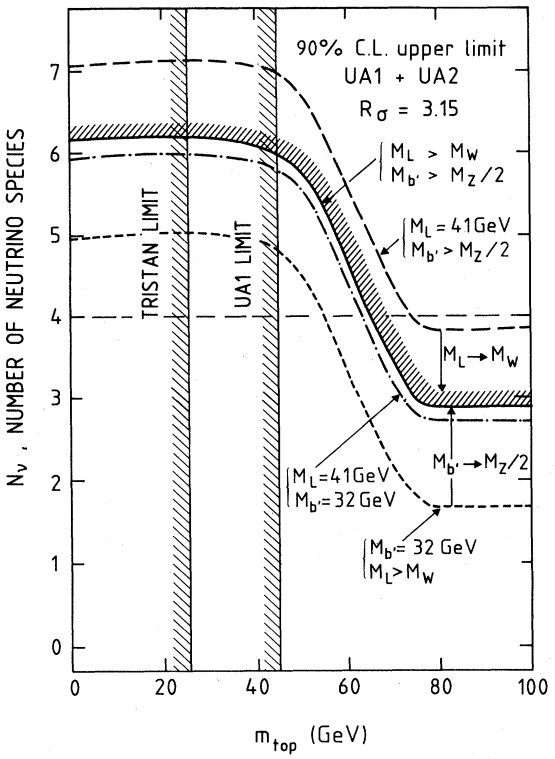

FIG. 32. Upper limits on the number of neutrino species from the combined UA1/2 measurement of R, as a function of m_{top}, for the various heavy lepton and/or heavy b' quark fourth-generation scenarios indicated (see text for details).

and the top-quark mass would be severely limited from above in this case. As $m_{b'}$ tends to $M_Z/2$, this limit moves up towards the one shown in Fig. 31.

Finally, for $m_{b'}=32$ GeV and $m_L=41$ GeV (dot-dashed curve in Fig. 32), the limit nearly coincides accidentally with the one for no L, no b'.

F. Conclusions on neutrino counting from $\sigma(W\to l\nu)/\sigma(Z\to l\bar{l})$ and future prospects

In conclusion, the measurement of R allows us to estimate the number of neutrino generations. The result depends on the top-quark mass. The upper bound that can be placed is no worse than $N_\nu<6.0$ at 90% C.L. A fourth-generation heavy lepton below the W mass would degrade this limit by at most one unit. A fourth-generation b' quark could only strengthen the limit.

This method depends on the ratio of $W\to l\bar{\nu}$ and $Z\to l\bar{l}$ events. It is therefore much less affected by absolute normalization uncertainties, both experimental and theoretical, than are the direct counting methods. The present experimental error of $\delta R/R\approx 14\%$ is largely due to limited Z^0 statistics. It corresponds to an uncertainty in N_ν of $\delta N_\nu^{\rm exp}\approx\pm 1.8$ units. It can be reduced to about $\delta N_\nu\approx\pm 0.5$ units with a factor of ≥ 12 increase in statistics, when systematics takes over (in the experimental conditions of UA1). The theoretical uncertainty $\delta R_\sigma \approx\pm 0.10$, corresponding to a contribution of $\delta N_\nu^{\rm th}\approx\pm 0.5$ units, is difficult to reduce without new data or new constraints on the structure functions.

It is nonetheless worth noticing that when going to Fermilab energies the dispersion of theoretical predictions for the ratio R_σ diminishes, as can be seen from Fig. 33. (The energy dependence of R_σ has been obtained with the EUROJET Monte Carlo method; sea contributions are included.) This can be understood from Fig. 29, as at $\sqrt{s}=1.8$ TeV the W and Z productions sample the structure functions at $x\sim 0.05$, and the ratios $F_2^n/F_2^p\sim\sigma_W/\sigma_Z$ come together with diminishing values of x. However, the uncertainty δR_σ cannot be reduced significantly until there are more-constraining measurements of F_2^n/F_2^p at high Q^2 and low values of x (Fig. 29) and the heavy-quark sea contributions are better known, or until other ways are found to reduce the ambiguity due to structure functions, as discussed, for example, by Berger *et al.* (1989). The ultimate accuracy of this method for neutrino counting is therefore about $\delta N_\nu\approx\pm 0.7$ to ± 0.4 neutrino units, depending on the top-quark mass and the $p\bar{p}$ collision energy.

VII. SUMMARY AND CONCLUSIONS

We have described four approaches for estimating the number of neutrino generations, with the monojet method providing only an upper limit. We remind the reader that our approach is to summarize, through estimates of N_ν and their errors, the information carried by each of the measurements we describe, independently of

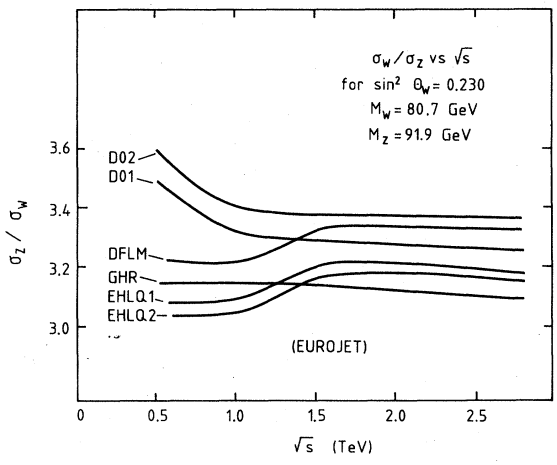

FIG. 33. Variation of the ratio of total production rates $R_\sigma=\sigma_W/\sigma_Z$ with $\sqrt{s}$ from CERN to FERMILAB $p\bar{p}$ collider energies, according to the various sets of structure functions indicated (EUROJET calculation).

any *a priori* knowledge on the number of neutrinos. Figures 34 and 35 and Table V summarize the results obtained.

The method based on the energy release in SN 1987A yields

$$N_\nu = 2^{+1.4}_{-0.7} .$$

The uncertainty in the total-energy release from the collapse of the iron core contributes about 0.5 neutrino units.

The current measurements of the primordial abundances lead to

$$N_\nu = 2.3 \pm 0.8 ,$$

if we assume that the ^{7}Li primordial abundance is given by the population-II stars. None of the fits with ^{7}Li abundance from population-I stars are good. The only acceptable one gives lower N_ν values.

The combined result from single-photon searches in all e^+e^- experiments give a central value

$$N_\nu = 1.0^{+2.9}_{-1.0} .$$

For the combined result of UA1 and UA2, the central value of N_ν is

$$N_\nu = 2.2^{+2.2}_{-1.5} \text{ for } m_{\text{top}} = 50 \text{ GeV}/c^2$$

and

$$N_\nu = 0^{+2.0}_{-1.3} \text{ for } m_{\text{top}} = 100 \text{ GeV}/c^2 .$$

The theoretical uncertainty in R_σ accounts for an error of half a unit.

The upper limits from laboratory experiments having a 95% confidence level are at the $N_\nu < 3$ to 5.8 level, depending on the mass of the top quark. It is quite remarkable that these four different methods (Figs. 34 and 35) give estimates of the same order of magnitude, although

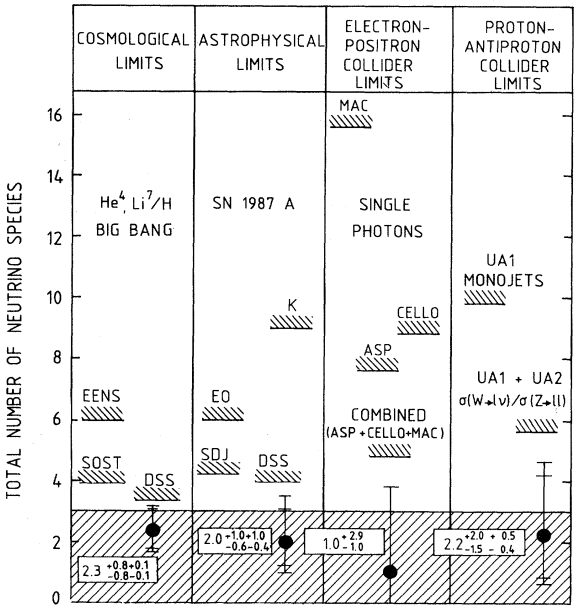

FIG. 34. Compilation of central values and 90% C.L. upper limits on the number of neutrino flavors N_ν from cosmology, astrophysics, and particle physics. The central value of N_ν from UA1 and UA2 is for the central theoretical expectation $R_\sigma = 3.25$ and for $m_{\text{top}} = 50$ GeV. The upper limit is for the "worst case:" $R_\sigma = 3.15$ and $m_{\text{top}} = 50$ GeV. The abbreviations used for the cosmological and astrophysical limits are EENS=Ellis *et al.*, 1986; SOST=Steigman *et al.*, 1986; K=Krauss, 1987; EO=Ellis and Olive, 1987; SDJ=Shaeffer *et al.*, 1987; and DSS=this paper.

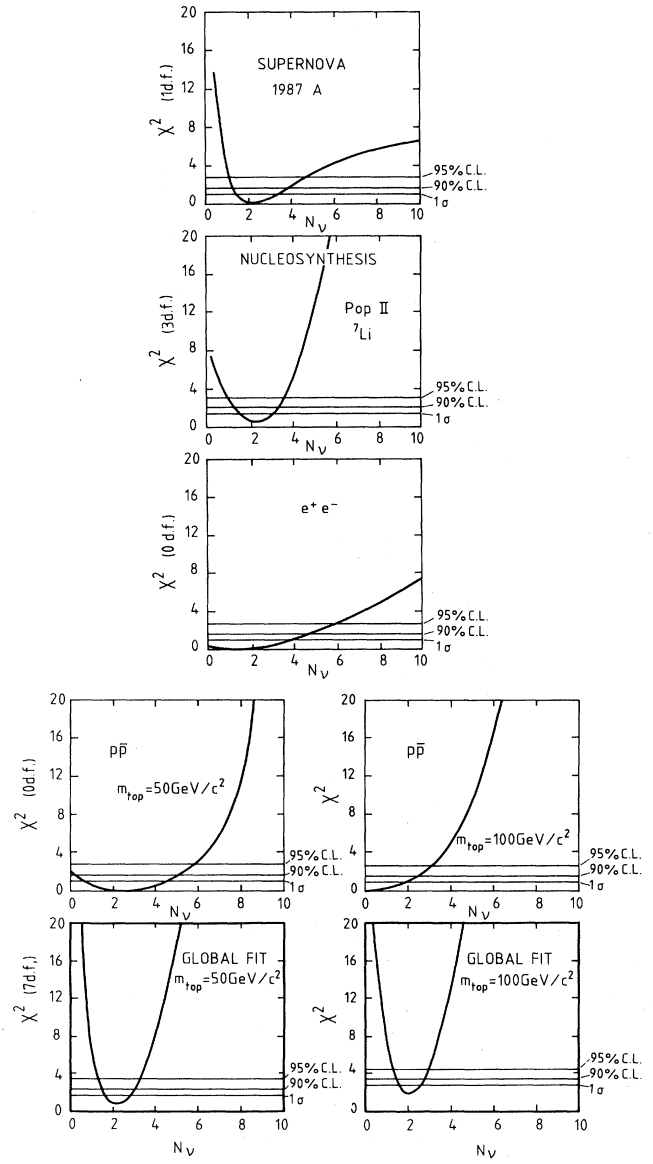

FIG. 35. χ^2 as a function of the number of neutrino families for the various methods and the global fits. The theoretical uncertainties have been treated as being random, as explained in the Appendix. The numbers of degrees of freedom of the fits are given in parentheses.

TABLE V. Results from the fits; systematic errors included.

Method	Central value	$\pm 1\sigma$	90% upper C.L.	95% upper C.L.	Goodness of fit
Supernova	2	$^{+1.4}_{-0.7}$	3.9	4.8	99%
Nucleosynthesis					
Population-II ^{7}Li					
$\eta=(4.35^{+0.4}_{-0.6})10^{-10}$	2.3	± 0.8	3.3	3.6	93%
Population-I ^{7}Li					
Solution II $\eta=(8.6\pm 0.6)\times 10^{-10}$	1.8	± 0.75	2.6	3.1	1.9%
Population-I ^{7}Li					
Solution III $\eta=(1.6\pm 0.6)\times 10^{-10}$	4.2	± 0.8	4.4	4.7	$<10^{-6}$
e^+e^-	1	$+2.9$	4.6	5.8	
W and Z production					
$M_{\rm top}=50$ GeV/c^2	2.2	$^{+2.2}_{-1.5}$	5.1	5.8	
$M_{\rm top}=100$ GeV/c^2	0	$^{+2.0}_{-1.3}$	2.5	3.1	
Global fit[a]					
$M_{\rm top}=50$ GeV/c^2	2.1	$^{+0.6}_{-0.4}$	2.9	3.2	99%
$M_{\rm top}=100$ GeV/c^2	2	$^{+0.6}_{-0.4}$	2.7	2.9	97%

[a]Using population-II ^{7}Li abundance.

in principle they are sensitive in a different way to particles other than light neutrinos. The supernova luminosity is sensitive to any energy loss through the emission of other light particles such as axions (Mayle *et al.*, 1986, 1987; Raffelt and Seckel, 1988; Burrows *et al.*, 1989). The primordial nucleosynthesis depends on the number of relativistic degrees of freedom at ~ 0.75 MeV. The e^+e^- and $\bar{p}p$ experiments limit the number of particles coupling to the Z, including, for instance, supersymmetric particles such as $\tilde{\nu}$ and $\tilde{h}$ of masses less than half the Z mass.

The agreement obtained indicates that these additional phenomena are not important and that the Standard Model is a good approximation of reality. Inside its framework, we could combine all our estimates. In order to do so, we minimize a global χ^2 constructed as explained in the Appendix (Fig. 35). Our procedure of treating systematic errors of random Gaussian variables is justified by the number of different methods and assumptions used.

Choosing the ^{7}Li abundance from population-II stars, we see that this global minimization procedure leads to

$$N_\nu = 2.1^{+0.6}_{-0.4} \text{ for } m_{\rm top}=50 \text{ GeV}/c^2$$

and

$$N_\nu = 2.0^{+0.6}_{-0.4} \text{ for } m_{\rm top}=100 \text{ GeV}/c^2$$

with the 90% and 95% confidence limits of

$$N_\nu < 2.9 \text{ or } 2.7 \text{ (90\% C.L.)}$$
$$\text{for } m_{\rm top}=50 \text{ GeV}/c^2 \text{ or } 100 \text{ GeV}/c^2,$$
$$N_\nu < 3.2 \text{ or } 2.9 \text{ (95\% C.L.)}$$
$$\text{for } m_{\rm top}=50 \text{ GeV}/c^2 \text{ or } 100 \text{ GeV}/c^2,$$

respectively.

Taken at face value, these numbers would lead to exclude as being unlikely the presence of a fourth generation and would suggest a relatively light top-quark mass. However, the χ^2 values obtained by four families (Table VI) are still acceptable, and, as argued in the Appendix, this may be a more conservative approach. We conclude therefore that in the *framework of the Standard Model, at most four generations are allowed.*

This result is in good agreement with the claim by Schramm, Steigman, and co-workers (e.g., Steigman *et al.*, 1986) on the basis of primordial nucleosynthesis. Our conclusion is somewhat more general, since we show that *all present determinations* lead to a rather low limit, and more precise, because of our systematic attempt to treat errors consistently.

It should be noted, however, that significant biases may exist. They are of various types. The Standard Model acts, to a certain extent, as an implicit constraint on the published experimental values, particularly in the case of primordial abundances. Moreover, direct counting experiments based on the rejection of events, such as the e^+e^- experiments, may be biased by an implicit intent to get rid of the "background," which will yield a value of the number of neutrinos.

These four determinations of the number of neutrino

TABLE VI. Goodness of fit for global fit (using population-II ^{7}Li abundances).

	No. of neutrinos		
	3	4	5
$M_{\rm top}=50$	95%	36%	1.7%
$M_{\rm top}=100$	77%	11%	0.1%

species are subject to considerably different types of theoretical uncertainties. The supernova estimates suppose a knowledge of the binding energy of the collapsing star. The nucleosynthesis values rely mainly on the assumption that primordial ^{7}Li abundance is given by population-II stars. In addition to being less attractive, the other choice of using population I for this purpose leads to a much poorer fit in the Standard Model. The final error also depends heavily on the assumed uncertainties in the modeling of H II regions when determining ^{4}He abundances. The e^+e^- result is rather direct, but relies on the assumption of a universal coupling between the neutrinos and the Z. The estimates are made for neutrinos whose masses are negligible as compared with the e^+e^- center-of-mass energy (29 to 43 GeV). The present calculations do not yet take into account higher-order corrections (Berends *et al.*, 1986), but the effect is expected to be small. The $p\bar{p}$ value also relies on universality and assumes that the neutrino masses are smaller than ~ 10 GeV. It is based on the ratio R_σ of W to Z production, which is well understood in the framework of the parton model, and is rather well constrained by μ and ν deep-inelastic scattering, in spite of current disagreement between the experiments (Benvenuti *et al.*, 1989). The $p\bar{p}$ value assumes that there are no significant contributions to $\Gamma_{\rm tot}^W$ and $\Gamma_{\rm tot}^Z$ beyond those expected from the Standard Model. The effect of a heavy lepton or a b' quark modifies the limit by $\approx \pm 1$ unit.

Incidentally, with the ^{7}Li abundance from population-II stars, this global fit gives for the baryon cosmological density

$$\Omega_b h^2 = (1.61^{+0.16}_{-0.22}) \times 10^{-2} ,$$

with upper limits of

$$\Omega_b h^2 < 1.85 \times 10^{-2} \quad (90\%\ \text{C.L.})$$
$$< 1.92 \times 10^{-2} \quad (95\%\ \text{C.L.})$$

essentially independently of the top-quark mass.

The problem of the number of neutrinos (at least for M_ν up to ~ 30 GeV) should be settled in the near future by the direct measurement of the Z^0 width at SLC or LEP, with an expected accuracy of $\Delta\Gamma_{\rm tot}^Z < 50$ MeV. This, in turn, will probably settle the question of the number of fermion generations. The elimination of this fundamental indeterminacy, together with the progress of measurements for each of the processes we considered, will allow a more precise testing of the consistency between all these determinations and possibly point to missing elements in our current understanding of stellar collapse, Big Bang nucleosynthesis, and particle spectra.

(1) Although the understanding of neutrino production in supernovae will probably not improve noticeably before we have a change to observe a supernova in our galaxy, the knowledge of the number of neutrinos will allow us to give a better estimate of the energy release and may strengthen limits on the production of light, weakly interacting particles (e.g., axions) in supernovae.

(2) The knowledge of the number of neutrinos will significantly constrain primordial nucleosynthesis and allow us to exploit fully the progress likely to be made in the understanding of the depletion of ^{7}Li, the determinations of the nuclear cross sections involved in its production, and the measurements of the ^{4}He and D abundances. The Hubble Space Telescope to be launched in 1990 and the currently studied Far Ultraviolet Satellite Explorer (FUSE) will probably have a great impact in the coming decade. Ultimately it should be possible to give a reliable value of the baryon density in the universe, a fundamental number in the discussion of the nature of dark matter. Should any discrepancy appear in the determination of the primary abundances with the number of neutrinos, they will point to the possibility of unstable neutrinos (if the current trend of the data toward a low neutrino number remains) or to a complete revision of the framework (e.g., the rejection of the present assumption of homogeneity).

(3) The precise measurement of the Z^0 width may well bring some surprises. A fractional "number of neutrinos" will be, for instance, evidence for the existence of new neutral particles coupling to the Z^0 (for example, relatively low-mass $\tilde{h}$ or $\tilde{\nu}$ supersymmetric particles).

(4) Finally, the knowledge of the precise width of the Z^0 from e^+e^-, a better measurement of the ratio of W and Z^0 production cross sections through the increase of statistics at the CERN and Fermilab $\bar{p}p$ colliders, and the discovery, or the absence, of the t quark in the W mass region will allow a more thorough test of SU(2)×U(1). For instance, an upper limit for the top mass could be derived.

In other words, far from ending a line of research, the determination of the number of generations will open new and fascinating possibilities for deeply probing the Standard Model through the combination of many subfields of particle astrophysics.

NOTE ADDED IN PROOF

This review and analysis was completed before the operation of the electron-positron colliders ("Z-factories") SLC and LEP. While this paper was being prepared for publication, several important results relating to neutrino counting have appeared from experiments at the CERN and Fermilab proton-antiproton colliders.

The CDF collaboration at Fermilab (Abe *et al.*, 1989) has determined the parameters of the Z^0 from 188 decays of Z^0 produced in 1.8-TeV proton-antiproton collisions into electron pairs or muon pairs. They report

$$M_Z = 90.9 \pm 0.3 \pm 0.2 \ \text{GeV}/c^2 ,$$

where the first error includes statistical and systematic errors and the second reflects the uncertainty in the energy scale, and

$$\Gamma_Z = 3.8 \pm 0.8 \pm 1.0 \ \text{GeV} ,$$

where the errors are statistical and systematic. They

have also presented (Abe *et al.*, 1990b) a measurement of the ratio of observed W and Z cross sections,

$$R = 10.2 \pm 0.8 \pm 0.4 ,$$

which implies that

$$N_\nu = 2.7 \pm 1.1 \pm 0.6 ,$$

if the decay $W \to t\bar{b}$ is kinematically forbidden, as seems likely from the recent lower limit to the top mass of 77 GeV/c^2 set by the same group (Abe *et al.*, 1990a).

The UA2 collaboration (Lefebre *et al.*, 1989; Weidberg *et al.*, 1989) has also given a preliminary value of the cross-section ratio from its observations in 630-GeV proton-antiproton collisions. They find

$$R = 10.35^{+1.5}_{-1.0} \pm 0.3 ,$$

which corresponds to

$$N_\nu = 2.6^{+2.1}_{-1.5} \pm 0.4 ,$$

if the decay $W \to t\bar{b}$ is kinematically forbidden.

The Mark II Collaboration (Abrams *et al.*, 1989a, 1989b) at the Stanford Linear Collider has measured the parameters of the Z^0 in 480 decays. They find

$$M_Z = 91.14 \pm 0.12 \text{ GeV}/c^2$$

and

$$\Gamma_Z = 2.42^{+0.45}_{-0.35} \text{ GeV} .$$

From their determination of the width for invisible decays,

$$\Gamma(Z \to \text{invisible}) = 0.46 \pm 0.10 \text{ GeV} ,$$

they infer

$$N_\nu = 2.8 \pm 0.6 .$$

The most statistically powerful results come from early running at the LEP Collider at CERN. These measurements are summarized in the following table:

Detector	Events	M_Z (GeV/c^2)	Γ_Z (GeV)	N_ν
ALEPH (Decamp *et al.*, 1989)	3112	91.174±0.070	2.68±0.15	3.27±0.30
DELPHI (Aarnio *et al.*, 1989)	1038	91.06±0.09±0.045	2.49±0.21	2.4±0.4±0.5
L3 (Adeva *et al.*, 1989)	2538	91.132±0.057±0.045	2.588±0.137	3.42±0.48
OPAL (Akrawy *et al.*, 1989)	4539	91.01±0.05±0.05	2.60±0.13	3.1±0.4

On 6 January 1990, Thresher (1990) presented at the DPF 90 meeting the most recent combined results for all the CERN experiments:

$$M_Z = 91.152 \pm 0.014, \quad M_Z = 2.569 \pm 0.032,$$

$$N_\nu = 3.18 \pm 0.10 ,$$

for a global model dependent fit (i.e., taking into account the expected height of the Z^0 peak) and

$$N_\nu = 3.04 \pm 0.20$$

for a model independent fit performed with the DELPHI and OPAN events.

These results are well within the region allowed by our analysis of the previous results and strengthen considerably our conclusion that the consistency of all N_ν determinations is an astounding success for the Standard Model and for the current descriptions of stellar collapse and the Big-Bang primordial nucleosynthesis.

ACKNOWLEDGMENTS

For the astrophysical determination, we are grateful for discussions with S. Woosley, R. Schaeffer, and S. Bludman. The input on nucleosynthesis from J. Audouze, D. Schramm, J. Silk, G. Steigman, M. Turner, S. Vauclair, and J. P. Zahn was greatly appreciated. This work has been partially supported by the U.S. Department of Energy, Contract No. DE-AC03-76SF00098.

APPENDIX: STATISTICAL METHOD

Although a Bayesian approach, which considers unknown parameters as random variables, would have been equally legitimate, we have followed the more general practice of considering the true values of the parameters as fixed, and their estimates as random variables. This attitude leads to the choice of prescriptions, such as confidence intervals, that will give wrong results only in a small proportion of the experiments. Note that it is inconsistent to mix Bayesian "confidence intervals" with the usual ones, since their definition and interpretation are quite different.

In order to be able to write down a χ^2, we have treated theoretical and observational uncertainties on a similar footing, assuming, for simplicity, that the preferred theoretical values were distributed in a normal (Gaussian) way. For the case in which only a range of acceptable values was known, we have assumed that it represented a $\pm 2\,\sigma$ interval of a normal variable. Therefore our definition of acceptability is that only $\approx 5\%$ of the time would such an estimated range not include the

true value of the parameter considered. Although this procedure is arbitrary for a small number of theoretical assumptions involved in a particular result, it becomes legitimate when a larger number of such assumptions are made, as shown by the central limit theorem (see, for instance, Eadie *et al.*, 1971).

We have constructed χ^2 functions and minimized them with respect to N_ν and the other free parameters. For instance, for the case of the primordial nucleosynthesis, we considered

$$\chi^2=\left[\frac{Y_p-\theta_1(\eta,\tau_{1/2},N_\nu)}{\sigma_{Y_p}}\right]^2+\left[\frac{\ln\frac{\mathrm{D}}{\mathrm{H}}-\theta_2(\eta)}{\sigma\left[\ln\frac{\mathrm{D}}{\mathrm{H}}\right]}\right]^2+\left[\frac{\ln\frac{^3\mathrm{He}}{\mathrm{H}}-\theta_3(\eta)}{\sigma\left[\ln\frac{^3\mathrm{He}}{\mathrm{H}}\right]}\right]^2$$
$$+\left[\frac{\ln\frac{\mathrm{D}+^3\mathrm{He}}{\mathrm{H}}-\theta_4(\theta)}{\sigma\left[\ln\frac{\mathrm{D}+^3\mathrm{He}}{\mathrm{D}}\right]}\right]^2+\left[\frac{\frac{^7\mathrm{Li}}{\mathrm{H}}-\theta_5(\eta)}{\sigma\left[\frac{^7\mathrm{Li}}{\mathrm{H}}\right]}\right]^2+\left[\frac{10.35-\tau_{1/2}}{0.12}\right]^2,$$

where the θ_i are the relevant theoretical functions taken from Yang *et al.* (1984), except for the ^{7}Li, which is taken from Kawano *et al.* (1988); the last term takes into account the uncertainty of the neutron lifetime; and the σ's are the corresponding experimental error.

For variables that were not Gaussian, we made an appropriate change of variables so that the new variable would be Gaussian. For instance, in the case of the $\bar{p}p$ determination, we made a change of variable $u=g(R)$, so that the $\pm1\sigma$ and 90% and 95% upper confidence-level values of R given in Sec. VI.B would correspond to $u=\pm1$, 1.28, and 1.64, respectively. The $g(R)$ is then distributed normally with zero mean and unity variance. The χ^2 can then be written

$$\chi^2=[g(R)]^2+\left[\frac{\frac{R}{R_\Gamma}(N_\nu)-R_\sigma}{\sigma_{R_\sigma}}\right]^2$$

and minimized with respect to R and N_ν.

The $\pm1\sigma$ interval (containing in $\approx68\%$ of the cases the true value of the parameter) and the 90% and 95% upper confidence intervals have been defined by the value of N_ν for which the χ^2, minimized with respect to all other parameters, is increased with respect to the minimum value by 1, $(1.28)^2$, and $(1.64)^2$, respectively.

It may be useful to recall the difference between confidence level and goodness of fit: they correspond to two different questions. A confidence level on N_ν is placed by asking what is the probability, for a given N_ν, of getting an estimate $\hat{N}_\nu$ that is further from N_ν than the current estimate. It relies on the fact that if N_ν is the true value asymptotically, then

$$\frac{(\hat{N}_\nu-N_\nu)^2}{\sigma^2_{N_\nu}}$$

(where $\sigma^2_{N_\nu}$ is the variance of the $\hat{N}_\nu$) should behave as a χ^2 of 1 degree of freedom. The value of N_ν at the "$\alpha\%$ upper confidence level" is the value of N_ν *above* the best estimate, for which this probability is $\alpha\%$. The "goodness of fit" for a given value of N_ν is the probability of having a χ^2 larger than the χ^2 obtained for this *given* value.

One may choose to reject a value of N_ν if it is bigger than the value at the $\alpha\%$ upper confidence level or, alternatively, if the goodness of fit is worse than a chosen value of $(1-\alpha\%)$. Both procedures are acceptable in the sense that the experimenter choosing systematically either prescription will, in the long run, be wrong in only $(1-\alpha\%)$ of the experiments. However, the confidence level is more powerful, i.e., more discriminating, against a wrong hypothesis regarding the number of neutrinos (see, e.g., Eadie *et al.*, 1971).

This discussion presupposes that the errors are properly estimated and that no bias has been introduced. In our case, where the best fit is unusually good, there is a significant difference between the two methods—the confidence-level prescription rejects four families, while the goodness of fit for four families is still acceptable (Table VI). Two attitudes may be taken.

(1) It could be argued that the too good value of the best fit χ^2 could be traced back to an overly conservative estimate of the errors. If this were true, the confidence-level method would be preferable because it is less sensitive to a wrong evaluation of the errors. This is the line of argument behind the usual choice of the confidence level in experimental physics, since in the most common case, in which errors are underestimated, this method is more conservative.

(2) It could also be argued that the extremely good fit could be attributed to an unconscious bias towards the Standard Model. In that case, the goodness of fit is more reliable. In our case, it is also more conservative, and we choose *not* to reject the possibility of four families.

In such a "classical" approach, we are not using the *a priori* information that we know that at least three neutrinos exist (we do not know, however, that they are all

light enough and stable enough to contribute to all the considered processes). In order to use this information, a Bayesian point of view would have to be adopted, with the *arbitrary* definition of *a priori* probabilities (truncated at 2 or 3, depending on the process) for the number of neutrinos contributing to each process. The *a posteriori* probability will be obtained by convolution with the likelihood functions given in Fig. 35. *Given* these *a priori* probabilities and the specification of the risks considered, an optimal decision rule on the number could be defined.

The comparison between the two approaches is a well-known discussion (see, e.g., Eadie *et al.*, 1971, Sec. 6.5). The "classical" approach can be considered as a way for the experimentalist to summarize a set of measurements in a manner that carries the maximum amount of information about the unknown parameters. This procedure is well defined and, in our case, comes down to the presentation of the likelihood curves of Fig. 35. But as soon as a decision has to be made about the value of the parameter, one must choose among different decision rules, each of which is only optimal for one value of the parameter and one definition of the risk, and there is some *fundamental indeterminacy.* This indeterminacy in the classical case is located in the choice of the decision rule (e.g., in our case the goodness-of-fit test). In the Bayesian case this fundamental uncertainty is embedded in the choice of the *a priori* probabilities.

REFERENCES

The institutions and organizations participating in the collaborations that are named in this list of references are as follows. ASP—SLAC, MIT, Washington, Boston University, Pennsylvania; BCDMS—Bologna, CERN, Dubna, Munich, Saclay. CELLO—Hamburg (DESY), Glasgow, Universität Hamburg, INFN, Karlsruhe (Kernforschungszentrum), Universität Karlsruhe, Munich (Max-Planck-Institute). Orsay (LAL), Paris, Rome, Saclay (CEN), Tel Aviv; MAC—Colorado, Frascati (INFN), University of Houston, Northeastern University (Boston), Stanford (SLAC and Department of Physics), Utah, Wisconsin; TASS—Aachen (Physikalisches Institut der RWTH), Bonn (Physikalisches Institut der Universität), Bristol, Hamburg (DESY), Universität Hamburg, Dortmund, Imperial College (London), Madrid, Oxford University, Queen Mary College (London), Rutherford Appleton Laboratory, Siegen, Weizmann Institute (Rehovot), Wisconsin; UA1—Aachen, Amsterdam (NIKHEF), Annecy (LAPP), Birmingham, CERN, Harvard, Helsinki, INFN, Kiel, Imperial College (London), Madrid (CIEMAT), MIT, Padua, Paris (Collège de France), Queen Mary College (London), Riverside, Rome, Rutherford Appleton Laboratory, Saclay (CEN), Victoria, Vienna, Wisconsin; UA2—Bern, CERN, Copenhagen (NBI), Heidelberg, Orsay (LAL), Pavia, Perugia, Pisa, Saclay (CEN).

Aarnio, P., *et al.*, DELPHI Collaboration, 1989, "Measurement of the mass and width of the Z^0 particle from multihadronic final states produced in e^+e^- collisions," Report No. CERN EP/89-134, unpublished.

Abe, F., *et al.*, CDF Collaboration, 1989, Phys. Rev. Lett. **63**, 720.

Abe, F., *et al.*, CDF Collaboration, 1990a, Phys. Rev. Lett. **64**, 142.

Abe, F., *et al.*, CDF Collaboration, 1990b, Phys. Rev. Lett. **64**, 152.

Abrams, G. S., *et al.*, Mark II Collaboration, 1989a, Phys. Rev. Lett. **63**, 724.

Abrams, G. S., *et al.*, Mark II Collaboration, 1989b, Phys. Rev. Lett. **63**, 2173.

Adeva, B., *et al.*, L3 Collaboration, 1989, "A determination of the properties of the neutral intermediate boson Z^0," Report No. L3-001, unpublished.

Aglietta, M., *et al.*, 1987, Europhys. Lett. **3**, 1315,1321.

Akrawy, A.Z., *et al.*, OPAL Collaboration, 1989, "Measurement of the Z^0 mass and width with the OPAL detector at LEP," Report No. CERN EP/89-133, unpublished.

Albajar, C., *et al.*, 1987a, UA1 Collaboration, Phys. Lett. B **185**, 233.

Albajar, C., *et al.*, 1987b, UA1 Collaboration, Phys. Lett. B **185**, 241.

Albajar, C., *et al.*, 1987c, UA1 Collaboration, Phys. Lett. B **198**, 261.

Albajar, C., *et al.*, 1987d, UA1 Collaboration, Phys. Lett. B **198**, 271.

Albajar, C., *et al.*, 1988, UA1 Collaboration, Z. Phys. C **37**, 489.

Albajar, C., *et al.*, 1989, UA1 Collaboration, Z. Phys. C **44**, 15.

Albert, D., W. J. Marciano, D. Wyler, and Z. Parsa, 1980, Nucl. Phys. **B166**, 460.

Alcock, C., G. Fuller, and G. Mathews, 1987, Astrophys. J. **320**, 439.

Alcock, C., G. Fuller, B. Myer, and G. Mathews, 1988, Phys. Rev. D **37**, 1380.

Alexeyev, E. N., L. N. Alexeyava, I. V. Krivosheina, and V. I. Volchenko, 1988, Phys. Lett. B **205**, 209.

Alpher, R.A., J. W. Follin, Jr., and R. C. Herman, 1953, Phys. Rev. **92**, 1347.

Alpher, R. A. and R. C. Herman, 1950, Rev. Mod. Phys. **22**, 153.

Altarelli, G., R. K. Ellis, M. Greco, and G. Martinelli, 1984, Nucl. Phys. **B246**, 12.

Altarelli G., R. K. Ellis, and G. Martinelli, 1985, Z. Phys. C **17**, 617.

Altarelli, G., 1986, "Precision tests of the electroweak theory at the Z^0," CERN 86-02, Physics at LEP yellow report, Vol. 1, p. 3.

Alvarez, T., A. Leites, and J. Terrón, 1987, Nucl. Phys. **B301**, 1.

Amaldi, U., *et al.*, 1987, Phys. Rev. D **36**, 1385.

Ansari, R., *et al.*, 1987a, UA2 Collaboration, Phys. Lett. B **186**, 440.

Ansari, R., *et al.*, 1987b, UA2 Collaboration, Phys. Lett. B **194**, 158.

Applegate, J. H., C. J. Hogan, and R. J. Scherrer, 1987, Phys. Rev. D **35**, 1151.

Arnett, W. D., 1973, in *Explosive Nucleosynthesis* (University of Texas, Austin).

Arnison, G., *et al.*, 1983a, UA1 Collaboration, Phys. Lett. **122B**, 103.

Arnison, G., *et al.*, 1983b, UA1 Collaboration, Phys. Lett. **126B**, 398.

Arnison, G., *et al.*, 1983c, UA1 Collaboration, Phys. Lett.

129B, 273.
Arnison, G., *et al.*, 1983d, UA1 Collaboration, Phys. Lett. **134B**, 469.
Arnison, G., *et al.*, 1986, UA1 Collaboration, Europhys. Lett. **1**, 327.
Aubert, J. J., *et al.*, 1987, Nucl. Phys. **B293**, 740.
Audouze, J., O. Boulade, G. Malinie, and Y. Poilane, 1983, Astron. Astrophys. **127**, 164.
Audouze, J., and B. Tinsley, 1976, Annu. Rev. Astron. Astrophys. **14**, 43.
Baade, D., and P. Magain, 1988, Astron. Astrophys. **194**, 237.
Bagnaia, P., *et al.*, 1983, UA2 Collaboration, Phys. Lett. **129B**, 130.
Bania, T. M., R. T. Rood, and T. L. Wilson, 1987, Astrophys. J. **323**, 30.
Banner, M., *et al.*, 1983, UA2 Collaboration, Phys. Lett. **122B**, 476.
Barbiellini, G., B. Richter, and J. L. Siegrist, 1981, Phys. Lett. **106B**, 414.
Barger, V., T. Han, N. G. Deshpande, and R. J. N. Phillips, 1987, Phys. Lett. B **192**, 212.
Barrow, J. D., 1983, in *Fundamentals of Cosmic Physics,* Vol. **8**, edited by V. M. Canuto and Bruce G. Elmegreen (Gordon and Breach, New York), p. 83.
Bartha, G., *et al.*, ASP Collaboration, Phys. Rev. Lett. **56**, 685.
Baym, G., H. A. Bethe, and C. J. Pethick, 1971, Nucl. Phys. A **175**, 225.
Baym, G., and C. Pethick, 1975, Annu. Rev. Nucl. Sci. **25**, 27.
Behrend, H. J., *et al.*, 1986, CELLO Collaboration, Phys. Lett. B **176**, 247.
Behrend, H. J., *et al.*, 1988, CELLO Collaboration, Phys. Lett. B **215**, 186.
Benvenuti, A. C., *et al.*, 1989, Phys. Lett. B **223**, 490.
Berends, F. A., G. J. H. Burgers, and W. L. Van Neerven, 1986, Phys. Lett. B **177**, 191.
Berger, E. L., F. Halzen, C. S. Kim, and S. Willenbrock, 1989, Phys. Rev. D **40**, 43; **40**, 3789(E).
Bethe, A. H., and G. Browne, 1985, Sci. Am. **252**, 60.
Bionta, R. M., *et al.*, 1987, Phys. Rev. Lett. **58**, 1494.
Blitz, L., and C. Heiles, 1987, Astrophys. J. Lett. **313**, L95.
Boesgaard, A. M., and G. Steigman, 1985, Annu. Rev. Astron. Astrophys. **23**, 319.
Braunschweig, W., *et al.*, 1988, TASSO Collaboration, Z. Phys. C **38**, 543.
Brown, L., and D. N. Schramm, 1988, Astrophys. J. **329**, L103.
Burke, D. L., 1987, "Neutrino counting in e^+e^- annihilation," (SLAC) Report No. SLAC-PUB 4284.
Burrows, A., 1984, Astrophys. J. **283**, 848.
Burrows, A., 1987a, Arizona State University Preprint No. 87-34.
Burrows, A., 1987b, in *Proceedings of Telemark 1987,* edited by V. Barger *et al.* (World Scientific, Singapore), p. 28.
Burrows, A., 1988, Astrophys. J. **334**, 891.
Burrows, A., M. S. Turner, and R. P. Brinkman, 1989, Phys. Rev. D **39**, 1020.
Cabibbo, N., 1983, in *Proceedings of the Third Topical Workshop on Proton-Antiproton Collider Physics, Rome, 1983,* Report No. CERN 83-04, edited by C. Bacci and G. Salvini (CERN, Geneva), p. 567.
Carswell, R., *et al.*, 1986 (unpublished).
Chaichian, M., and M. Hayashi, 1984, Phys. Rev. D **30**, 243.
Chandrasekhar, S., 1957, *An Introduction to the Study of Stellar Structure* (Dover, New York).
Clayton, D. D., 1968, *Principles of Stellar Evolution and Nucleosynthesis* (McGraw-Hill, New York).
Clayton, D. D., 1985, Astrophys. J. **290**, 428.
Cline, D., and J. Rolf, 1983, CERN Report No. UA1 TN 83/40.
Cline, D., D. N. Schramm, and G. Steigman, 1987, Comments Nucl. Part. Phys. **17**, No. 3, 145.
Colas, P., D. Denegri, and C. Stubenrauch, 1988, Z. Phys. C **40**, 527.
Costa, G., J. Ellis, G. L. Fogli, D. V. Nanopoulos, and F. Zwirner, 1988, Nucl. Phys. B **297**, 244.
D'Antona, F., and I. Mazzitelli, 1983, Astron. Astrophys. **138**, 431.
Dearborn, D., D. Schramm, G. Steigman, and T. Truran, 1989, "The shocking development of lithium (and boron) in supernovae," Fermilab Report No. FERMILAB-CONF-89/50-A.
Dearborn, D. S. P., D. N. Schramm, and G. Steigman, 1986, Astrophys. J. **302**, 35.
Decamp, D., *et al.*, ALEPH Collaboration, 1989, "Determination of the number of light neutrino species," Report No. CERN EP/89-132, unpublished.
Delbourgo-Salvador, P., C. Gry, G. Malinie, and J. Audouze, 1985, Astron. Astrophys. **150**, 53.
Denegri, D., 1984, Report Nos. UA1 TN 84/03, January 1984, and UA1 TN 85-28.
Denegri, D., 1986, in *Proceedings of the 6th Topical Workshop on Proton-Antiproton Collider Physics, Aachen, Germany, July, 1986* (World Scientific, Singapore), p. 32.
De Rújula, A., 1987, Phys. Lett. **193**, 525.
Deshpande, N. G., G. Eilam, V. Barger, and F. Halzen, 1985, Phys. Rev. Lett. **54**, 1757.
Diemoz, M., F. Ferroni, E. Longo, and G. Martinelli, 1988, Z. Phys. C **39**, 31.
Di Lella, L., *et al.*, 1987, in "Proton Antiproton Collider Physics," lectures at the Cargèse 1987 School (Plenum, New York), p. 556.
Dimopoulos, S., R. Esmailzadeh, L. Hall, and G. Starkman, 1988a, Astrophys. J. **330**, 545.
Dimopoulos, S., R. Esmailzadeh, L. Hall, and G. Starkman, 1988b, Phys. Rev. Lett. **60**, 7.
Dimopoulos, S., R. Esmailzadeh, L. Hall, and G. Starkman, 1989, Nucl. Phys. **B311**, 699.
Dolgov, A. D., L. B. Okun, and V. I. Z. Zacharov, 1972, Nucl. Phys. **B41**, 197.
Duke, D. W., and J. F. Owens, 1984, Phys. Rev. D **30**, 49.
Eadie, W. T., D. Drijard, F. E. James, M. Roos, and B. Sadoulet, 1971, *Statistical Methods in Experimental Physics* (North-Holland, Amsterdam).
Ellis, J., K. Enqvist, D. V. Nanopoulos, and S. Sarkar, 1986, Phys. Rev. **167B**, 457.
Ellis, J., and K. A. Olive, 1987, Phys. Lett. **B193**, 525.
Feldman, G., 1986, MARKII/SLC Physics Working Group Note 02, Asilomar.
Ferlet, R., A. Vidal-Madjar, C. Laurent, and D. G. York, 1980, Astrophys. J. **242**, 576.
Fernandez, E., *et al.*, 1985, MAC Collaboration, Phys. Rev. Lett. **54**, 1118.
Ford, W. T., *et al.*, 1986, MAC Collaboration, Phys. Rev. D **33**, 3472.
Fujimoto, M. Y., and R. E. Taam, 1986, Astrophys. J. **305**, 246.
Fuller, G. M., C. R. Mathews, and C. R. Alcock, 1988, Phys. Rev. D **37**, 1380.
Gaemers, K. J. F., R. Gastmans, and F. M. Renard, 1979, Phys. Rev. D **19**, 1605.
Gamow, G., 1946, Phys. Rev. **70**, 572.
Gamow, G., 1948, Phys. Rev. **74**, 505.

Glück, M., E. Hoffmann, and E. Rey, 1982, Z. Phys. C **13**, 119.
Gry, C., C. Laurent, and A. Vidal-Madjar, 1983, Astron. Astrophys. **124**, 99.
Haines, T. J., 1987, in *Proceedings of Telemark IV: Neutrino Masses and Neutrino Astrophysics, Ashland, 1987* (World Scientific, Singapore), p. 63.
Halzen, F., 1986, Phys. Lett. B **182**, 388.
Halzen, F., and K. Marsula, 1983, Phys. Rev. Lett. **51**, 857.
Harrison, B. K., K. S. Thorne, M. Wakano, and J. Wheeler, 1965, *Gravitational Theory and Gravitational Collapse* (University of Chicago, Chicago).
Hearty, C., *et al.*, 1987, ASP Collaboration, Phys. Rev. Lett. **58**, 1711.
Hillebrandt, W., 1987, in *High Energy Phenomena around Collapsed Stars,* edited by F. Pacini (Reidel, Dordrecht), p. 73.
Hirata, K., *et al.*, 1987, Phys. Rev. Lett. **58**, 1490.
Hitlin, D., 1988, in *Proceedings of the International Symposium on Lepton and Photon Interactions at High Energies, Hamburg, 1987* (North-Holland, Amsterdam), p. 179.
Hobbs, L. M., and D. K. Duncan, 1987, Astrophys. J. **317**, 796.
Hobbs, L. M., and C. Pilachowski, 1986, Astrophys. J. **311**, L37.
Hobbs, L. M., and C. Pilachowski, 1988, Astrophys. J. **334**, 734.
Irvine, J. M., 1978, *Neutron Stars* (Clarendon, Oxford), and references therein.
Johnson, A. S., 1987, in *XXII Rencontres de Moriond, Les Arcs 1987,* edited by T. Monmerle and Tran Thanh Van (Editions Frontières, Gif-sur-Yvette), Vol. 1, p. 119.
Kawano, L., D. Schramm, and G. Steigman, 1988, Astrophys. J. **327**, 750.
Krauss, L. M., 1987, Nature (London) **329**, 689.
Kühn, J. H., A. Reiter, and P. M. Zerwas, 1986, Nucl. Phys. B **272**, 560.
Kunth, D., 1986, Publ. Astron. Soc. Pac. **98**, 984.
Kunth, D., and W. L. W. Sargent, 1983, Astrophys. J. **273**, 81.
Lamb, D. Q., *et al.*, 1987, *Supernova 1987A in the Large Magellanic Cloud, Proceedings of the George Mason Workshop,* edited by M. Kafatos (Cambridge, University Press, New York), in press.
Laurent, C., A. Vidal-Madjar, and D. G. York, 1979, Astrophys, J. **229**, 923.
Locci, E.,1987, in *Proceedings of the International European Conference on High-Energy Physics, Uppsala, 1987* (University of Uppsala, Sweden).
Lefebre, M., *et al.*, UA2 Collaboration, 1989, presented at the 8th Topical Workshop on $\bar{p}p$ Collider Physics, Castiglione della Pescaia, Italy.
LoSecco, J. M., 1989, Phys. Rev. D **39**, 1013.
Ma, E., and J. Okada, 1978, Phys. Rev. Lett. **41**, 287.
Malone, R. C., M. B. Johnson, and H. A. Bethe, 1975, Astrophys. J. **199**, 741.
Marciano, W., 1987, "Weak Currents and Future Z-mass Measurements," talk given at the 1987 SLAC Summer Institute Topical Conference, August 1987; BNL Report No. 40379.
Matzner, R. A., 1986, "Cosmic Nucleosynthesis," Publ. Astron. Soc. Pac. **98**, 1049.
Mayle, R., and J. Wilson, 1987, Lawrence Livermore Laboratory Preprint.
Mayle, R., *et al.*, 1988, Phys. Lett. B **203**, 188.
Mayle, R., *et al.*, 1989, Phys. Lett. B **219**, 515.
Michaud, G., G. Fontaine, and G. Beaudet, 1984, Astrophys. J. **282**, 206.
Milsztajn, A., 1989, Thèse d'Etat (Université Paris XI).
Mohammadi, M., 1987, Ph.D. thesis (University of Wisconsin, Madison).
Olive, K. A., D. N. Schramm, and G. Steigman, 1981, Nucl. Phys. **B180**, 497.
Olive, K. A., D. N. Schramm, G. Steigman, M. S. Turner, and J. Yang, 1981, Astrophys. J. **246**, 557.
Pagel, B. E. J., *et al.*, 1986, "New measurements of helium in H II galaxies," Publ. Astron. Soc. Pac. **98**, 1005.
Pandharipande, V. R., 1971, Nucl. Phys. **A178**, 123.
Peebles, P. J. E., 1966, Astrophys. J. **146**, 542.
Peebles, P. J. E., 1971, *Physical Cosmology* (Princeton University, Princeton, N.J.).
Peimbert, M., 1986, "On the helium and heavy-element enrichment of the interstellar medium," Publ. Astron. Soc. Pac. **98**, 1057.
Penzias, A. A., and R. W. Wilson, 1965, Astrophys. J. **142**, 419.
Piran, T., and D. Spergel, 1988, in *Dark Matter,* Proceedings of the XXIIIrd Rencontre de Moriond, Les Arcs, Savoie, France, 1988, edited by J. Audouze and J. Tran Thanh Van (Editions Frontières, Gif-sur-Yvette), p. 453.
Pomanski, A., 1987, communication at the XXII Rencontres de Moriond, Les Arcs, March 5–14, unpublished.
Raffelt, G., and D. Seckel, 1988, Phys. Rev. Lett. **60**, 1793.
Rebolo, R., P. Molaro, C. Abía, and J. E. Beckman, 1988, Astron. Astrophys. **193**, 193.
Rebolo, R., P. Molaro, and J. E. Beckman, 1988, Astron. Astrophys. **192**, 192.
Rood, R. T., T. M. Bania, T. L. Wilson, 1984, Astrophys. J. **280**, 629.
Sadoulet, B., 1988, in *Proceedings of the Fifteenth SLAC Summer Institute on Particle Physics,* edited by E. C. Brenan (Stanford University, Stanford), p. 277.
Sahu, K. C., M., Sahu, and R. Pottasch, 1988, Astron. Astrophys. Lett. **207**, L1.
Schaeffer, R., 1984, *Ecole d'été de Physique des particules, Gif-sur-Yvette* (CNRS, Paris), p. 19.
Schaeffer, R., Y. Declais, and S. Jullian, 1987, Nature (London) **330**, 142.
Schramm, D. N., 1987, Comments Nucl. Part. Phys. **17**, 239.
Schramm, D. N., 1988, in *Proceedings of the International Symposium on Lepton and Photon Interactions at High Energies, Hamburg, 1987* (North-Holland, Amsterdam), p. 471.
Schramm, D. N., 1989, unpublished.
Shields, G. A., 1987, in *Proceedings of the 13th Texas Symposium on Relativistic Astrophysics,* edited by M. P. Ulmer (World Scientific, Singapore), p. 192.
Simopoulou, E., 1986, CERN 86-02, LEP yellow report, Vol. 1, p. 197.
Spergel, D. N., T. Piran, A. Loeb, J. Goodman, and J. N. Bahcall, 1987, Science **237**, 1471.
Spite, F., and M. Spite, 1982, Nature (London) **297**, 483.
Steigman, G., 1987, in *Proceeedings of the 13th Texas Symposium on Relativistic Astrophysics,* edited by M. P. Ulmer (World Scientific, Singapore), p. 173.
Steigman, G., G. Gallagher, and D. N. Schramm, 1989, Comments Astron. Astrophys. (in press).
Steigman, G., K. A. Olive, D. N. Schramm, and M. S. Turner, 1986, Phys. Lett. B **176**, 33, and references therein.
Stubenrauch, C., 1987, "Etude de la Production des Bosons W et Z dans l'expérience UA1," Thèse d'Etat (Université de Paris-Sud), note CEA-N-2532.
Thresher, J., 1990, "Plenary talk at the DPF 90 meeting of the Division of Particles and Fields of the American Physical Society, Rice University, January 6."
Trimble, V., 1982, Rev. Mod. Phys. **54**, 1183.

Trimble, V., 1983, Rev. Mod. Phys. **55**, 511.
Trimble, V., 1987, in *High Energy Phenomena around Collapsed Stars,* edited by F. Pacini (Reidel, Dordrecht), p. 105.
Vand der Velde, J., 1988, in *Dark Matter,* Proceedings of the XXIIIrd Rencontre de Moriond, Les Arcs, Savoie, France, 1988, edited by J. Audouze and J. Tran Thanh Van (Editions Frontières, Gif-sur-Yvette), p. 429.
Vauclair, S., 1988a, in *Dark Matter,* Proceedings of the XXIIIrd Rencontre de Moriond, Les Arcs, Savoie, France, 1988, edited by J. Audouze and J. Tran Thanh Van (Editions Frontières, Gif-sur-Yvette), p. 269.
Vauclair, S., 1988b, Astrophys. J. **335**, 971.
Vidal-Madjar, A., 1983, Astron. Astrophys. **120**, 58.
Voss, R., 1988, in *Proceedings of the International Symposium on Lepton and Photon Interactions at High Energies, Hamburg, 1987* (North-Holland, Amsterdam,), p. 581.
Wagoner, R. V., 1973, Astrophys. J. **179**, 343.
Wagoner, R. V., W. A. Fowler, and F. Hoyle, 1967, Astrophys. J. **148**, 3.
Weaver, T. A., and S. E. Woosley, 1980, in *Supernova Spectra,* edited by R. Meyerott and G. H. Gillespie (AIP, New York), p. 1973.
Weidberg, A., *et al.*, UA2 Collaboration, presented by the XIV International Symposium on Lepton and Photon Interactions at High Energies, Stanford, August, 1989, unpublished).
Weinberg, S., 1972, *Gravitation and Cosmology* (Wiley, New York).
Wilkinson, D., 1987, in *Proceedings of the 13th Texas Symposium on Relativistic Astrophysics,* edited by M. P. Ulmer (World Scientific, Singapore), p. 209.
Woosley, S. E., 1987, UCRL Preprint No. UCRL-98001.
Woosley, S. E., J. R. Wilson, and R. Mayle, 1986, Astrophys. J. **302**, 19.
Yang, J., D. N. Schramm, G. Steigman, and R. T. Rood, 1979, Astrophys. J. **227**, 697.
Yang, J., M. S. Turner, G. Steigman, D. N. Schramm, and K. A. Olive, 1984, Astrophys. J. **281**, 493.
York, D. G., 1983, Astrophys. J. **264**, 172.
Zahn, J. P., 1987, in *The Internal Solar Angular Velocity,* edited by B. R. Durney and S. Sofia (Reidel, Dordrecht), p. 201.